UNIVERSITY OF CALIFORNIA, SAN DIEGO

Quantitative Neuroimaging: Applications to Normal Aging and Neurodegenerative Disease

A dissertation submitted in partial satisfaction of the requirement for the degree Doctor of Philosophy

in

Neurosciences

by

Elizabeth Ann Murphy

Committee in charge:

Professor James B. Brewer, Chair
Professor David P. Salmon, Co-Chair
Professor Terry L Jernigan
Professor Linda K. McEvoy
Professor William C. Mobley

2013

The dissertation of Elizabeth Ann Murphy is approved, and is acceptable in quality and form for publication on microfilm and electronically:

_____

_____

_____

_____
Co-Chair

_____
Chair

University of California, San Diego

2013

DEDICATION

To those I love (two, four and even six-legged).

Collection of data for this dissertation allowed me to spend considerable time with elderly subjects and their caregivers, and I believe there is much to learn from those who have traveled long journeys. In most cases, the caregivers were children or spouses who had been married to their then-demented partners for decades. Seeing love so strong it weathers the devastation of dementia is what gives me an eternal faith in *love*. While my subjects were in the scanner, I often had the opportunity to speak with their spouses, and these selfless souls were often delighted to find a listening ear in me. The spouses faced tremendous pain in watching their loved ones fade into an existence that bore no resemblance to their former selves. But despite the pain, what I saw in these spouses was tremendous courage and inspiring loyalty. Only the greatest love survives such a blow.

I will not soon forget the wife who told me in tears that her husband with Alzheimer's had peed in the oven that morning, and then later said in complete sincerity that he was the love of her life. The daughter who could laugh as she told me her mother painted her lips with mascara.

Nor will I soon forget my subject who had dementia with Lewy bodies and woke every morning in tears. He cried for at least one hour because he was under the delusion his wife was the one who was sick and believed she was dying from cancer.

When I finished scanning this man and brought him to his wife, he kissed her and told her she was the *best* wife.

I saw surprising evidence of love in what others may deem barren soil. One of my subjects diagnosed with dementia with Lewy bodies insisted that when I scanned her I was to find a stroke rather than "those Lewy bodies." She was adamant it was a stroke that had caused her symptoms. I suppose the diagnosis of a stroke would be less frightening than the diagnosis of a degenerative disorder. With a stroke, the worst is behind; with a degenerative disorder, the worst is yet to come. The scan was a fragile process of negotiation. As long as I gave her the choice to stop or continue every seven minutes or so, she bellowed "a little bit longer!" She was motivated to find a stroke, but the scan showed no stroke. This feisty woman had a full-time aid who was my saving grace during the scan. He was a behemoth, black man with tattoos on his neck. It took him several minutes to take off all his jewelry and piercings before going into the scan room (he sat with my subject during the scan and rubbed her feet to keep her calm; I wouldn't have managed without him). He was so kind and patient toward my subject, and she absolutely adored him. At one point, I accidentally got in his way as he was moving her, and she screamed at me, "Don't you give Ricky* a hard time! He knows better than anyone! Don't you pick on him!" I was touched to see a little old lady scream at me in defense of a man like Ricky.

In meeting with my subjects, I realized that at some point in life, most of us will be entirely dependent on the kindness of others.

In the face of tragedy—the tragedy of a pathology that steals away the mind—I saw strife as well: families who could not decide how a subject's treatment should be handled, families who faced off between denial and acceptance, families who bickered about the final cents attached to an individual's last days. I scanned one woman with Alzheimer's who was relatively young although her intracranial space was more fluid than brain. I talked to her daughter during the scan. She lived with her mom and cared for her while also trying to hold a full-time job. The daughter needed to talk, so I listened. She was fighting against her aunt, who staunchly denied her mother had Alzheimer's, and her brother, who disagreed with the decided path of management. Conversations such as that one made me realize how universal are the roots of human suffering, despite unique branches. Much of this daughter's frustration was derived from feeling overwhelmed, wrongfully accused, under-appreciated and misunderstood. The universality of such feelings allows for deep compassion.

Of course, in dealing with dementia, I had my private moments of giggling too. There was one woman with frontal temporal lobe dementia whom I could not approach without caution for she took great delight in lifting up my skirt.

There was the 97-year-old non-demented control subject, who was deaf and mute once his hearing aids and dentures were removed. His wife had died a few months prior, and he had already taken up residence with a younger mistress in her 70s (she was a nurse, which is certainly an attractive trait in golden-age courtship). The mistress had been a neighbor and friend to my patient and his wife for many years. When his wife died, he had asked the mistress to dinner at the Soup Plantation.

She accepted, and then agreed to go home with him that evening to watch a little TV. While the TV was roaring, he disappeared into the bedroom for a while and then came back out with a rather forward request: "Nancy*, I've turned down a side of my bed for you." She said, "Oh, John*, I don't think I'm ready for that" and went home. But all that night, she could only imagine how she would feel watching *other* hussies walk past her house to enter John's. So the next morning, she marched down to his house, and asked, "John? Is the offer still open?" They had been sleeping together ever since. When I delivered this man from the MRI room to his mistress-in-waiting, he fell into her for a lengthy, denture-free make-out session. I can really only describe the sight and sound as what you would expect in observing a fish French kissing.

And then one of my favorite subjects of all, Jacque*: Mexican and Swiss by birth, French by association only. He too was a non-demented control subject. He was 90 years old, lived alone, navigated public transportation (in San Diego, no less!), and was as fiery as they come. I scanned him four times, and he and I were very much on first name, cell phone basis. He called frequently to check on the status of something or another or just to chat. The first time I scanned him, he and I had a number of spats involving the finer points of MRI. During those challenging (but oh so entertaining) 45 minutes, my favorite snippet was this:

Him: I need to take off my pants.
Me: Why do you need to take off your pants?
Him: They have a metal zipper.
Me: That will be fine. The zipper is not magnetic enough to cause a problem in the scanner. We scan people with zippers in their pants all the time.
Him: But my pants have three zippers in them. One in the center and one on each pocket.
Me: Thank you for letting me know, but again, that should be fine. The only slight

possibility is that you might feel a bit of heat in the area. I will check with you frequently to make sure you're comfortable, and if you feel any heat, we can stop the scan.
Him: My pants also have staples in them. Do you scan people with staples in their pants?
Me: Mmmmm. What do you mean staples?
Him: When I get holes in my pants I staple them.
Me: Ok. Again, that should be fine. Just let me know if you start to feel heat.
Him: But I want to take off my pants.
Me: Did you bring another pair of pants or shorts to change into?
Him: No. But I'm wearing underwear. I don't mind if you see me in my underwear.
Me: Alright. Let's just keep your pants on. It should be fine.
Him: You could give me a blanket to cover myself.
Me: No, let's just keep the pants on please.

I must say I was exasperated and also tickled to death when I received a call on my cell phone from an endearing gentleman who introduced himself as Jacque's brother and said he too *ought* to participate in my study. The brothers were quite enraptured to watch one another be scanned. When Jacque emerged from the scanner, Pierre* told him we had found a mouse in his brain. When Pierre emerged from the scanner, Jacque told him that 84 of his 166 slices were perfect matches to Einstein's brain...just not Albert's. Jacque was working on getting his affairs in order so it would be easy for Pierre to take over his estate. First on his list was to remodel the front porch of his house.

Before heading out the door arm-in-arm beneath matching flat caps, Jacque and Pierre sat captivated for nearly an hour as I explained to them about the brain. Jacque took notes (even stopping to verify the spelling of hippocampus) and told Pierre the two of them should go over the notes together later that day.

Another of my favorites was Natalia*, an 84-year-old writer who also participated in my research as a healthy control. Dr. Natalia, to be precise (yes, this

84-year-old woman had her PhD!). I liked Natalia from the start because she said the chirps of the MRI machine sounded like birds. I think it says something about the soul when a person can walk into a cold, sterile medical room filled with the noise of heavy technology and hear birds. I like these sorts of people the best. After her first scan, Natalia and I embarked upon a beautiful friendship in spite of a six-decade age differential. I am always welcomed into her home with a hug, honest discourse and the gift of poetry.

This is why I have loved the data collection aspect of my research the best. These subjects and their caregivers have brought me to tears and to laughter, and most beautifully of all, they have often brought me to my knees in prayer. For even in diseases as awful as dementia, I have seen incredible evidence that God is good.

*Names changed to protect subject confidentiality.

TABLE OF CONTENTS

LIST OF FIGURES

LIST OF TABLES

ACKNOWLEDGMENTS

I would like to acknowledge Dr. James Brewer for his support as my graduate school adviser and as the chair of my dissertation committee. I would also like to acknowledge Kelly Landy, members of the Human Memory Laboratory—Sarah Gimbel, Jena Hales, Tyler Seibert, Reas, Erik Kaestner and Nichol Ferng—the Shiley-Marcos Alzheimer's Disease Research Center, and members of The Brain Observatory for their assistance and friendship.

Chapter 1, in full, is a reprint of the material as it appears in NeuroImage, 2010. Murphy EA; Holland D; Donohue M; McEvoy LK; Hagler Jr. DJ; Dale AM; Brewer JB. The dissertation author was the primary investigator and author of this paper.

Chapter 2, in full, is a reprint of the material as it appears in Brain Imaging and Behavior, 2011. Murphy EA; Roddey JC; McEvoy LK; Holland D; Hagler Jr. DJ; Dale AM; Brewer JB. The dissertation author was the primary investigator and author of this paper.

Chapter 3, in full, is currently being prepared for submission for publication of the material. Murphy EA; Seibert TM; Holland D; Hagler Jr. DJ; Dale AM; Brewer JB. The dissertation author was the primary investigator and author of this paper.

VITA

2007	Bachelor of Arts in Mathematics, University of California, San Diego
2013	Doctor of Philosophy in Neurosciences, University of California, San Diego

PUBLICATIONS

Murphy EA, Seibert TM, Holland D, Hagler Jr. DJ, Dale AM, Brewer JB. Spatial and temporal patterns of change identified in longitudinal study of Lewy body dementia using volumetric and diffusion tensor imaging. (In submission).

Murphy EA, Roddey JC, McEvoy LK, Holland D, Hagler Jr. DJ, Dale AM, Brewer JB; Alzheimer's Disease Neuroimaging Initiative. CETP polymorphisms associate with brain structure, atrophy rate, and Alzheimer's disease risk in an APOE-dependent manner. *Brain Imaging and Behavior* 2012; 6(1):16-26.

Seibert TM, **Murphy EA**, Kaestner EJ, Brewer JB. Interregional correlations in Parkinson disease and Parkinson-related dementia with resting functional MR imaging. *Radiology* 2012; 263(1):226-234.

Murphy EA, Holland D, Donohue M, McEvoy LK, Hagler Jr. DJ, Dale AM, Brewer JB; Alzheimer's Disease Neuroimaging Initiative. Six-month atrophy in MTL structures is associated with subsequent memory decline in elderly controls. *Neuroimage* 2010; 52(4): 1310-1317.

ABSTRACT OF THE DISSERTATION

Quantitative Neuroimaging: Applications to Normal Aging and Neurodegenerative Disease

by

Elizabeth Ann Murphy

Doctor of Philosophy in Neurosciences

University of California, San Diego, 2013

Professor James B. Brewer, Chair

Magnetic resonance imaging (MRI) techniques provide a noninvasive, quantitative means to assess spatial and temporal patterns of change that occur in the brain, both as a function of healthy aging and as a function of neurodegenerative disease. In particular, structural MRI can be used to quantify cortical thickness and subcortical volumes across the brain at sub-millimeter accuracy. By tracking these measurements in an individual across time using longitudinal analysis, it is possible to assess the rate and spatial distribution of gross anatomical change, which is believed to correlate with neuronal loss and shrinkage. Further, diffusion tensor imaging (DTI) allows assessment of the brain at the level of local microstructure and is believed to be

sensitive to changes in white matter integrity. These quantitative neuroimaging techniques have been applied to three distinct studies in this dissertation. In Chapter One, it is shown that neurodegeneration can be quantified in healthy elderly subjects across a time period as short as six months, and this quantification might help identify those at risk for subsequent cognitive decline. In Chapter Two, these imaging techniques are used as quantitative phenotypes in a genetic analysis to show that polymorphisms in the cholesteryl ester transfer protein (CETP) gene associate with and therefore may contribute to the genetic variability of brain structure, atrophy rate and Alzheimer's disease susceptibility. Chapter Three of this dissertation applies these techniques to the study of Lewy body dementia, in which it is found that structural change in the Lewy body dementias appears intermediate between that of Alzheimer's disease and healthy aging, whereas DTI data reveals relatively equivalent severities between Alzheimer's disease and dementia with Lewy bodies. These results suggest that Lewy body dementia may be characterized more prominently by microstructural change rather than neuronal loss.

INTRODUCTION

From the depths of a large, horizontal tube that houses a magnet so strong it could be used to pick up cars, a man grins and exclaims with bravado: “Ready for blast-off!” This man has a neurodegenerative disorder named dementia with Lewy bodies, and we are about to embark upon a fascinating journey through his brain. We will glide over every ridge and valley on its surface and plummet through deep internal structures. As he lies in the magnet untouched, this man’s brain will be reconstructed in fascinating detail on the computer before us.

To understand how magnetic resonance imaging (MRI) works, we must return to the 1970s when scientists discovered that spinning, subatomic particles in the human body called protons tend to align in the presence of a strong magnetic field. Once aligned, the spin of these protons can be manipulated by applying brief pulses of radio wave energy. This phenomenon produces an electromagnetic signal that differs according to tissue density, thereby revealing an image of the body’s internal structure.

Since its discovery, MRI has been a mainstay in diagnostic radiology and particularly useful in examining the soft tissue of the brain. Not only does MRI provide a noninvasive look inside the brain, but it does so without exposing individuals to radioactivity unlike many other imaging methods.

In neurology clinics today, MRI is mostly used to distinguish normal tissue from pathologic tissue, for example, in ruling out the presence of a stroke, tumor or bleed. However, such uses of MRI vastly under-utilize its capabilities. In fact, the resolution of modern MR technology enables the entire brain to be digitally reconstructed within sub-millimeter accuracy. The resulting image can then be analyzed using automated and semi-automated computer software in order to make calculations about the brain's structure and function. These calculations form the basis for what is called quantitative magnetic resonance neuroimaging, a field that shows tremendous promise in the study of aging and neurodegenerative disease.

When a person agrees to spend approximately 30 minutes in an MRI scanner, an enormous wealth of data about his or her brain is collected. A high-resolution, three-dimensional image is constructed to enable measurements across hundreds of regions within the brain, taking particular note of those regions in which neurodegenerative disease first manifests as the loss of brain volume and thickness. An MRI technique called diffusion tensor imaging (DTI) assesses the structural integrity of fiber tracts connecting different regions of the brain.

These measurements can not only be compared to expected values given a person's age, but sophisticated computational methods allow tracking of changes in the same individual with information gathered from follow-up scans.

As research groups across the world embark upon similar journeys through thousands of brains in various stages of healthy and pathological aging, the field has begun to understand the spatial and temporal patterns of changes that occur in

neurodegenerative disease, even before clinical symptoms appear. It is hoped that this research will significantly impact the clinical approach to disease by allowing physicians to identify individuals at risk, detect the disease in its earliest stages, and monitor the success of treatments.

The studies described in this dissertation employ these quantitative MR techniques in three distinct applications: early detection of neurodegeneration among elderly control subjects (Chapter One); assessment of genetic influence at the level of brain structure (Chapter Two); and differential diagnosis of neurodegenerative disease with overlapping clinical presentations (Chapter Three). Two primary MRI techniques are utilized in the exploration of these goals, namely structural MRI and DTI.

Structural MRI

Although structural MRI is perhaps one of the most rudimentary of MR techniques, evidence suggests it is extremely useful in identifying change that occurs in normal aging and in neurodegenerative disease. In particular, a high-resolution, three-dimensional, T1-weighted volume can be used to quantify cortical thickness and subcortical volumes across the entirety of the brain. By tracking these measurements in an individual across time using longitudinal analysis, it is possible to assess the rate and spatial distribution of tissue loss in the individual's brain.

A quantification of this change has been shown to correlate with subsequent cognitive performance and may thus have significant future implications for both the diagnosis and prognosis of neurodegenerative disease. For example, a quantification

of neurodegeneration in patients with mild cognitive impairment (MCI) has been shown to predict progression to Alzheimer's disease (AD) (McEvoy et al, 2009). Further, as suggested by the findings in the first chapter of this dissertation, longitudinal MRI shows promise for identifying rapid atrophy in otherwise healthy subjects. This presents the possibility that quantitative neuroimaging might be used to supplement existing clinical diagnostic techniques to evaluate risk of memory decline. Further, these techniques might be used in clinical trials to assess whether or not a therapeutic agent slows brain atrophy and associated decline in memory. Neuroimaging may even offer an advantage over clinical testing in therapeutic trials by allowing earlier detection of a drug's effect in the prodromal phase, when an effect on atrophy may be demonstrable prior to an effect on cognition.

Additionally, by assessing temporal and spatial patterns of structural brain change, it may be possible to more accurately elucidate the underlying pathology contributing to an individual's dementia. Diagnosis of neurodegenerative dementia is only definitive post-mortem; in the clinical setting, patients are assigned "probable" diagnoses based on the characterization of symptoms, but these diagnoses suffer inaccuracy. In particular, clinical diagnosis of the Lewy body dementias (the second most common form of neurodegenerative dementia after AD) tends to have notoriously low sensitivity (Luis et al, 1999) due to significant heterogeneity in clinical presentation and substantial overlap with the clinical presentations of other neurodegenerative diseases like AD. Chapter Three of this dissertation demonstrates

that quantitative neuroimaging shows promise with regard to Lewy body dementia to enable insight into its biologic basis and to enhance differential diagnosis.

The measurement of cortical thickness and subcortical volumes may further be applied in the field of neuroimaging genetics, in which phenotypes are defined by quantitative measures of brain structure or function rather than clinical characteristics such as disease, symptoms or behavior. By using these quantitative measures of brain structure and function in lieu of complex behaviors or cognitive states, association analyses may provide a more direct assessment of genetic influence at the level of neuronal circuitry (Mattay et al, 2008), thereby rendering these analyses less susceptible to non-genetic variability. For example, as seen in Chapter Two of this dissertation, structural neuroimaging has potential to address whether specific genes may affect brain structure during development or pathological processes.

Diffusion Tensor Imaging

The second quantitative neuroimaging technique applied in this dissertation is DTI, which assesses local microstructure of the brain, and is believed to be sensitive to changes in white matter integrity, fiber density, myelination and axonal diameter (Hagler et al, 2009). As degenerative changes occur, diffusivity of water in the brain increases due to the break-down of structural barriers that restrict Brownian motion, and directionality of diffusion becomes more random and less-defined by white matter tracts. DTI therefore provides information in addition to the gross anatomical findings of structural MRI. Whereas changes in cortical thickness and subcortical volumes

detected by structural MRI are largely believed to represent neuronal loss and shrinkage, DTI is more sensitive to changes at a microstructural level. As demonstrated in Chapter Three of this dissertation, DTI may be particularly useful in the study of neurodegenerative dementias such as the Lewy body dementias, in which neuronal loss is not believed to be a prominent feature.

References

Hagler DJ Jr, Ahmadi ME, Kuperman J, Holland D, McDonald CR, Halgren E, Dale AM. Automated white-matter tractography using a probabilistic diffusion tensor atlas: Application to temporal lobe epilepsy. Hum Brain Mapp 2009;30(5):1535-1547.

Luis CA, Barker WW, Gajaraj K, Harwood D, Petersen R, Kashuba A, et al. Sensitivity and specificity of three clinical criteria for dementia with Lewy bodies in an autopsy-verified sample. Int J Geriatr Psychiatry 1999;14:526-533.

Mattay VS, Goldberg TE, Sambataro F, Weinberger DR. Neurobiology of cognitive aging: insights from imaging genetics. Biological Psychology 2008; 79(1), 9–22.

McEvoy LK, Fennema-Notestine C, Roddey JC, Hagler Jr DJ, Holland D, Karow DS, Pung CJ, Brewer JB, Dale AM, Alzheimer's Disease Neuroimaging Initiative. Alzheimer disease: quantitative structural neuroimaging for detection and prediction of clinical and structural changes in mild cognitive impairment. Radiology 2009; 251 (1), 195–205

CHAPTER 1:

SIX-MONTH ATROPHY IN MTL STRUCTURES IS ASSOCIATED WITH SUBSEQUENT MEMORY DECLINE IN ELDERLY CONTROLS

Abstract

Neurodegeneration precedes the onset of dementias such as Alzheimer's by several years. Recent advances in volumetric imaging allow quantification of subtle neuroanatomical change over time periods as short as six months. This study investigates whether neuroanatomical change in medial temporal lobe subregions is associated with later memory decline in elderly controls. Using high-resolution, T1-weighted magnetic resonance images acquired at baseline and six months follow-up, change in cortical thickness and subcortical volumes was measured in 142 healthy elderly subjects (aged 59 – 90 years) from the ADNI cohort. Regression analysis was used to identify whether change in fourteen subregions, selected *a priori*, was associated with declining performance on memory tests from baseline to two years follow-up. Percent thickness change in the right fusiform and inferior temporal cortices and expansion of the right inferior lateral ventricle were found to be significant predictors of subsequent decline on memory-specific neuropsychological measures. These results demonstrate that six-month regional neurodegeneration can be quantified in the healthy elderly and might help identify those at risk for subsequent cognitive decline.

Introduction

Loss of cognitive function during the transition from health to dementia can be linked to regional damage as pathological processes spread in the brain. Previous research suggests that the neurodegeneration occurring during this pathological spread can be quantified and used to predict further cognitive decline. For example, a quantification of neurodegeneration in patients with mild cognitive impairment (MCI) has been shown to predict progression to Alzheimer's disease (AD) (McEvoy et al., 2009). However, few studies have attempted to quantitatively assess regional neurodegeneration during the preclinical stage, before the onset of memory symptoms, and to see whether it is predictive of which individuals will subsequently undergo cognitive decline at a rate faster than that of normal aging. This has been challenging, in part, because healthy elderly subjects show minimal cognitive decline over the time course of most studies and therefore a large numbers of subjects are needed. By enrolling more than 200 normal controls in a three-year observational study, the Alzheimer's Disease Neuroimaging Initiative (ADNI) has made it possible to measure changes in cortical thickness and subregional brain volumes in the healthy elderly, thus enabling identification of those individuals who are in the earliest stages of neurodegeneration. As disease-modifying interventions become available, early detection of neurodegenerative illness becomes imperative, especially since the preclinical stage may be the period most amenable to disease-modifying therapy.

Longitudinal magnetic resonance imaging (MRI) can be used as a tool to aid early diagnosis of neurodegenerative illness by providing information about the rate of

brain tissue loss, as evidenced by changes in cortical thickness and subcortical volumes. Further, the measurement of subregional change, coupled with knowledge about regional progression of various neurodegenerative diseases, may assist in differential diagnosis. Prior studies using longitudinal MRI for early detection of dementia have obtained measures of change through manual tracing (Jack et al., 1997), automated procedures for global volumetric change such as the boundary shift integral (Ridha et al., 2008), or methods based on statistical parametric mapping, such as voxel-based morphometry (Ashburner et al., 2003). The automated method in this paper uses nonlinear registration between baseline and follow-up scans to calculate volumetric change on a voxel-by-voxel basis. This is combined with image segmentation and cortical surface reconstruction to obtain average structural change in each subregion (Holland et al., 2009). The method is high-throughput and requires little manual input, making it applicable to large research studies and promising for extension to the clinical setting. Further, it has been shown to be sensitive to changes in the healthy elderly over one-year intervals. A recent study using this method in the ADNI elderly control cohort found that all identified subcortical and ventricular regions except the caudate nucleus and fourth ventricle changed significantly over one year (Fjell et al., 2009). It remains unclear whether these structural changes might be detectable over an even shorter time-period, how they relate to cognitive performance, and whether they are a harbinger of later cognitive decline.

The aim of this study was to investigate whether six-month, subregional change in the medial temporal region could be detected in elderly subjects with no diagnosis

of dementia upon entry to the study and if so, whether it is predictive of subsequent cognitive decline on memory-specific tasks. High-resolution, three-dimensional MRI scans were acquired six months apart and analyzed to obtain percentage change across fourteen cortical and subcortical regions. These fourteen regions for which longitudinal volumetric change measures were publicly available for download from the ADNI database on January 1, 2010 were selected for inclusion in a regression analysis. In addition to regional temporal lobe measures, global measures of neurodegeneration were analyzed using change in cerebral and ventricular volumes.

Four memory-specific neuropsychological measures derived from the Logical Memory Test (from the Wechsler Memory Scale-Revised) and the Rey Auditory Verbal Learning Test (AVLT) were chosen as clinically relevant indicators of decline. Two-year changes in scores were used as distinct outcomes in separate regression analyses. Memory-specific tests were chosen as outcome measures because it is well recognized that memory impairment is an early symptom of Alzheimer's disease, and it has been proposed that tests specifically designed to measure memory functioning are sensitive to detecting early AD (Pike and Savage, 2008). Two of the neuropsychological measures were specifically chosen to assess episodic memory since impairment in this realm is considered a hallmark symptom of early AD (Sperling, et al., 2010). Further, performance on these specific tests has been previously associated with neurodegeneration in the medial temporal region (Apostolova et al., 2010).

Based on previous findings, the hypotheses were that six-month neurodegeneration could be detected in healthy elderly subjects, and that this neurodegeneration could be used to predict subsequent deterioration in memory performance as measured by neuropsychological testing.

Methods

Alzheimer's Disease Neuroimaging Initiative

Raw data used in this paper were obtained from the Alzheimer's Disease Neuroimaging Initiative (ADNI) public database (http://www.loni.ucla.edu/ADNI/). ADNI is a multi-site, five-year observational study of elderly individuals started in 2004 by the National Institute on Aging, the National Institute of Biomedical Imaging and Bioengineering, the Food and Drug Administration, private pharmaceutical companies and nonprofit organizations. Elderly controls, subjects with mild cognitive impairment (MCI) and AD subjects underwent longitudinal MRI scans and neuropsychological assessment at specified intervals for two to three years.

The Principal Investigator of this initiative is Michael W. Weiner, M.D. at the VA Medical Center and University of California, San Francisco. ADNI is the result of the efforts of many co-investigators from a broad range of academic institutions and private corporations, and subjects have been recruited from over 50 sites across the U.S. and Canada. For more information, see www.adni-info.org.

Standard protocol approvals, enrolment and patient consents

ADNI was conducted according to Good Clinical Practice guidelines, the Declaration of Helsinki, US 21CFR Part 50—Protection of Human Subjects, and Part 56—Institutional Review Boards, and pursuant to state and federal HIPAA regulations. Written informed consent for the study was obtained from all subjects and/or authorized representatives and study partners (http://www.ADNI-info.org).

Subjects

ADNI eligibility criteria are described at http://adni-info.org/TakingPartInADNI.aspx. In general, all enrolled subjects were between 55 and 90 (inclusive) years of age, had a study partner available to provide an independent evaluation of functioning, and spoke either English or Spanish. Control subjects were cognitively normal, based on an absence of significant impairment in cognitive functions or activities of daily living, and were in good general health with no depression or additional diseases expected to interfere with the study. They had baseline Mini Mental State Examination (MMSE) scores between 24 and 30 (inclusive), global Clinical Dementia Ratings (CDR) of 0, and normal memory function determined by specific cutoffs on the Logical Memory Test (delayed paragraph recall) from the Wechsler Memory Scale-Revised. All control subjects were given the diagnosis of normal at baseline by physicians who were experienced neurologists or psychiatrists. This diagnosis was reviewed by physicians at each

follow-up visit after 6 months, 12 months and 24 months to determine whether there was conversion to MCI or AD.

In this study, data were included on all ADNI control subjects for whom the following criteria were satisfied by December 2009: baseline and six-month MR imaging data were available and passed a quality control review (described in Holland et al., 2009), and baseline and 24-month neuropsychological data were available. Of the 229 ADNI control subjects, 142 were included and 87 were excluded. Demographics of the included subjects are described in Table 1. The differences between included and excluded subjects for mean age (75.88 vs 76.49 years, respectively), percent female subjects (.47 vs .49), mean education level (16.10 vs 15.94), percent carriers of the *APOE* ε4 allele (.28 vs .24), and mean MMSE at baseline (29.22 vs. 28.94) did not meet statistical significance at the $\alpha = 0.05$ level. However, the included subjects had significantly higher global cognition at baseline on mean Alzheimer's Disease Assessment Scale-Cognitive (ADAS-cog) (5.89 vs. 6.69, $p = 0.046$).

Neuropsychological assessment

Two memory-specific neuropsychological tests administered at baseline and 24 months were used to determine cognitive decline: Logical Memory Test (Delayed Paragraph Recall) from the Wechsler Memory Scale-Revised and Rey Auditory Verbal Learning Test (AVLT). In the Logical Memory (LM) Test, which assesses episodic memory, subjects were read aloud a short story containing 25 units of

Table 1.1: Subject baseline characteristics.

	All (n=142) [a,c]	**Conv. (n=7)** [b,c]
Age (years)	75.88 ± 4.86	74.81 ± 5.82
Percent female subjects	47 %	29 %
Education (years)	16.12 ± 2.73	16.57 ± 1.81
Percent carriers of *APOE* ε4	28 %*	71 %*
Baseline MMSE	29.22 ± .92	28.57 ± .79
Baseline ADAS-cog	5.89 ± 2.85*	9.19 ± 3.26*

[a] Contains information about all 142 subjects whose data was included in the analysis. [b] Contains information about only those 7 subjects who converted to a diagnosis of mild cognitive impairment (MCI) during the two-year follow-up. [c] Data are given as mean ± SD unless otherwise specified as a percent. * The subjects who converted to MCI had a significantly higher frequency of the *APOE* ε4 allele and significantly more impaired ADAS-cog scores at baseline ($p<0.05$).

information. The total number of units (maximum score = 25) recalled immediately and after a 30-minute delay were recorded. Retention of the information was computed by dividing the delayed recall score by the immediate recall score. Two-year change in both the delayed recall score and the retention score were calculated as absolute change between baseline and 24 months, where cognitive decline was defined as a positive value.

The AVLT assesses multiple aspects of learning and memory. Subjects participated in five learning trials in which they were presented orally with the same 15 unrelated nouns at the rate of one word per second. The number of words freely recalled immediately after each trial was recorded for each of the 5 trials. After the first five trials, a second list of words was read, and the subjects were asked to freely recall as many words as possible immediately afterward (trial B). After a 20-minute delay, free recall of the original 15 words was elicited again (trial 6). Additionally, a yes/no recognition test containing the 15 original words interspersed with 15 new words was administered, and the numbers of true and false positive responses were recorded (delayed recognition). Two-year change in both the sum across all trials 1 through 6 plus B (maximum score = 105) and the delayed recognition score (maximum score = 15) were calculated as absolute change between baseline and 24 months, where cognitive decline was defined as a positive value.

MR acquisition and analysis

Two three-dimensional, T1-weighted volumes per subject per visit were downloaded from the public ADNI database (http://www.loni.ucla.edu/ADNI/). All image processing and analyses occurred at the Multimodal Imaging Laboratory at the University of California, San Diego. The methods are described in detail in Holland et al., 2009. Briefly, images were corrected for gradient nonlinearities (Jovicich et al., 2006). The two baseline images were rigid-body aligned, averaged to improve signal-to-noise ratio and resampled to isotropic 1-mm voxels. An automated segmentation procedure based on FeeSurfer software (Fischl, et al., 2002) and customized Matlab code was used to obtain volumetric segmentation. Cortical surface reconstruction yielded a measure of thickness at each vertex, and the surface was parceled into distinct regions of interest (ROIs). To obtain six-month change, follow-up images were fully affine-registered to the baseline images and corrected for intensity nonuniformity. Nonlinear registration was then used to align voxel centers in the baseline with the appropriate location in the follow-up scans, and a volume-change field was calculated. This field was averaged over each ROI to compute the percentage change from baseline. This method has been validated using models where amount of change was known and where noise was added to approximate that seen in human brain imaging of demented patients. In these studies, technical measurement error for the computed change in volume was within 0.2 percent of the structure volume. That is, for a 6000 mm^3 hippocampal volume undergoing a change of 1 percent, the technical measurement error in estimating the 60 mm^3 volumetric change

would be ±12 mm^3 in an individual subject if voxels were each 1mm isotropic (Holland, submitted).

Statistical analysis

All statistical analysis was performed using SPSS 15.0. To determine whether the population of subjects included in this study were representative of all ADNI control subjects, independent samples t-tests were used to compare age, sex, education, *APOE* ε4 carrier status, and baseline cognition (MMSE and ADAS-cog) with a significance level of $\alpha = 0.05$.

To investigate whether six-month change in subregional brain volumes predicts two-year cognitive decline, regression analysis was used. Four different neuropsychological measures were treated as distinct dependent variables, and a separate regression analysis was done for each. The four outcome measures include two-year change in scores on LM delayed recall, LM retention, AVLT sum and AVLT delayed recognition. Six-month change in the whole brain, ventricles and twelve subregions of interest were selected to be independent variables in the regression analyses because these were the regions for which longitudinal data was available in the public ADNI database. The regions of interest included bilateral hippocampus, inferior lateral ventricle, middle temporal gyrus, inferior temporal gyrus, entorhinal cortex and fusiform gyrus. Risk factors for AD including age, sex, education and *APOE* ε4 carrier status were also included in the regression analysis as independent variables.

Univariate analyses were first conducted to determine which independent variables should be included in a stepwise multivariate regression. All variables that met significance at $p < .10$ in the univariate analyses were entered into the multivariate model. Residual analysis was conducted to evaluate the validity of regression assumptions. Additionally, independent variables that met significance ($p < .01$) in the multivariate model were tested for multicollinearity and undue influence. If a subject was found to have undue influence on the regression model, the subject's data was examined for abnormalities, the analysis was repeated after excluding the subjects with undue influence, and both results were reported.

To determine whether six-month neuroanatomical change provides additional predictive information beyond that which is obtained by assessing six-month change in cognition, the regression analysis was repeated using baseline ADAS-cog scores and six-month change in ADAS-cog, MMSE, AVLT sum and AVLT delayed recognition as independent variables. Six-month change in LM delayed recall and retention were not included because these measures were not assessed in the ADNI dataset at six months. Because six-month change on AVLT sum and AVLT delayed recognition are encompassed within two-year change on these same measures and are therefore not independent variables, the dependent variable in these analyses was change between the six-month and two-year visits rather than between the baseline and two-year visits.

A secondary set of regression analyses was also performed to identify how the multivariate models change when data from the seven subjects who converted to MCI

over the course of two years is weighted twice as heavily as data from subjects who retained a diagnosis of normal. After assigning a weight of 2/149 (0.013423) to all data from subjects who converted to MCI and a weight of 1/149 (0.006711) to all other subjects, the regression procedures detailed above were repeated.

Composite neuroanatomical change scores were calculated for each subject by converting each subject's change within the regional temporal lobe ROIs to standardized z-scores and then averaging the scores across these ROIs. Similarly, composite cognitive change scores were calculated for each subject by converting each subject's change on the neuropsychological measures to standardized z-scores and then averaging these scores across the four outcome measures.

Results

Of the 142 healthy elderly subjects included in this study, there were 67 females and 75 males, the mean age was 75 years (range 59 to 90), the mean education 16 years (range 6 to 20), and 40 were carriers of the *APOE* ε4 allele. The mean MMSE at baseline was 29.22 (range 25 to 30) and the mean ADAS-cog at baseline was 5.89 (range 1 to 16.33).

On three of the four memory-specific neuropsychological assessments, subjects showed a slight mean improvement with repeat testing over the course of two years. The two-year mean change on LM delayed recall (maximum score 25) was an improvement of 0.64 points (range 10-point decline to 9-point improvement), the mean change on LM retention (maximum score 1) was a decline of 0.05 points (range

0.93-point decline to 0.43-point improvement), the mean change on AVLT sum (maximum score 105) was an improvement of 1.20 points (range 42-point decline to 30-point improvement), and the mean change on AVLT delayed recognition (maximum score 15) was an improvement of 0.09 points (range 11-point decline to 10-point improvement).

There was significant evidence of medial temporal atrophy over a six-month period (Fig. 1). Although not all subjects had measurable atrophy, there was a mean loss of subcortical volume and cortical thickness in all regions of interest, with the exception of the inferior lateral ventricles, which expanded. There were mean decreases in the volumes of the left and right hippocampus (-1.02 and -0.98 %, respectively) and mean decreases in the thicknesses of the left and right middle temporal gyri (both -0.64%), left and right inferior temporal gyri (-0.55 and -0.65%), left and right entorhinal cortices (-0.45 and -0.43 %), and left and right fusiform gyri (-0.55 and -0.50 %, respectively). There were mean expansions in the volumes of the left and right inferior lateral ventricles (1.74 and 1.90 %, respectively). Additionally, there was a mean loss of volume in the whole brain (-0.31%) and a mean gain in volume in all ventricles (1.73%).

Univariate regression analysis revealed that six-month neurodegenerative change in several medial temporal regions significantly predicted two-year cognitive decline at a significance level $\alpha < .01$ (Table 2). The multivariate regression models designated three of these regions as the best predictors of cognitive decline when compared to other risk factors such as age, education and *APOE* ε4 carrier status. A

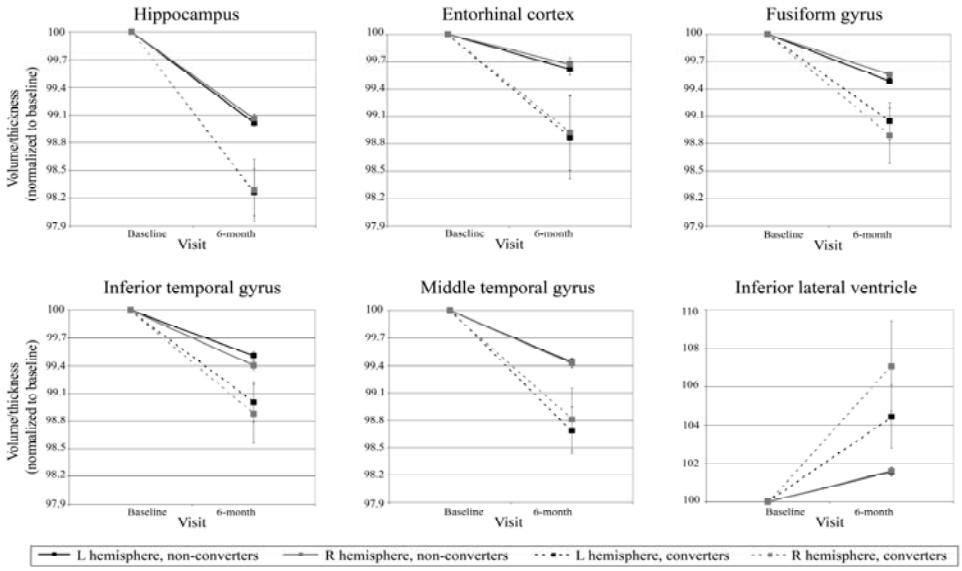

Figure 1.1: Neuroanatomical change between baseline and 6-month follow-up visits across medial temporal lobe (MTL) regions. All volumes were normalized to baseline. Data points represent mean volumes for all subjects who retained a diagnosis of cognitively normal over the two-year follow-up (solid lines, n=135) and for those subjects who converted to mild cognitive impairment (MCI) during the follow-up (dashed lines, n=7). Error bars represent standard error of the mean. A mean loss in volume was seen in all medial temporal lobe regions, with the exception of the inferior lateral ventricle, in which there was mean expansion.

Table 1.2: Variables of significance in univariate and multivariate regression models

	Univariate [b] t ($p < 0.1$)	Multivariate [a,b] t ($p < 0.01$)
Outcome: Logical Memory Delayed Recall		
Right fusiform	**-3.190 (.002)**	**-3.453 (.001)**
Left hippocampus	**-2.954 (.004)**	
Right inferior lateral ventricle	**2.791 (.006)**	
Right inferior temporal gyrus	-2.490 (.014)	
Total cerebral	-2.461 (.015)	
Right hippocampus	-2.172 (.032)	
Left fusiform	-2.058 (.041)	
Right entorhinal cortex	-2.007 (.047)	
Left inferior lateral ventricle	1.742 (.084)	
Outcome: Logical Memory Retention		
Right inferior lateral ventricle	**3.066 (.003)**	**3.105 (.002)**
Left hippocampus	-2.536 (.012)	
Left inferior lateral ventricle	2.424 (.017)	
Right fusiform	-1.918 (.057)	
All ventricles	1.876 (.063)	
Outcome: AVLT Sum		
Right inferior temporal gyrus	**-2.935 (.004)**	**-2.935 (.004)**
Left entorhinal cortex	-2.605 (.010)	
Left hippocampus	-2.244 (.026)	
Education	-2.160 (.033)	
Right entorhinal cortex	-1.851 (.066)	
Outcome: AVLT Delayed Recognition		
Total cerebral	**-2.765 (.006)**	**-2.639 (.009)**
Right fusiform	**-2.732 (.007)**	
Right inferior temporal	-2.113 (.036)	
APOE	2.043 (.043)	
Age	2.020 (.045)	
Education	-1.827 (.070)	
Left hippocampus	-1.687 (.094)	
Left entorhinal cortex	-1.673 (.097)	

[a] All variables that met significance at $p < 0.1$ in the univariate analysis were included in the multivariate model. [b] Data is reported as t-value (p-value).Variables that met significance at $p < 0.01$ are highlighted in bold for both the univariate and multivariate analyses.

decrease in the thickness of the right fusiform gyrus predicted decline on LM delayed recall ($p = .001$), with a 1% decrease in thickness corresponding to a 1.22 ± 0.35 point decline. Expansion of the right inferior lateral ventricle was a significant predictor of decline on LM retention ($p = .002$), with an expansion of 10% corresponding to a decline in the retention ratio by 0.09 ± 0.03. A decrease of thickness in the right inferior temporal gyrus predicted decline on AVLT sum ($p = .004$), with a 1% decrease in thickness corresponding to a $2.57 \pm .43$ point decline. Additionally, a decrease in whole brain volume predicted decline on AVLT delayed recognition ($p=.009$) with a 1% decrease in volume corresponding to a $1.39 \pm .53$ point decline. Age, sex, education and *APOE* ε4 carrier status were not significant predictors of cognitive decline.

When baseline ADAS-cog scores and six-month change in ADAS-cog, and MMSE scores were entered into the regression model as independent variables, they failed to be significant predictors of two-year cognitive decline and the regression models did not change. Six-month change on AVLT sum did predict change on AVLT sum over the subsequent eighteen months ($p=.000$), and six-month change on AVLT delayed recognition predicted change on AVLT delayed recognition over the subsequent eighteen months ($p=.000$). In addition, six-month change on AVLT sum predicted two-year change on LM delayed recall ($p=.007$).

Data from two subjects who converted to MCI during the two-year follow-up period were found to exert undue influence in the regression models for LM delayed recall and LM retention. When these subjects were removed from the regression

analyses, neither the right fusiform nor the right inferior lateral ventricle were significant predictors at $p < .01$, although the right fusiform remained significant at $p < .05$. Change in the right fusiform predicted decline on LM delayed recall ($p = .016$), with a 1% decrease in thickness corresponding to a 0.92 ± 0.38 point decline. Additionally, change in the left hippocampus became significant ($p = .012$) with a 1% decrease in thickness corresponding to a decline in the retention ratio by $0.39 \pm .15$.

During the two-year follow-up period, a total of seven subjects converted to MCI. The subjects who converted were not significantly different at baseline in age, education or MMSE than those who retained a normal diagnosis. However, the converters had a significantly higher frequency of the *APOE* ε4 allele (0.71 vs 0.26, $p = .049$) and significantly more impaired ADAS-cog scores at baseline (mean 9.19 vs. 5.72, $p = .030$).

In a secondary regression analysis, data from the seven subjects who converted to MCI, including the two subjects mentioned above who exerted undue influence in the regression models, were weighted twice as heavily as data from all other subjects in order to create a prediction model biased toward identifying changes in the brain that predict conversion to MCI (Table 3). Change in the right fusiform became a more significant predictor ($p < .001$) of decline on LM delayed recall, with a 1% decrease in thickness corresponding to a $1.46 \pm .33$ point decline. Additionally, change in the right fusiform became a significant predictor ($p = .005$) of AVLT delayed recognition, with a 1% decrease in volume corresponding to a $.83 \pm .29$ point decline. Expansion of the right inferior lateral ventricle also became a more significant predictor ($p < .001$) of

Table 1.3: Variables of significance in regression analysis after weighting data from subjects who converted to MCI [a]

	Univariate [c] t ($p < 0.1$)	Multivariate [b,c] t ($p < 0.01$)
Outcome: Logical Memory Delayed Recall		
Right fusiform	**-4.118 (p < .000)**	**-4.371 (p < .000)**
Right inferior lateral ventricle	**4.013 (p < .000)**	
Left hippocampus	**-3.708 (p < .000)**	
Right inferior temporal gyrus	**-3.215 (.002)**	
Total cerebral	**-3.150 (.002)**	
Right hippocampus	**-3.048 (.003)**	
Left fusiform	**-2.750 (.007)**	
Left inferior lateral ventricle	**2.643 (.009)**	
Right entorhinal cortex	-2.625 (.010)	
Right middle temporal gyrus	-2.424 (.017)	
All ventricles	2.399 (.018)	
Left inferior temporal gyrus	-1.925 (.056)	
Age	1.906 (.059)	
Outcome: Logical Memory Retention		
Right inferior lateral ventricle	**3.547 (.001)**	**3.577 (p < .000)**
Left hippocampus	**-2.889 (.004)**	
Left inferior lateral ventricle	**2.704 (.008)**	
Right fusiform	-2.519 (.013)	
All ventricles	2.444 (.016)	
Total cerebral	-1.995 (.048)	
Right hippocampus	-1.868 (.064)	
Left fusiform	-1.813 (.072)	
Right middle temporal gyrus	-1.681 (.095)	

[a] Subjects who converted to a diagnosis of mild cognitive impairment (MCI) during the two-year follow-up were weighted twice as heavily as all other subjects in this regression analysis. [b]All variables that met significance at $p < 0.1$ in the univariate analysis were included in the multivariate model. [c] Data is reported as t-value (p-value).Variables that met significance at $p < 0.01$ are highlighted in bold for both the univariate and multivariate analyses.

Table 1.3, Continued: Variables of significance in regression analysis after weighting data from subjects who converted to MCI [a]

	Univariate [c] t ($p < 0.1$)	Multivariate [b,c] t ($p < 0.01$)
Outcome: AVLT Sum		
Right inferior temporal gyrus	**-3.034 (.003)**	
Left entorhinal cortex	**-2.922 (.004)**	
Left hippocampus	-2.531 (.013)	
Right entorhinal cortex	-2.086 (.039)	
Education	-2.042 (.043)	
Right hippocampus	-1.989 (.049)	
Right middle temporal gyrus	-1.827 (.070)	
Right fusiform	-1.779 (.077)	
Outcome: AVLT Delayed Recognition		
Right fusiform	**-3.133 (.002)**	**-2.841 (.005)**
Total cerebral	**-3.005 (.003)**	
APOE	**2.741 (.007)**	
Right inferior lateral ventricle	2.331(.021)	
Right inferior temporal gyrus	-2.323 (.022)	
Age	2.097 (.038)	
Left hippocampus	-2.079 (.039)	
Left entorhinal cortex	-2.066 (.041)	
Left fusiform	-1.981 (.050)	
Left inferior lateral ventricle	1.777 (.078)	
Right entorhinal cortex	-1.697 (.092)	

[a] Subjects who converted to a diagnosis of mild cognitive impairment (MCI) during the two-year follow-up were weighted twice as heavily as all other subjects in this regression analysis. [b]All variables that met significance at $p < 0.1$ in the univariate analysis were included in the multivariate model. [c] Data is reported as t-value (p-value).Variables that met significance at $p < 0.01$ are highlighted in bold for both the univariate and multivariate analyses.

decline on LM retention, with a 10% increase corresponding to a decline in the ratio by 0.10 ± 0.03. No regions remained significant predictors of decline on AVLT sum at the $\alpha = .01$ level, but there was a trend toward change in the left entorhinal cortex predicting decline on AVLT sum ($p = .017$), with a 1% decrease in thickness corresponding to a 1.34 ± .55 point decline.

Among the nine subjects with the greatest composite neuroanatomical change (defined as being greater than one standard deviation relative to our sample), two converted to a diagnosis of MCI, and five had cognitive change greater than the mean for the group. In no case did a subject above the 93rd percentile for composite neuroanatomical change fail to have greater than average decline on the composite memory measure. Further, in no case did a subject below the 32nd percentile for composite neuroanatomical change convert to a diagnosis of MCI.

Discussion

This study provides evidence that loss of cortical thickness and subcortical volume can not only be detected and quantified over a six-month period in healthy elderly subjects, but can also be used to predict subsequent cognitive decline. Specifically, six-month neurodegeneration in certain medial temporal regions, including the right fusiform gyrus, right inferior lateral ventricle and right inferior temporal gyrus, predicted two-year decline on memory-specific neuropsychological measures in ADNI normal controls. These results suggest that longitudinal MRI may provide an early biomarker for cognitive decline in healthy elderly subjects. Further,

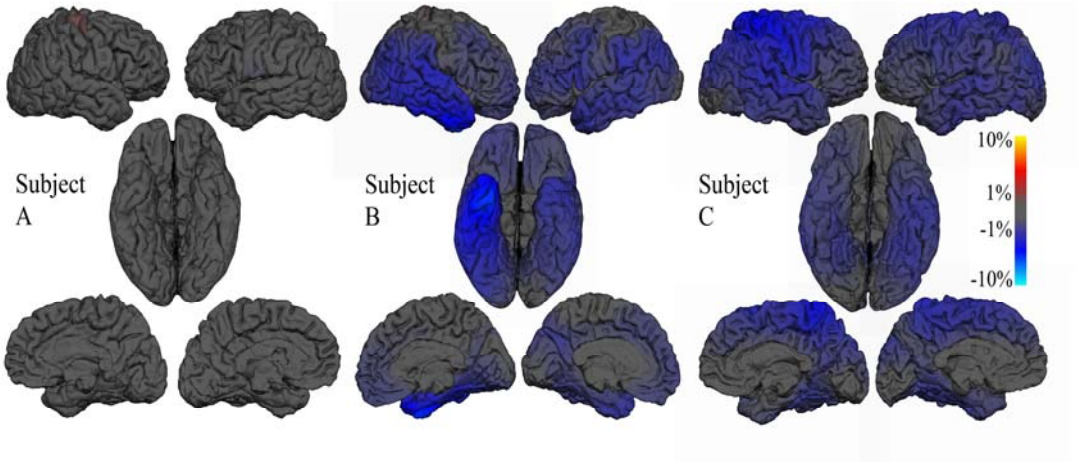

Figure 1.2: Six-month neuroanatomical change overlaid on baseline brain images for three sample subjects using a heat-scale color mapping where blue represents shrinkage and red represents expansion. Subject A was a 77 year-old female who retained a diagnosis of cognitively normal throughout the two-year follow-up period. Subject B was a 77 year-old female who converted to a diagnosis of mild cognitive impairment (MCI) at the six-month follow-up. Subject C was a 79 year-old male who converted to a diagnosis of MCI at the 24-month follow-up.

the predictive information gained by longitudinal MRI cannot be obtained by assessing six-month change in global cognitive scores such as ADAS-cog or MMSE. It is less obvious that the usefulness of six-month MRI data in predicting subsequent decline on memory-specific measures exceeds that of six-month scores on these same memory-specific tests. Six-month change on AVLT sum and AVLT delayed recognition were found to be significant predictors of change on these same tests over the subsequent eighteen months. However, they did not predict change on one another and only AVLT sum predicted two-year change on LM delayed recall. At a minimum, the information provided by six-month imaging data enhances information gained by extensive neuropsychological testing. Further, imaging measures have certain advantages over neuropsychological tests in that they are not influenced by volition or attention.

This study is the first to detect and quantify six-month change across multiple medial temporal regions in healthy elderly subjects and to relate these changes to later cognitive decline with a relatively short follow-up. Prior studies have examined a limited number of structures using volumes obtained through manual tracing (Jack et al., 1997) or qualitative ratings (Scheltens et al., 1992). The current procedure is high-throughput and requires little manual input, thus making it applicable to the clinical setting or large research studies.

Other studies examining neurodegeneration in healthy elderly subjects have focused on either baseline volumes or change over longer time periods, at least one year in duration. It is likely that additional information is gained by including baseline

volumes in a predictive model (Adak et al, 2004), but the purpose of this study was to specifically examine change over a six-month period. Baseline volumes can be interpreted as the sum of all changes occurring prior to the six-month period of interest. These results show that regardless of baseline volumes, a six-month follow-up is sufficient to identify neurodegenerative changes. Because six months is the shortest follow-up period in the ADNI dataset, it remains to be seen whether neurodegenerative changes could be detected in even shorter time periods, such as three months. Further studies are needed to compare the quality of predictive information gained by assessing change over different time periods.

It is unclear whether the neurodegeneration detected in this study is entirely explained by general aging or whether early pathological processes occurring in some subjects drive the prediction models. It is well established that there is a gradual loss of brain volume with normal aging (Scahill et al., 2003), and there is not sufficient follow-up in the ADNI dataset to determine if these subjects will go on to develop AD. However, the pattern of neurodegeneration seen in the subjects whose subregional brain volumes change the most in six months is consistent with what is known about the regional progression of pathology in AD, which starts in medial temporal lobe structures and spreads laterally through the neocortex (Braak and Braak, 1991). Although prior studies have focused on early changes in the hippocampus and entorhinal cortex as being predictive of AD (Devanand, et al. 2007; Hampel, et al., 2008), the fusiform gyrus, inferior lateral ventricles and inferior temporal gyrus lie along the known path of pathological progression and would be expected to change in

disease as well. Further, the findings of this study are consistent with prior studies in MCI and AD that have found significant volume changes in the fusiform gyrus (Holland et al., 2009; McDonald, 2009), inferior temporal gyrus (Holland et al., 2009; McDonald, 2009) and inferior lateral ventricles (Kovacevic et al., 2009). Thus, it is reasonable that these three regions were the best predictors of cognitive decline in the regression models.

Additionally, there is information about the seven subjects who did convert to a diagnosis of MCI over the two-year follow-up. Although not enough subjects converted to MCI to provide sufficient statistical power, a qualitative analysis of their imaging data reveals that the six-month change seen in their brains is highly consistent with what is expected in the early forms of AD (Fig. 2). These seven subjects, in whom a clinically relevant change was noted, are clearly of particular interest. The secondary regression analysis was used to examine how the regression models would change when their data was weighted more heavily, thus influencing the regression models toward the specific changes that occurred in subjects known to be converters. In doing so, subregional change in the fusiform gyrus and inferior lateral ventricle became stronger predictors of cognitive decline. Again, these regions are consistent with the known path of pathologic progression in AD, and it is therefore likely that accelerated change in these regions suggests pathology rather than general aging although longer follow-up and pathological confirmation would be required to confirm this.

When further examining the seven subjects who converted to MCI, it appears that *APOE* genotype is meaningful. Five of the seven converters were carriers of the *APOE* ε4 allele, compared to 35 carriers of the allele among the 135 subjects who did not convert to MCI. This suggests that *APOE* genotype may assist in knowing whether neurodegenerative change detected by quantitative neuroimaging is clinically relevant and likely to result in a change in diagnosis from normal cognition to MCI.

Although the pattern of atrophy observed in some subjects in this study is consistent with expected changes in AD, the hemispheric asymmetry is unexpected. Namely, these results suggest that atrophy in right hemisphere regions is more strongly predictive of later cognitive decline than is atrophy in the left hemisphere. Many prior studies have reported greater involvement of the left hemisphere than the right hemisphere in AD (Karas et al., 2003; Baron et al., 2001) and MCI (Seo et al., 2007) although one study found greater atrophy in the right medial temporal region than in the left in MCI (Karas et al., 2004), and another study using the ADNI dataset reported greater thinning in the right hippocampal and entorhinal cortices in patients with MCI (Fennema-Notestine et al., 2009). It is important to note that the results of this study do not suggest that greater atrophy occurs in right hemispheric regions. In fact, mean percent changes in volume were not statistically different between the right and left hemispheres for any regions examined. However, the results do suggest that right hemispheric atrophy is more predictive of later cognitive decline. It is unclear why such a laterality exists, and this is an issue that merits further study.

Finally, despite the potential for future application of these procedures in the clinical setting, it should be mentioned that such use would require additional investigation into their power to detect such subtle changes in the individual subject, as well as overcoming a host of other practical issues that have impeded the translation of volumetry into the clinical setting (Brewer et al, 2009). Further, the ADNI dataset does not accurately represent the population at large, which limits generalizability of the findings. In particular, the normal subjects included in this study had a high average level of education (16.12 years) compared to the general population. This warrants further research because other investigators have found that low education levels are associated with an increased risk of dementia (Chen et al., 2009). Thus, one might expect more neurodegeneration and cognitive decline in a sample more representative of the general population.

The present findings suggest that longitudinal MRI shows promise for identifying rapid atrophy in otherwise healthy subjects. It is too early to tell whether the atrophy identified in this population represents significant disease that should be targeted for therapy, especially since histological underpinnings might vary. Nevertheless, the results suggest that such MR neuroimaging techniques might be used to supplement existing research and diagnostic techniques to evaluate risk of memory decline. For example, this subregional approach using longitudinal MRI may supplement measures of global atrophy currently used in clinical trials to assess whether or not a therapeutic agent slows brain atrophy and associated decline in memory. Neuroimaging may even offer an advantage over cognitive testing in clinical

trials targeting the earliest disease stages by allowing earlier detection of a drug's effect in the prodromal phase, when an effect on atrophy would appear to be demonstrable prior to an effect on cognition. Thus, these techniques may have significant future implications for both diagnosis and prognosis, even among the healthy elderly.

Acknowledgments

Chapter 1, in full, is a reprint of the material as it appears in NeuroImage, 2010. Murphy EA; Holland D; Donohue M; McEvoy LK; Hagler Jr. DJ; Dale AM; Brewer JB. The dissertation author was the primary investigator and author of this paper.

Data collection and sharing for this project was funded by the Alzheimer's Disease Neuroimaging Initiative (ADNI) (National Institutes of Health Grant U01 AG024904). ADNI is funded by the National Institute on Aging, the National Institute of Biomedical Imaging and Bioengineering, and through generous contributions from the following: Abbott, AstraZeneca AB, Bayer Schering Pharma AG, Bristol-Myers Squibb, Eisai Global Clinical Development, Elan Corporation, Genentech, GE Healthcare, GlaxoSmithKline, Innogenetics, Johnson and Johnson, Eli Lilly and Co., Medpace, Inc., Merck and Co., Inc., Novartis AG, Pfizer Inc, F. Hoffman-La Roche, Schering-Plough, Synarc, Inc., and Wyeth, as well as non-profit partners the Alzheimer's Association and Alzheimer's Drug Discovery Foundation, with participation from the U.S. Food and Drug Administration. Private sector

contributions to ADNI are facilitated by the Foundation for the National Institutes of Health (www.fnih.org). The grantee organization is the Northern California Institute for Research and Education, and the study is coordinated by the Alzheimer's Disease Cooperative Study at the University of California, San Diego. ADNI data are disseminated by the Laboratory for Neuro Imaging at the University of California, Los Angeles. This research was also supported by NIH grants P30 AG010129, K01 AG030514, and the Dana Foundation.

J.B.B. is supported by NINDS K23NS050305; E.A.M. is supported in part by NIGMS Training Grant GM007198.

A.M.D. receives funding to his laboratory from General Electric Medical Systems as part of a Master Research Agreement with UCSD; and is a founder of, holds equity in, and serves on the scientific advisory board for CorTechs Labs, Inc. The terms of this arrangement have been reviewed and approved by UCSD in accordance with its conflict of interest policy.

References

Adak, S., Illouz, K., Gorman, W., Tandon, R., Zimmerman, E.A., Guariglia, R., Moore, M.M., Kaye, J.A., 2004. Predicting the rate of cognitive decline in aging and early Alzheimer disease. Neurology 63(1), 108-14.

Apostolova, L.G., Morra, J.H., Green, A.E., Hwang, K.S., Avedissian, C., Woo, E., Cummings, J.L., Toga A.W., Jack C.R., Jr., Weiner, M.W., Thompson, P.M., Alzheimer's Disease Neuroimaging Initiative, 2010. Automated 3D mapping of baseline and 12-month associations between three verbal memory measures and hippocampal atrophy in 490 ADNI subjects. Neuroimage. 51(1): 488-99.

Ashburner, J., Csernansky, J.G., Davatzikos, C., Fox, N.C., Frisoni, G.B., Thompson, P.M., 2003. Computer-assisted imaging to assess brain structure in healthy and diseased brains. Lancet Neurol 2(2), 79-88.

Baron, J.C., Chetelat, G., Desgranges, B., Perchey, G., Landeau, B., de la Sayette, V., Eustache, F., 2001. In vivo mapping of gray matter loss with voxel-based morphometry in mild Alzheimer's disease. Neuroimage 14(2), 298-309.

Braak, H., and Braak E., 1991. Neuropathological staging of Alzheimer-related changes. Acta Neuropathol, 82, 239-259.

Brewer, J.B., 2009. Fully-automated volumetric MRI with normative ranges: translation to clinical practice. Behav Neurol. 21(1): 21-8.

Chen, J.H., Lin, K.P., Chen, Y.C., 2009. Risk factors for dementia. J Formos Med Assoc. 108(10): 754-64.

Devanand, D.P., Pradhaban, G., Liu, X., Khandji, A., De Santi, S., Segal, S., Rusinek, H., Pelton, G.H., Honig, L.S., Mayeux, R., Stern, Y., Tabert, M.H., de Leon, M.J., 2007. Hippocampal and entorhinal atrophy in mild cognitive impairment: prediction of Alzheimer disease. Neurology 68(11): 828-36.

Fennema-Notestine, C., Hagler, D.J. Jr., McEvoy, L.K., Fleisher, A.S., Wu, E.H., Karow, D.S., Dale, A.M., Alzheimer's Disease Neuroimaging Initiative, 2009. Structural MRI biomarkers for preclinical and mild Alzheimer's disease. Hum Brain Mapp. 30(10): 3238-53.

Fischl, B., Salat, D.H., Busa, E., Albert, M., Dieterich, M., Haselgrove, C., van der Kouwe, A., Killiany, R., Kennedy, D., Klaveness, S., Montillo, A., Makris, N., Rosen, B., Dale, A.M., 2002. Whole brain segmentation: automated labeling of neuroanatomical structures in the human brain. Neuron 33(3): 341-55.

Fjell, A.M., Walhovd, K.B., Fennema-Notestine, C., McEvoy, L.K., Hagler, D.J., Holland, D., Brewer, J.B., Dale, A.M., 2009. One-year brain atrophy evident in healthy aging. J. Neurosci. 29(48),15223-15231.

Hampel, H., Burger, K., Teipel, S.J., Bokde, A.L., Zetterberg, H., Blennow, K., 2008. Core candidate neurochemical and imaging biomarkers of Alzheimer's disease. Alzheimers Dement. 4(1): 38-48.

Holland, D., Brewer, J.B., Hagler, D.J., Fennema-Notestine, C., Dale, A.M., and the Alzheimer's Disease Neuroimaging Initiative, 2009. Subregional neuroanatomical change as a biomarker for Alzheimer's disease. Proc Natl Acad Sci USA 106(49), 20954-20959.

Jack, Jr, C.R., Petersen, R.C., Xu, Y.C., Waring, S.C., O'Brien, P.C., Tangalos, E.G., Smith, G.E., Ivnik, R.J., Kokmen, E., 1997. Medial temporal atrophy on MRI in normal aging and very mild Alzheimer's disease. Neurology 49(3), 786-794.

Jovicich, J., Czanner, S., Greve, D., Haley, E., van der Kouwe, A., Gollub, R., Kennedy, D., Schmitt, F., Brown, G., Macfall, J., Fischl, B., Dale, A., 2006. Reliability in multi-site structural MRI studies: effects of gradient non-linearity correction on phantom and human data. Neuroimage 30(2), 436-43.

Karas, G.B., Scheltens, P., Rombouts, S.A.R.B., Visser, P.J., van Schijndel, R.A., Fox, N.C., Barkhof, F., 2004. Global and local gray matter loss in mild cognitive impairment and Alzheimer's disease. Neuroimage 23(2), 708-716.

Karas, G.B., Burton, E.J., Roumbouts, S.A., van Schijndel, R.A., O'Brien, J.T., Scheltens, P., McKeith, I.G., Williams, D., Ballard, C., Barkhof, F., 2003. A comprehensive study of gray matter loss in patients with Alzheimer's disease using optimized voxel-based morphometry. Neuroimage 18(4), 895-907.

Kovacevic, S., Rafii, M.S., Brewer, J.B., and the Alzheimer's Disease Neuroimaging Initiative, 2009. High-throughput, fully-automated volumetry for prediction of MMSE and CDR decline in mild cognitive impairment. Alzheimer Dis Assoc Disord 23(2): 139-145.

McDonald, C.R., McEvoy, L.K., Gharapetian, L., Fennema-Notestine, C., Hagler Jr., D.J., Holland, D., Koyama, A., Brewer, J.B., Dale, A.M. and the Alzheimer's Disease Neuroimaging Initiative, 2009. Regional rates of neocortical atrophy from normal aging to early Alzheimer disease. Neurology 73(6), 457-65.

McEvoy, L.K., Fennema-Notestine, C., Roddey, J.C. Hagler, Jr, D.J., Holland, D., Karow, D.S., Pung, C.J., Brewer, J.B., Dale, A.M. and for the Alzheimer's Disease Neuroimaging Initiative 2009. Alzheimer Disease: Quantitative structural neuroimaging for detection and prediction of clinical and structural changes in Mild Cognitive Impairment. Radiology 251(1), 195-205.

Pike, K.E. and Savage, G., 2008. Memory profiling in mild cognitive impairment: can we determine risk for Alzheimer's disease? J Neuropsychol. 2(Pt 2): 361-72.

Ridha, B.H., Anderson, V.M., Barnes, J., Boyes, R.G., Price, S.L., Rossor, M.N., Whitwell, J.L., Jenkins, L., Black, R.S., Grundman, M., Fox, N.C., 2008. Volumetric MRI and cognitive measures in Alzheimer disease: comparison of markers of progression. J Neurol. 255(4): 567-74.

Scahill, R.I., Frost, C., Jenkins, R., Whitwell, J.L., Rossor, M.N., Fox, N.C., 2003. A longitudinal study of brain volume changes in normal aging using serial registered magnetic resonance imaging. Arch Neurol 60(7), 989-994.

Scheltens, P., Leys, D., Barkhof, F., Huglo, D., Weinstein, H.C., Vermersch, P., Kuiper, M., Steinling, M., Wolters, E.C., Valk, J., 1992. Atrophy of medial temporal lobes on MRI in "probable" Alzheimer's disease and normal ageing: diagnostic value and neuropsychological correlates. J Neurosurg Psychiatry 55(10), 967-72.

Seo, S.W., Im, K., Lee, J.M., Kim, Y.H., Kim, S.T., Kim, S.Y., Yang, D.W., Kim, S.I., Cho, Y.S., Na, D.L., 2007. Cortical thickness in single- versus multiple-domain amnestic mild cognitive impairment. Neuroimage 36(2), 289-297.

Sperling, R.A., Dickerson, B.C., Pihlajamaki, M., Vannini, P., LaViolette, P.S., Vitolo O.V., Hedden, T., Becker, J.A., Rentz, D.M., Selkoe, D.J., Johnson, K.A., 2010. Functional alterations in memory networks in early Alzheimer's disease. Neuromolecular Med. 12(1) 27-43.

CHAPTER 2:

CETP POLYMORPHISMS ASSOCIATE WITH BRAIN STRUCTURE, ATROPHY RATE, AND ALZHEIMER'S DISEASE RISK IN AN APOE-DEPENDENT MANNER

Abstract

Two alleles in cholesteryl ester transfer protein (CETP) gene polymorphisms have been disputably linked to enhanced cognition and decreased risk of Alzheimer's disease (AD): the V and A alleles of I405V and C-629A. This study investigates whether these polymorphisms affect brain structure in 188 elderly controls and 318 AD or mild cognitive impairment (MCI) subjects from the Alzheimer's Disease Neuroimaging Initiative cohort. Nominally significant associations were dependent on APOE ε4 carrier status. In APOE ε4 carriers, the V and A alleles, both of which decrease CETP and increase HDL, associated with greater baseline cortical thickness and less twelve-month atrophy in the medial temporal lobe. Conversely, in APOE ε4 non-carriers, the I allele, which increases CETP and decreases HDL, associated with greater baseline thickness, less atrophy and lower risk of dementia. These results suggest CETP may contribute to the genetic variability of brain structure and dementia susceptibility in an APOE-dependent manner.

Introduction

The role of genetics in brain development and disease susceptibility has recently gained insight from the field of neuroimaging genetics, in which phenotypes are defined by quantitative measures of brain structure or function rather than clinical characteristics such as disease, symptoms or behavior. Association analyses between genetic data and information obtained from structural and functional neuroimaging provide a more direct assessment of genetic influence at the level of neuronal circuitry than other traditional analyses, which only indirectly assess the impact of genes on complex behaviors or cognitive states (Mattay et al., 2008). Thus, the use of imaging measures may provide a closer description of underlying pathology (Saykin et al., 2010) and therefore render association analyses less susceptible to non-genetic variability. Accordingly, neuroimaging genetics may have the potential to examine the biologic impact of genes with greater precision and accuracy than traditional genetic association analyses by examining atrophy as a possible link between genes and behavioral deficits (Stein et al., 2010).

In particular, structural neuroimaging has considerable potential to address whether specific genes may affect brain structure during development or pathological processes. One such gene of interest is the cholesteryl ester transfer protein (CETP) gene, which is located on chromosome 16q21 and contains 14 exons (Arias-Vásquez et al., 2007). CETP is involved in the transfer of insoluble cholesteryl esters between lipoproteins as part of the reverse cholesterol transport system and is known to be synthesized and secreted in the brain (Albers et al., 1992). It has been speculated that

CETP may play a role in cholesterol transport within the brain (Albers et al., 1992), perhaps by promoting neuronal uptake of high density lipoprotein (HDL) particles via interactions with receptors for apolipoprotein E (APOE), which is the most common genetic risk factor of Alzheimer's disease (AD) (Rodríguez et al., 2006). Several studies have shown that cholesterol metabolism is indeed altered in AD (Kivipelto et al., 2001; Pregelj, 2008), providing a biologically plausible role for CETP in AD susceptibility (Barzilai et al., 2003, 2006; Sanders et al., 2010).

CETP has been previously implicated in metabolic syndrome, a conglomeration of metabolic risk factors including dyslipidemia, hypertension and altered glucose metabolism, which increases in prevalence with age. Variations in the CETP gene lead to altered CETP serum concentration and activity and subsequent changes in HDL levels and lipoprotein particle sizes (Thompson et al., 2003). Specifically, CETP deficiency is characterized by decreased CETP mass and activity and increased HDL and lipoprotein size (Qureischie et al., 2008). Two functional CETP polymorphisms associated with CETP deficiency have been controversially implicated as protecting against cognitive decline and neurodegenerative disease susceptibility: the A allele of promoter polymorphism C-629A (rs1800775) and the V allele of the amino acid exchange polymorphism I405V in exon 14 (rs5882). Three studies have reported that I405V VV genotype was associated with increased cognitive function and decreased risk of dementia (Barzilai et al., 2003, 2006; Sanders et al., 2010), although these effects have not been replicated in other studies (Arias-Vásquez et al., 2007; Johnson et al., 2007; Qureischie et al., 2009; Rodriguez et al.,

2006). Likewise, one study reported a decreased risk of AD associated with C-629A AA genotype (Rodriguez et al., 2006), but this has been contradicted by others (Qureischie et al., 2008, 2009).

Inconsistent findings involving these two polymorphisms may be due to a variety of factors, including discrepancies in the age and ethnic composition of study samples, or the possibility that these polymorphisms are merely surrogates for another polymorphism that acts as the true causal variant for modulating disease susceptibility. Further, it is possible that the associations found were due to chance alone. However, the inability to replicate findings may also be due to imprecision of the phenotype when defined by neuropsychological measures or clinical disease status. To address this concern, we examined the effect of the CETP C-629A and I405V polymorphisms on structural brain measures in 188 healthy elderly controls and 318 subjects with AD or mild cognitive impairment (MCI) from the Alzheimer's Disease Neuroimaging Initiative (ADNI). To reduce the number of statistical comparisons, the analysis was restricted to the hippocampus, parahippocampal gyrus and entorhinal cortex, three brain regions in which structural change is considered to be a sensitive indicator of memory impairment and early pathological processes occurring in AD (Braak and Braak, 1991; Dickerson et al., 2009; Jack et al., 1997; McEvoy et al., 2009).

Methods

Alzheimer's Disease Neuroimaging Initiative

Raw data used in this paper were obtained from the ADNI public database (http://www.loni.ucla.edu/ADNI/). ADNI is a multi-site, five-year observational study of elderly individuals started in 2004 by the National Institute on Aging, the National Institute of Biomedical Imaging and Bioengineering, the Food and Drug Administration, private pharmaceutical companies and nonprofit organizations. Elderly controls, subjects with MCI and AD subjects underwent longitudinal MRI scans and neuropsychological assessment at specified intervals for two to three years.

The Principal Investigator of this initiative is Michael W. Weiner, M.D. at the VA Medical Center and University of California, San Francisco. ADNI is the result of the efforts of many co-investigators from a broad range of academic institutions and private corporations, and subjects have been recruited from over 50 sites across the U.S. and Canada. For more information, see www.adni-info.org.

Standard protocol approvals, enrolment and patient consents

ADNI was conducted according to Good Clinical Practice guidelines, the Declaration of Helsinki, US 21CFR Part 50—Protection of Human Subjects, and Part 56—Institutional Review Boards, and pursuant to state and federal HIPAA regulations. Written informed consent for the study was obtained from all subjects and/or authorized representatives and study partners (http://www.ADNI-info.org).

Subjects

ADNI eligibility criteria are described at http://adni-info.org. In general, all enrolled subjects were between 55 and 90 (inclusive) years of age, had a study partner available to provide an independent evaluation of functioning, and spoke either English or Spanish. A total of 188 healthy controls (HC), 327 subjects with MCI, and 149 AD subjects were included in this study based on their availability of genetic data and baseline MRI data that passed local quality control. One-hundred and nine ADNI subjects were excluded on account of missing data or failure of imaging data to pass local quality control.

To increase the power of analysis, subjects with MCI and AD were treated as a single diagnostic group after selecting only the 169 MCI subjects who were classified as most at risk for imminent conversion to AD based on their AD-like pattern of regional atrophy, as described in McEvoy et al. (2009). Briefly, stepwise linear discriminant analysis was used to identify eight cortical and subcortical regions to best aid discrimination of HC and AD subjects. A classifier trained on data from HC and AD subjects was applied to data from all 327 MCI subjects to determine whether they had patterns of regional atrophy characteristic of mild AD. The discrimination analysis correctly classified 92% of HC subjects and 86% of AD subjects, which is comparable to the clinical diagnostic accuracy of AD (Gearing et al., 1995; Mok et al., 2004; Schneider et al., 2007). The discriminant model was predictive of the rate of clinical decline and progression of MCI patients to an AD diagnosis. Further, the rates of

Table 2.1: Subject characteristics

	Healthy Controls (n=188)	**MCI & AD Subjects (n=318)**
Age (years)	76.12 ± 5.13	74.91 ± 7.52
Percent female subjects	46 %	46 %
Education (years)	16.10 ± 2.81*	15.34 ± 3.01*
Percent carriers of APOE ε4	28 %*	64 %*
MMSE	29.13 ± .97*	25.16 ± 2.49*
ADAS-cog	6.15 ± 2.85*	15.38 ± 5.86*

Data are given as mean ± SD unless otherwise specified as a percent. *The MCI and AD subjects had a significantly lower level of education ($p=.005$), higher frequency of the APOE ε4 allele ($p < .001$) and significantly more impaired MMSE ($p < .001$) and ADAS-cog ($p < .001$) scores at baseline than the healthy controls.

cognitive decline in these prodromal AD patients were in line with those of AD patients in ADNI (McEvoy et al., 2009).

Demographics of the 188 HC, and 318 MCI and AD subjects are described in Table 1. Of the 506 total subjects, 420 had twelve-month follow-up imaging data that passed local quality control and were thus included in the longitudinal analysis.

Genotyping

DNA was extracted from blood and genotyped with the Illumina Human610-Quad BeadChip. Since the Illumina chip does not include the APOE alleles, the Alzheimer's Disease Neuroimaging Initiative (ADNI) did a separate DNA extraction from blood samples, and APOE genotyping was done via PCR amplification and HhaI restriction enzyme digestion (Potkin et al., 2009). Smartpca was used to identify ADNI subjects who were outliers relative to the genetic cluster of ADNI subjects who self-reported their race as exclusively "White," and one subject who reported "More than one race" (Joyner et al., 2009). Fifty-three genetic outliers were identified. These and 30 subjects with missing genetic data were excluded from the study and, therefore, are not included in the total subjects enumerated above.

MR acquisition and analysis

Two three-dimensional, T1-weighted volumes per subject per visit were downloaded from the public ADNI database (http://www.loni.ucla.edu/ADNI/). All image processing and analyses occurred at the Multimodal Imaging Laboratory at the

University of California, San Diego. Images were corrected for gradient nonlinearities (Jovicich et al., 2006) and B1 field inhomogeneity (Sled et al., 1998). The two baseline images were rigid-body aligned, averaged to improve signal-to-noise ratio and resampled to isotropic 1-mm voxels. An automated segmentation procedure based on FeeSurfer software (Fischl et al., 2002) and customized Matlab code was used to obtain volumetric segmentation. Cortical surface reconstruction yielded a measure of thickness at each vertex, and the surface was parceled into distinct regions of interest (ROIs) (Dale and Sereno, 1993; Dale et al., 1999; Fischl et al., 1999, 2004).

The methods to obtain twelve-month change are described in detail in Holland et al. (2009). Briefly, follow-up images were fully affine-registered to the baseline images and corrected for intensity nonuniformity. Nonlinear registration was then used to align voxel centers in the baseline with the appropriate location in the follow-up scans, and a volume-change field was calculated. This field was averaged over each ROI to compute the percentage change from baseline. This method has been validated using models where amount of change was known and where noise was added to approximate that seen in human brain imaging of demented patients. In these studies, technical measurement error for the computed change in volume was within 0.2 percent of the structure volume. That is, for a 6000 mm^3 hippocampal volume undergoing a change of 1 percent, the technical measurement error in estimating the 60 mm^3 volumetric change would be ±12 mm^3 in an individual subject if voxels were each 1mm isotropic (Murphy et al., 2010).

The methods to visualize CETP by APOE interactions at each vertex on the cortical surface are described in detail in Joyner et al. (2009). Briefly, the cortical surface was reconstructed to measure thickness at each vertex. Continuous maps of cortical surface area were smoothed with a Gaussian kernel and mapped onto a standardized spherical atlas space. Association of cortical thickness and CETP by APOE interactions was assessed at each surface vertex after controlling for the effects of age, sex and diagnosis, and the strength of association was mapped as negative log p-values.

Statistical analysis

All statistical analysis was performed using PASW Statistics 18. Genotype distributions and allele frequencies were compared using χ^2-statistics. Genotype was modeled as minor allele SNP-dosage (homozygote of minor allele = 2, heterozygote = 1, homozygote of major allele = 0) and separated into two regressor variables to account for sex-specific effects. Thus, genotype was modeled as dosage of the A allele at C-629A and the V allele at I405V. Sex was additionally included as a covariate in regression analyses to ensure that males and females homozygous for major alleles would not be equivalent in the overall model.

To examine the relationship between CETP genotype and diagnosis, binary logistic regression analysis was used with age, sex and APOE ε4 carrier status as covariates. Independent-sample t-tests were used to compare the effects of specific genotypes on diagnosis. To study the association between genotype and brain

structure, standardized morphometric measures were entered as dependent variables into linear regression models. Morphometric measures were standardized by converting raw values to standardized residuals in a linear regression model built upon data from only the HC subjects. Cortical thickness measures were standardized with respect to age and sex. Subcortical volumes were standardized with respect to age, sex and intracranial volume. Likewise, longitudinal morphometric measures were entered as dependent variables into linear regression models to determine whether genotype influenced atrophy. These analyses were also performed with stratification for APOE ε4 carrier status to determine whether the effects were dependent on genotype at this locus. Given the imaging and genetic data currently available, we conducted a restricted exploratory analysis without correction for multiple comparisons. The two-sided significance level was set at α=.05 for all regression models, each of which was repeated for two CETP polymorphisms and nine subject groups to demonstrate the effect of these polymorphisms on every possible combination of subject diagnosis and APOE ε4 carrier status.

To determine whether the aging process had different effects on brain structure and atrophy depending upon genotype at the two CETP polymorphisms, a univariate General Linear Model factor by covariate analysis of variance was used. Genotype was a grouping factor and genotype*age, age, sex, diagnosis and APOE ε4 carrier status were covariates. In this analysis, cortical thickness measures were standardized with respect to sex, and subcortical volumes with respect to sex and intracranial volume, but no measures were adjusted for age. Likewise, to determine whether

APOE ε4 carrier status affected the influence of CETP genotype on brain structure, genotype*APOE ε4 carrier status was entered along with the main effects in the following interaction model: $y = b0 + b1*CETP + b2*APOE + b3*CETP*APOE + b4*age + b5*sex + b6*diagnosis$.

Results

Influence of CETP polymorphisms on risk of MCI and AD

Genotype distributions and allele frequencies of CETP I405V and C-629A for the 188 HCs and 318 subjects with AD or MCI are presented in Table 2. Both polymorphisms were in Hardy-Weinberg equilibrium in the study sample (I405V: χ^2 = .043, p=.979; C-629A: χ^2 = 2.289, p=.318).

Logistic regression analysis revealed no association of either CETP polymorphism with the risk of MCI and AD. Likewise, age and sex were not significantly associated with the risk of MCI and AD although APOE ε4 carrier status was significantly associated with the risk of MCI and AD (χ^2 = 61.60, *df*=1, p= 4.21E-15).

When the study sample was stratified by gender and APOE ε4 carrier status, I405V genotype was associated with the risk of MCI and AD in both male (n=135, χ^2 = 9.89, *df*=2, p=.007) and female (n=115, χ^2 = 9.89, *df*=2, p=.019) non-carriers. Males with genotype IV were more likely to have MCI or AD than males with genotype II (t(122)= -3.151, p=.002), and likewise, females with genotype IV showed a trend of being more likely to have MCI or AD than females with genotype II (t(96)= -1.973,

Table 2.2: Genotype distribution and allele frequencies of CETP polymorphisms

Diagnosis (n)	**Genotypes**			**Allele frequencies**		**χ^2-test**		
C-629A	**CC(%)**	**AC(%)**	**AA(%)**	**C**	**A**	**χ^2**	***df***	**p**
HC (188)	50 (26.7)	97 (51.9)	40 (21.4)	52.7	47.3	2.289	2	.318*
MCI, AD (318)	76 (23.9)	172 (54.1)	70 (22.0)	50.9	49.1			
I405V	**II(%)**	**IV(%)**	**VV(%)**	**I**	**V**	**χ^2**	***df***	**p**
HC (188)	99 (52.7)	73 (38.8)	16 (8.5)	72.1	27.9	0.043	2	.979*
MCI, AD (318)	139 (43.7)	147 (46.2)	32 (10.1)	66.8	33.2			

Distribution of the CETP C-629A and I405V polymorphisms in healthy controls and subjects with MCI or AD. *Both polymorphisms were in Hardy-Weinberg equilibrium in the study population.

p=.051). In APOE ε4 carriers, I405V genotype showed no influence on diagnosis. Thus, the I405V polymorphism appeared to influence the risk of MCI and AD only in the absence of the APOE ε4 allele. In contrast, C-629A genotype was not significantly associated with the risk of MCI and AD in either carriers or non-carriers of APOE ε4.

3.2 Influence of CETP polymorphisms on brain structure

In the female population, C-629A and I405V genotype were associated with morphometric measures in two of the three brain structures tested, dependent upon diagnosis and APOE ε4 carrier status (Table 3). In particular, the I allele of the I405V polymorphism was associated with greater entorhinal (β=.222; SE = .232; p=.007) and parahippocampal thickness (β=.197; SE = .120; p=.016) in APOE ε4 non-carriers, and this effect appeared primarily driven by healthy individuals (β=.233; SE = .191; p=.032 for entorhinal; β=.256; SE = .139; p=.017 for parahippocampal), as it was not seen in the MCI and AD group. In contrast, the protective allele relationship was reversed in APOE ε4 carriers, where the V allele was associated with greater parahippocampal thickness (β=.194; SE = .130; p=.018), and this effect appeared primarily driven by individuals with MCI or AD (β=.230; SE = .139; p=.011). For the C-629A polymorphism, the A allele was associated with greater entorhinal (β=.547; SE = .376; p=.016) and parahippocampal thickness (β=.577; SE = .212; p=.020) in healthy controls. No significant associations were detected with hippocampal volume in females.

Table 2.3: Regression coefficients and significance levels (p-values) for associations between CETP polymorphisms and brain structure in *a priori* selected ROIs in females

SNP	Diagnosis	APOE ε4 Carrier Status	N	Entorhinal Cortex Thickness β (p-value)	Parahippocampal Gyrus Thickness β (p-value)
C-629A	All	All	506	0.047 (0.507)	0.003 (0.966)
	HC	All	188	**0.267 (0.023*) (A)**	**0.250 (0.031*) (A)**
	MCI, AD	All	318	-0.017 (0.850)	-0.118 (0.178)
	All	Non-carriers	250	0.005 (0.956)	0.040 (0.684)
	HC	Non-carriers	135	0.098 (0.479)	0.164 (0.224)
	MCI, AD	Non-carriers	115	-0.115 (0.439)	-0.128 (0.387)
	All	Carriers	256	0.052 (0.606)	-0.096 (0.321)
	HC	Carriers	53	**0.547 (0.016*) (A)**	**0.577 (0.020*) (A)**
	MCI, AD	Carriers	203	0.042 (0.703)	-0.135 (0.212)
I405V	All	All	506	0.088 (0.134)	0.203 (0.686)
	HC	All	188	0.151 (0.115)	**0.242 (0.011*) (I)**
	MCI, AD	All	318	0.033 (0.658)	-0.125 (0.090)
	All	Non-carriers	250	**0.222 (0.007*) (I)**	**.0197 (0.016*) (I)**
	HC	Non-carriers	135	**0.233 (0.032*) (I)**	**0.256 (0.017*) (I)**
	MCI, AD	Non-carriers	115	0.100 (0.442)	0.023 (0.861)
	All	Carriers	256	-0.076 (0.370)	**-0.194 (0.018*) (V)**
	HC	Carriers	53	-0.066 (0.741)	0.236 (0.282)
	MCI, AD	Carriers	203	-0.061 (0.506)	**-0.230 (0.011*) (V)**

Regression coefficients and significance levels were obtained from linear regression models in which CETP genotype was the independent variable and morphometric measures were the dependent variables. The valence assigned to β coefficients corresponds to the directionality of association. For CETP C-629A, positive values mean that the A allele is associated with greater volumes, and negative values mean that the C allele is associated with greater volumes. For CETP I405V, positive values mean that the I allele is associated with greater volumes, and negative values mean that the V allele is associated with greater volumes. CETP polymorphisms are associated with two morphometric measures in females, dependent upon diagnosis and APOE ε4 carrier status. No significant associations were detected with hippocampal volume in females. The only significant associations detected in males were between C-629A and hippocampal volume in MCI and AD carriers of APOE ε4; I405V and entorhinal cortex thickness in non-carriers of APOE; and I405V and hippocampal volume in non-carriers of APOE ε4. *Statistically significant p-values ($p<.05$) are represented in bold, and the allele corresponding to greater thickness (i.e. the "protective" allele) is denoted in parentheses.

Fewer significant associations among these polymorphisms and brain structures were detected in males, but those that were found matched well with the findings in females. Namely, the I allele of the I405V polymorphism was associated with greater entorhinal cortex thickness (β=.165; SE = .249; p=.048) and hippocampal volume (β=.176; SE = .215; p=.036) in APOE ε4 non-carriers; the A allele of the C-629A polymorphism was associated with greater hippocampal volume in APOE ε4 carriers with MCI or AD (β=.230; SE = .127; p=.017).

An interaction between CETP I405V and APOE ε4 carrier status was found with parahippocampal gyrus thickness after controlling for age, sex and diagnosis (F=2.459; p=.007). Namely, the I allele was found to be associated with thicker parahippocampal cortex in APOE ε4 non-carriers but with thinner parahippocampal cortex in APOE ε4 carriers (Figures 1, 2). Likewise, an interaction between CETP C-629A and APOE ε4 carrier status was found with parahippocampal gyrus thickness after controlling for age, sex and diagnosis (F=1.983; p=.031). The A allele was found to be associated with thicker parahippocampal cortex in APOE ε4 carriers but with thinner parahippocampal cortex in APOE ε4 non-carriers.

3.3 Influence of CETP polymorphisms on brain atrophy

Not only did genotype at these two CETP polymorphisms affect baseline brain structure, but also it influenced twelve-month brain atrophy in a consistent manner (Table 4). In females, the A allele of the C-629A polymorphism was protective against

Table 2.4: Proposed model of CETP effects on MCI/AD risk, baseline volumes and one-year atrophy in medial temporal lobe structures

	Protective for Baseline Volumes	Protective for One-year Atrophy	Protective for Risk of MCI/AD
APOE ε4 Carriers	V allele (low CETP)	-	-
HC	A allele (low CETP)	-	-
MCI or AD	V allele (low CETP) A allele (low CETP)	A allele (low CETP)	-
APOE ε4 Non-carriers	I allele (high CETP)	I allele (high CETP)	I allele (high CETP)
HC	I allele (high CETP)	-	-
MCI or AD	-	I allele (high CETP)	-

Alleles conferring low CETP and high HDL (V at I405V and A at C-629A) appear to be protective in APOE ε4 carriers, whereas alleles conferring high CETP and low HDL (I at I405V and C at C-629A) appear protective in non-carriers.

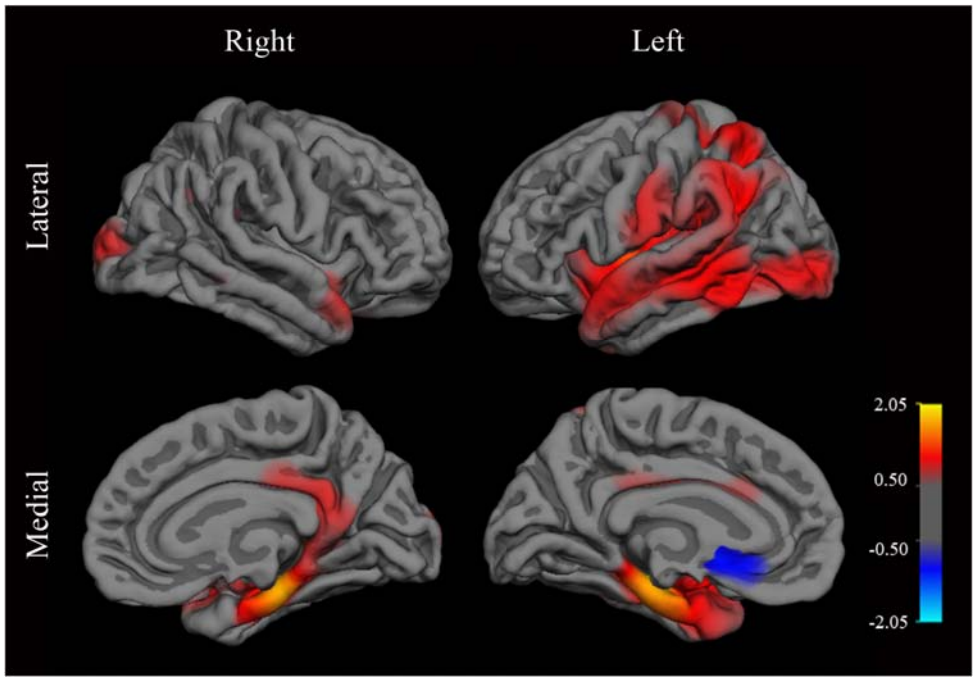

Figure 2.1: Association of baseline cortical thickness at each vertex with the interaction of CETP SNP I405V by APOE ε4 carrier status in all subjects after controlling for the effects of age, gender and diagnosis. The map shows the distribution of nominal –log p-values across the reconstructed cortical surface. The sign represents the direction of the effect. Red values correspond to the I allele associating with greater cortical thickness in APOE ε4 non-carriers and the V allele associating with greater cortical thickness in APOE ε4 carriers. Blue values represent the reverse relationship. The most significant effects of this genotype interaction are seen in the parahippocampal gyrus.

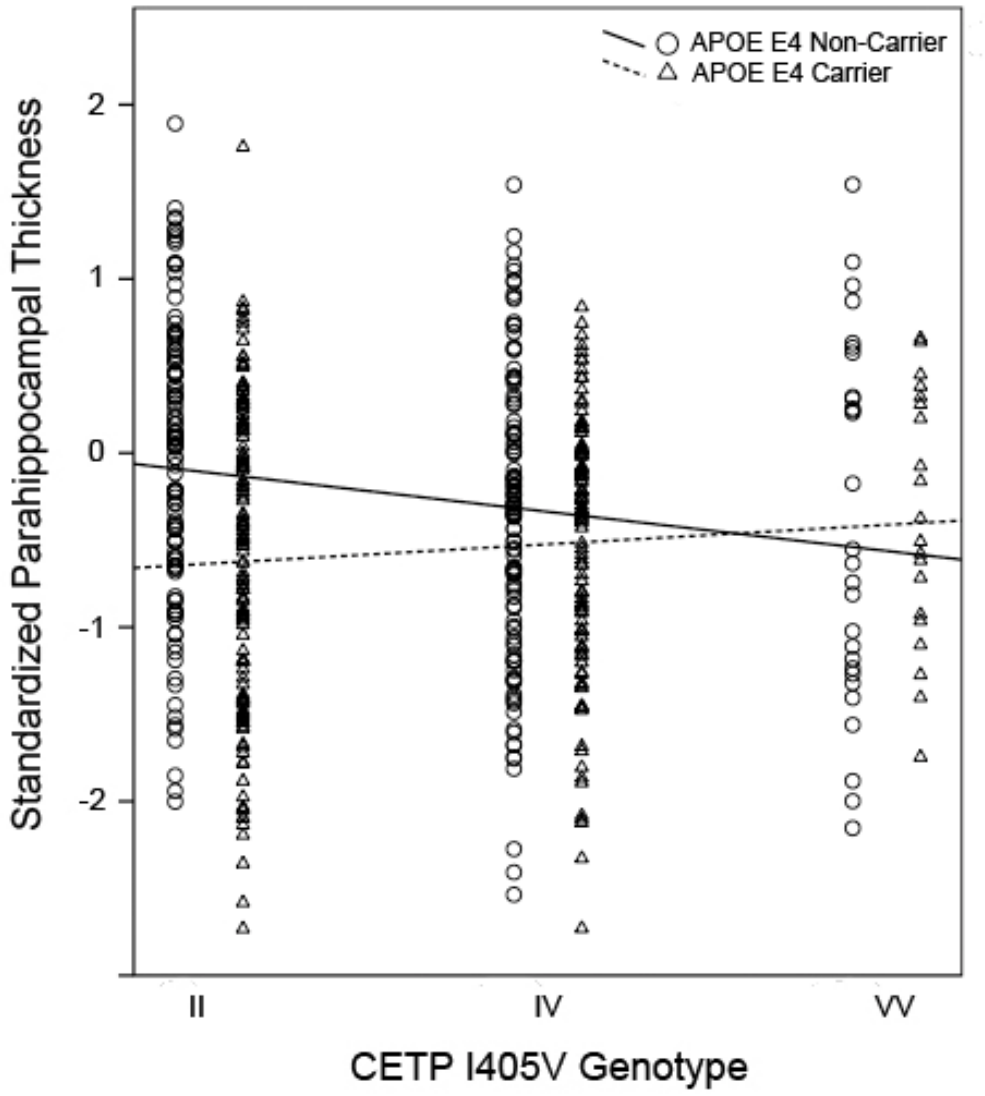

Figure 2.2: Standardized values for parahippocampal gyrus thickness plotted against CETP I405V genotype for APOE ε4 non-carriers (circles; solid line) and carriers (triangles; dashed line). In APOE ε4 non-carriers, the II genotype seems to be protective with respect to parahippocampal thickness. In contrast, in APOE ε4 carriers, VV seems protective. Regression lines computed using the least squares method to best fit the data points. For APOE ε4 non-carriers, $R^2 = .029$. For APOE ε4 carriers, $R^2 = .007$.

thinning of the entorhinal cortex (β=.188; SE = .142; p=.011). This protective effect remained significant when considering only those with a diagnosis of MCI or AD (β=.233; SE = .164; p=.013), as well as only those with a diagnosis of MCI or AD who were APOE ε4 carriers (β=.240; SE = .189; p=.043). In males, the I allele of the I405V genotype was protective against volume reduction in the hippocampus in APOE ε4 non-carriers (β=.227; SE = .235; p=.011), an effect still seen when the sample was limited to non-carriers with MCI or AD (β=.324; SE = .443; p=.031).

3.4 Effect of age on the interaction between CETP polymorphism and brain structure

In the female population, CETP I405V genotype by age interactions were found with parahippocampal gyrus thickness after controlling for diagnosis and APOE ε4 carrier status (Table 5). Females with the I405V II genotype showed less decline in parahippocampal gyrus thickness with age than those with VV (F=4.374; p=.013). No significant CETP C-629A genotype by age interactions were found in the three brain structures tested, nor were any significant effects found in males

Discussion

The present findings suggest that genotype at CETP polymorphisms I405V and C-629A may contribute to the genetic variability of brain structure and neurodegenerative disease susceptibility. This study is the first to detect APOE-specific associations between the I405V and C-629A polymorphisms and brain structure, and to relate these findings to longitudinal change in brain structure with

Table 2.5: Effects of age on CETP I405V influence on parahippocampal gyrus thickness

Variable	**df**	**F**	**Sig.**
Male I405V	2	2.309	.100
Female I405V	2	4.504	**.012***
Male I405V*Age	2	2.343	.097
Female I405V*Age	2	4.374	**.013***
Age	1	15.208	**1.10E-4***
Diagnosis	1	125.971	**3.45E-26***
Sex	1	.166	.684
APOE ε4 Status	1	.251	.617

Univariate General Linear Model factor by covariate analysis of variance was used for parahippocampal gyrus thickness, with I4045V genotype as a grouping factor and age, sex, diagnosis and APOE ε4 carrier status as covariates. There were no significant I405V genotype by age interactions with entorhinal cortex thickness or hippocampal volume. There were no significant C-629A genotype by age interactions in any of the three brain structures tested. *Statistically significant p-values ($p<.05$) are represented in bold.

aging. In APOE ε4 non-carriers, the I allele of the I405V polymorphism, which leads to increased CETP and decreased HDL, was associated with larger medial temporal lobe structures at baseline, less twelve-month atrophy in these structures, and lower risk of MCI and AD. This relationship was reversed in APOE ε4 carriers, in whom the V allele of I405V and the A allele of C-629A, both of which lower CETP and raise HDL, were found to be protective. Although the primary ROI analysis was restricted to three medial temporal structures selected *a priori*, a cortical surface analysis revealed the greatest effects of these polymorphisms were indeed found in the medial temporal lobe, and specifically in the parahippocampal gyrus.

The results suggest that these CETP polymorphisms may modify brain structure and neurodegenerative disease susceptibility in a manner dependent upon APOE. I405V genotype influenced the risk of MCI and AD in this study sample only in non-carriers of APOE ε4, and the protective allele relationships reversed in carriers and non-carriers of APOE ε4. Two prior studies found the effects of these polymorphisms on the risk of AD to be similarly dependent upon APOE. One study of 286 AD subjects found that risk of AD was lower in carriers of APOE ε4 with the C-629A AA genotype (Rodríguez et al., 2006), and another study of 544 AD subjects reported that risk of AD was higher in non-carriers of APOE ε4 with the I405V VV genotype (Arias-Vásquez et al., 2007), analogous to the present finding that the I allele was protective in non-carriers. The finding of alleles that lower CETP levels being protective in APOE ε4 carriers is further supported by a study of 107 AD subjects in

which another CETP polymorphism, D442G, was associated with lower levels of CETP and decreased risk of AD in APOE ε4 carriers (Chen et al., 2008).

It has been demonstrated that protein-protein interactions occur between CETP and APOE due to their joint participation in cholesterol metabolism (Sorlí et al., 2005). CETP-immunoreactivity has been demonstrated in astrocytes from AD brain tissue, a cell known to produce APOE (Yamada et al., 1995), and a physiological cooperation between CETP and APOE has been established in cholesterol ester transport in plasma (Marcel et al., 1990). Thus, it is reasonable that the influence of CETP on brain cholesterol metabolism and structure might be modulated by APOE activity within the brain, and that a dysfunction in cholesterol metabolism involving both proteins may play a central role in the AD pathology (Yamada et al., 1995).

The APOE-dependent reversal of the protective allele relationship observed in this study might be explained by such interactions between CETP and APOE. For example, it has been proposed that CETP may modify the risk of AD by altering HDL concentration in the brain, whereas the amount of HDL generated varies with APOE isoform (Rodríguez et al., 2006). CETP is believed to promote neuronal uptake of HDL particles via interactions with APOE receptors (Rodríguez et al., 2006). Indeed, gene-gene interactions between APOE and CETP have been shown to influence HDL concentrations (Sorlí et al., 2005), and it is known that HDL particles interact with amyloid beta to inhibit its aggregation into fibrils (Olesen and Dago, 2000).

The results further suggest that these two polymorphisms have a differential degree of influence on brain structure in males and females. Although both males and

females were affected by these polymorphisms in a similar manner, the majority of associations between genotype and brain structure were found in females. This may be due to sex-related differences in cholesterol metabolism (De Gennes et al., 1983) or due to underlying structural differences in the male and female brains imposed by distinct hormonal or genetic expression environments during the time of development (Negri-Cesi et al., 2004).

In APOE ε4 non-carriers, risk of MCI and AD increased with carriage of V at I405V. Since the V allele corresponds to lower levels of CETP and subsequently higher levels of HDL (Arias-Vásquez et al., 2007), this suggests that low CETP and high HDL may actually increase the risk of AD in non-carriers. One mechanism for this increased risk proposed by Arias Vásquez et al. (2007) is that low CETP levels lead to a reduction in neuronal repair. Other studies have found that variations in I405V had no effect on cognitive function in 525 subjects who participated in the Scottish Mental Survey of 1932 (Johnson et al., 2007) and did not influence the risk of vascular dementia in 163 subjects (Qureischie et al., 2009). Two additional studies reported no difference in distribution of allele and genotype frequencies for I405V between AD subjects and elderly controls (Arias-Vásquez et al., 2007; Rodríguez et al., 2006); however, after segregating by APOE ε4 status, VV homozygosity was more frequent in AD non-carriers than in elderly control non-carriers (Arias-Vásquez et al., 2007), similar to the present findings.

A recent prospective cohort study by Sanders et al., 2010, followed 523 mixed-ethnicity subjects aged 70 years or older over a time period during which 40 subjects

developed dementia. This group reported that the I405V VV genotype was associated with slower age-associated memory decline and lower risk of incident dementia and AD. Further, the hazard ratio of dementia for IV heterozygotes was between that for II and VV homozygotes, suggesting a possible gene-dose relationship (Sanders et al., 2010). This finding supported two previous studies in the Ashkenazi Jewish population that found the VV genotype to be more prevalent in 158 subjects with exceptional longevity (aged ≥ 95 years) and to be associated with better cognitive function in these subjects (Barzilai et al., 2003, 2006), although the specific ethnic composition of these studies limit their generalizability. Further, the fact that these studies adjusted for APOE ε4 status rather than stratifying by this allele makes their findings difficult to compare with those of the present study.

The effect of variations in C-629A on cognition and disease susceptibility is similarly unclear. One group found that AA homozygotes had a significantly decreased risk of AD associated with carriage of the APOE ε4 allele (Rodríguez et al., 2006), consistent with the present findings. Another group studying 388 AD subjects found no influence of C-629A on risk of AD in either carriers or non-carriers of APOE ε4 (Qureischie et al., 2008) but later reported increased risk of vascular dementia in AA homozygotes who were APOE ε4 non-carriers (Qureischie et al. 2009).

The discrepancies between prior research and the present study may be due to myriad factors, including variation in the age and ethnic compositions of study samples. One characteristic to note in this study sample is the high rate of APOE ε4 carriers among MCI and AD subjects as compared to rates reported among other study

samples (Crean et al., 2011), which is a difference that may limit the generalizability of these findings. Additionally, the discrepancies between prior research and the present study may reflect the limitation of examining polymorphisms in the CETP gene whose functional consequences are uncertain (Qureischie et al., 2008). For example, it is possible that the I405V polymorphism is a surrogate for another polymorphism that acts as the true causal variant for modulating brain structure and disease susceptibility; I405V may be a better surrogate for this true variant in the Ashkenazi Jewish population, which would be expected to have wider linkage disequilibrium blocks than in the ADNI study sample. Variable findings in prior research may also reflect the difficulty in trying to evaluate the genetic contribution of a single polymorphism to a heterogenous disorder such as AD, which is likely impacted by the interaction of multiple genes, proteins and non-genetic factors. That the apparent heritability of late-onset AD is seemingly unexplained by the known contributions of APOE and other well-replicated genes (e.g., presenilin-1, presenilin-2, APP) (Seshadri et al., 2010) suggests the likelihood that many genes contribute to AD susceptibility to a lesser degree. Additionally, this study suggests the importance of accounting for interactions with APOE, as failure to do so may produce inconsistent findings.

A limitation of this study is its inability to elucidate whether genetic variation in CETP modulates brain structure at the time of development, during aging, or solely in the context of disease. However, the regional specificity of findings suggests that CETP may influence susceptibility to AD given that these polymorphisms are

associated with cortical thickness in the parahippocampal gyrus and entorhinal cortex, regions particularly damaged in AD (Braak and Braak, 1991). Further, the significant I405V genotype by age interaction in females, independent of disease status, was also seen in the parahippocampal gyrus. This could suggest that these age-related effects might still be related to AD pathology, including pathology present in healthy controls.

Although a sample size of 188 elderly controls and 318 AD or MCI subjects may seem inadequate to identify a genetic risk factor for atrophy and disease susceptibility, the ADNI dataset is currently the largest dataset with complete genetic and imaging information available for such an analysis. Prior studies found similar effects using comparably sized, and even smaller (Chen et al., 2008), samples. Given the data currently available, this study was limited to a restricted exploratory analysis for subtle effects using relaxed correction for multiple comparisons. To reduce the need to correct for multiple comparisons across all brain regions and genetic variants, the study examined an *a priori* selection of targeted brain regions involved in Alzheimer's disease (Braak and Braak, 1991; Dickerson et al., 2009; Jack et al., 1997; McEvoy et al., 2009) and targeted genetic variants based on extant evidence of their involvement in aging and neurodegeneration (Barzilai et al., 2003, 2006; Sanders et al., 2010; Rodriguez et al., 2006). No doubt, the future will bring wider access to even larger datasets with complete genetic and imaging information in order to independently replicate our results. These results build on evidence of an interaction

between APOE, cholesterol metabolism, and neurodegeneration with aging and AD and indicate the need for future studies examining this interplay.

Acknowledgments

Chapter 2, in full, is a reprint of the material as it appears in Brain Imaging and Behavior, 2011. Murphy EA; Roddey JC; McEvoy LK; Holland D; Hagler Jr. DJ; Dale AM; Brewer JB. The dissertation author was the primary investigator and author of this paper.

Data collection and sharing for this project was funded by the Alzheimer's Disease Neuroimaging Initiative (ADNI) (National Institutes of Health Grant U01 AG024904). ADNI is funded by the National Institute on Aging, the National Institute of Biomedical Imaging and Bioengineering, and through generous contributions from the following: Abbott, AstraZeneca AB, Bayer Schering Pharma AG, Bristol-Myers Squibb, Eisai Global Clinical Development, Elan Corporation, Genentech, GE Healthcare, GlaxoSmithKline, Innogenetics, Johnson and Johnson, Eli Lilly and Co., Medpace, Inc., Merck and Co., Inc., Novartis AG, Pfizer Inc, F. Hoffman-La Roche, Schering-Plough, Synarc, Inc., and Wyeth, as well as non-profit partners the Alzheimer's Association and Alzheimer's Drug Discovery Foundation, with participation from the U.S. Food and Drug Administration. Private sector contributions to ADNI are facilitated by the Foundation for the National Institutes of Health (www.fnih.org). The grantee organization is the Northern California Institute for Research and Education, and the study is coordinated by the Alzheimer's Disease

Cooperative Study at the University of California, San Diego. ADNI data are disseminated by the Laboratory for Neuro Imaging at the University of California, Los Angeles. This research was also supported by NIH grants P30 AG010129, K01 AG030514, and the Dana Foundation.

J.B.B. is supported by NINDS K02 NS067427, NIA U01 AG10483, NIA P50 AG005131, NIA RC2AG036535 and General Electric Medical Foundation and is an investigator for, and receives research funds from Janssen Alzheimer Immunotherapy. He has served on advisory boards for Elan and Avanir Pharmaceuticals, holds stock options in CorTechs Labs, Inc., and serves as an editor for the International Journal of Alzheimer's Disease; E.A.M. is supported in part by NIGMS Training Grant GM007198.

A.M.D. receives funding to his laboratory from General Electric Medical Systems as part of a Master Research Agreement with UCSD; and is a founder of, holds equity in, and serves on the scientific advisory board for CorTechs Labs, Inc. The terms of this arrangement have been reviewed and approved by UCSD in accordance with its conflict of interest policy.

References

Albers, J.J., Tollefson, J.H., Wolfbauer, G., Albright, R.E., Jr., 1992. Cholesteryl ester transfer protein in human brain. Int J Clin Lab Res 21(3), 264-6.

Arias-Vásquez, A., Isaacs, A., Aulchenko, Y.S., Hofman, A., Oostra, B.A., Breteler, M., van Duijn, C.M., 2007. The cholesteryl ester transfer protein (CETP) gene and the risk of Alzheimer's disease. Neurogenetics 8(3), 189-93.

Barzilai, N., Atzmon, G., Derby, C.A., Bauman, J.M., Lipton, R.B., 2006. A genotype of exceptional longevity is associated with preservation of cognitive function. Neurology 67(12), 2170-5.

Barzilai, N., Atzmon, G., Schechter, C., Schaefer, E.J., Cupples, A.L., Lipton, R., Cheng, S., Shuldiner, A.R., 2003. Unique lipoprotein phenotype and genotype associated with exceptional longevity. JAMA 290(15), 2030-40.

Braak, H., Braak, 1991. E., Neuropathological stageing of Alzheimer-related changes. Acta Neuropathol 82(4), 239-59.

Chen, D.W., Yang, J.F., Tang, Z., Dong, X.M., Feng, X.L., Yu, S., Chan, P., 2008. Cholesteryl ester transfer protein polymorphism D442G associated with a potential decreased risk for Alzheimer's disease as a modifier for APOE epislon4 in Chinese. Brain Res. 1187, 52-7.

Crean, S., Ward, A., Mercaldi, C.J., Collins, J.M., Cook, M.N., Baker, N.L., Arrighi, H.M., 2011. Apolipoprotein E ε4 prevalence in Alzheimer's disease patients varies across global populations: a systematic literature review and meta-analysis.

Dale, A.M., Sereno, M.I., 1993. Improved localization of cortical activity by combining EEG and MEG with MRI cortical surface reconstruction: a linear approach. J Cogn Neurosci 5, 162-176.

Dale, A.M., Fischl, B., Sereno, M.I., 1999. Cortical surface-based analysis. I. Segmentation and surface reconstruction. Neuroimage 9, 179-194.

De Gennes, J.L., Dairou, F., Gardette, J., Truffert, J., 1983. Sex hormones and metabolism of lipoproteins. Ann Endocrinol 44(1), 59-65.

Dickerson, B.C., Feczko, E., Augustinack, J.C., Pacheco, J., Morris, J.C., Fischl, B., Buckner, R.L., 2009. Differential effects of aging and Alzheimer's disease on medial temporal lobe cortical thickness and surface area. Neurobiol Aging 30(3), 432-40.

Fischl, B., Salat, D.H., Busa, E., Albert, M., Dieterich, M., Haselgrove, C., van der Kouwe, A., Killiany, R., Kennedy, D., Klaveness, S., Montillo, A., Makris, N., Rosen, B., Dale, A.M., 2002. Whole brain segmentation: automated labeling of neuroanatomical structures in the human brain. Neuron 33(3), 341-55.

Fischl, B., van der Kouwe, A., Destrieux, C., Halgren, E., Segonne, F., Salat, D.H., Busa, E., Seidman, L.J., Goldstein, J., Kennedy, D., Caviness, V., Makris, N., Rosen, B., Dale, A.M., 2004. Automatically parcellating the human cerebral cortex. Cereb Cortex 14, 11-22.

Gearing, M., Mirra, S.S., Hedreen, J.C., Sumi, S.M., Hansen, L.A., Heyman, A., 1995. The Consortium to Establish a Registry for Alzheimer's Disease (CERAD). X. Neuropathology confirmation of the clinical diagnosis of Alzheimer's disease. Neurology 45, 461-466.

Holland, D., Brewer, J.B., Hagler, D.J., Fennema-Notestine, C., Dale, A.M., and the Alzheimer's Disease Neuroimaging Initiative, 2009. Subregional neuroanatomical change as a biomarker for Alzheimer's disease. Proc Natl Acad Sci USA 106(49), 20954-20959.

Jack, C.R., Jr., Petersen, R.C., Xu, Y.C., Waring, S.C., O'Brien, P.C., Tangalos, E.G., Smith, G.E., Ivnik, R.J., Kokmen, E., 1997. Medial temporal atrophy on MRI in normal aging and very mild Alzheimer's disease. Neurology 49(3), 786-94.

Johnson, W., Harris, S.E., Collins, P., Starr, J.M., Whalley, L.J., Deary, I.J., 2007. No association of CETP genotype with cognitive function or age-related cognitive change. Neurosci Lett 420(2), 189-92.

Jovicich, J., Czanner, S., Greve, D., Haley, E., van der Kouwe, A., Gollub, R., Kennedy, D., Schmitt, F., Brown, G., Macfall, J., Fischl, B., Dale, A., 2006. Reliability in multi-site structural MRI studies: effects of gradient non-linearity correction on phantom and human data. Neuroimage 30(2), 436-43.

Joyner, A.H., Roddey, J.C., Bloss, C.S., Bakken, T.E., Rimol, LM., Melle, I., Agartz, I., Djurovic, S., Topol, E.J., Schork, N.J., Andreassen, O.A., Dale, A.M., 2009. A common MECP2 haplotype associates with reduced cortical surface area in humans in two independent populations. Proc Natl Acad Sci USA 106(36), 15483-8.

Kivipelto, M., Helkala, E.L., Laaksom, M.P., Hanninen, T., Hallikainen, M., Alhainen, K., Soininen, H., Tuomilehto, J., Nissinen, A., 2001. Midlife vascular risk factors and Alzheimer's Disease in later life: longitudinal, population based study. BMJ 322, 1447-1451.

Marcel, Y.L., McPherson, R., Hogue, M., Czarnecka, H., Zawadzki, Z., Weech, P.K., Whitlock, M.E., Tall, A.R., Milne, R.W., 1990. Distribution and concentration of cholesteryl ester transfer protein in plasma of normolipemic subjects. J Clin Invest 85, 10-17.

Mattay, V.S., Goldberg, T.E., Sambataro, F., Weinberger, D.R., 2008. Neurobiology of cognitive aging: insights from imaging genetics. Biol Psychol. 79(1), 9-22.

McEvoy, L.K., Fennema-Notestine, C., Roddey, J.C., Hagler Jr., D.J., Holland, D., Karow, D.S., Pung, C.J., Brewer, J.B., Dale, A.M. for the Alzheimer's Disease

Neuroimaging Initiative, 2009. Alzheimer Disease: Quantitative Structural Neuroimaging for Detection and Prediction of Clinical and Structural Changes in Mild Cognitive Impairment. Radiology 251(1), 195-205.

Mok, W., Chow, T.W., Zheng, L., Mack, W.J., Miller, C., 2004. Clinicopathological concordance of dementia diagnoses by community versus tertiary care clinicians. Am J Alzheimers Dis Other Demen 19, 161-165.

Murphy, E.A., Holland, D., Donohue, M., McEvoy, L.K., Hagler, D.J., Jr., Dale, A.M., Brewer, J.B., Alzheimer's Disease Neuroimaging Initiative, 2010. Six-month atrophy in MTL structures is associated with subsequent memory decline in elderly controls. Neuroimage 53(4):1310-7.

Negri-Cesi, P., Colciago, A., Celotti, F., Motta, M., 2004. Sexual differentiation of the brain: role of testosterone and its active metabolites. J Endocrinol Invest 27(6), 120-127.

Olesen, O.F., Dago, L., 2000. High density lipoprotein inhibits assembly of amyloid beta-peptides into fibrils. Biochem Biophys Res Commun. 270(1), 62-6.

Potkin, S.G., Guffanti, G., Lakatos, A., Turner, J.A., Kruggel, F., Fallon, J.H., Saykin, A.J., Orro, A., Lupoli, S., Salvi, E., Weiner, M., Macciardi, F., Alzheimer's Disease Neuroimaging Initiative, 2009. Hippocampal atrophy as quantitative trait in genome-wide association study identifying novel susceptibility genes for Alzheimer's disease. PLoS One 4(8), e6501.

Pregelj, P., 2008. Involvement of cholesterol in the pathogenesis of Alzheimer's disease: role of statins. Psychiatr Danub 20(2), 162-7.

Qureischie, H., Heun, R., Popp, J., Jessen, F., Maier, W., Schmitz, S., Hentschel, F., Kelemen, P., Kölsch, H., 2009. Association of CETP polymorphisms with the risk of vascular dementia and white matter lesions. J Neural Transm 116(4), 467-72.

Qureischie, H., Heun, R., Lütjohann, D., Popp, J., Jessen, F., Ledschbor-Frahnert, C., Thiele, H., Maier, W., Hentschel, F., Kelemen, P., Kölsch, H., 2008. CETP polymorphisms influence cholesterol metabolism but not Alzheimer's disease risk. Brain Res 1232, 1-6.

Rodríguez, E., Mateo, I., Infante, J., Llorca, J., Berciano, J., Combarros, O., 2006. Cholesteryl ester transfer protein (CETP) polymorphism modifies the Alzheimer's disease risk associated with APOE ε4 allele. J Neurol 253(2), 181-5.

Sanders, A.E., Wang, C., Katz, M., Derby, C.A., Barzilai, N., Ozelius, L., Lipton, R.B., 2010. Association of a functional polymorphism in the cholesteryl ester

transfer protein (CETP) gene with memory decline and incidence of dementia. JAMA 303(2), 150-8.

Saykin, A.J., Shen, L., Foroud, T.M., Potkin, S.G., Swaminathan, S., Kim, S., Risacher, S.L., Nho, K., Huentelman, M.J., Craig, D.W., Thompson, P.M., Stein, J.L., Moore, J.H., Farrer, L.A., Green, R.C., Bertram, L., Jack, C.R., Jr., Weiner, M.W., Alzheimer's Disease Neuroimaging Initiative, 2010. Alzheimer's Disease Neuroimaging Initiative biomarkers as quantitative phenotypes: Genetics core aims, progress, and plans. Alzheimers Dement 6(3), 265-73.

Schneider, J.A., Arvanitakis, Z., Bang, W., Bennett, D.A., 2007. Mixed brain pathologies account for most dementia cases in community-dwelling older persons. Neurology 69, 2197-2204.

Seshadri, S., Fitzpatrick, A.L., Ikram, M.A., DeStefano, A.L., Gudnason, V., Boada, M., Bis, J.C., Smith, A.V., Carassquillo, M.M., Lambert, J.C., Harold, D., Schrijvers, E.M., Ramirez-Lorca, R., Debette, S., Longstreth, W.T. Jr, Janssens, A.C., Pankratz, V.S., Dartigues, J.F., Hollingworth, P., Aspelund, T., Hernandez, I., Beiser, A., Kuller, L.H., Koudstaal, P.J., Dickson, D.W., Tzourio, C., Abraham, R., Antunez, C., Du, Y., Rotter, J.I., Aulchenko, Y.S., Harris, T.B., Petersen, R.C., Berr, C., Owen, M.J., Lopez-Arrieta, J., Varadarajan, B.N., Becker, J.T., Rivadeneira, F., Nalls, M.A., Graff-Radford, N.R., Campion, D., Auerbach, S., Rice, K., Hofman, A., Jonsson, P.V., Schmidt, H., Lathrop, M., Mosley, T.H., Au, R., Psaty, B.M., Uitterlinden, A.G., Farrer, L.A., Lumley, T., Ruiz, A., Williams, J., Amouyel, P., Younkin, S.G., Wolf, P.A., Launer, L.J., Lopez, O.L., van Duijn, C.M., Breteler, M.M.; CHARGE Consortium; GERAD1 Consortium; EADI1 Consortium, 2010. Genome-wide analysis of genetic loci associated with Alzheimer disease. JAMA 303(18), 1864-5.

Sled, J.G., Zijdenbos, A.P., Evans, A.C., 1998. A nonparametric method for automatic correction of intensity nonuniformity in MRI data. IEEE Trans Med Imaging 17(1), 87-97.

Sorlí, J.V., Corella, D., Francés, F., Ramírez, J.B., González, J.I., Guillén, M., Portolés, O., 2006. The effect of the APOE polymorphism on HDL-C concentrations depends on the cholesterol ester transfer protein gene variation in a Southern European population. Clin Chim Acta 366(1-2), 196-203.

Stein, J.L., Hua, X., Morra, J.H., Lee, S., Hibar, D.P., Ho, A.J., Leow, A.D., Toga, A.W., Sul, J.H., Kang, H.M., Eskin, E., Saykin, A.J., Shen, L., Foroud, T., Pankratz, N., Huentelman, M.J., Craig, D.W., Gerber, J.D., Allen, A.N., Corneveaux, J.J., Stephan, D.A., Webster, J., DeChairo, B.M., Potkin, S.G., Jack, C.R., Jr., Weiner, M.W., Thompson, P.M., Alzheimer's Disease Neuroimaging Initiative, 2010. Genome-wide analysis reveals novel genes influencing temporal

lobe structure with relevance to neurodegeneration in Alzheimer's disease. Neuroimage 51(2), 542-54.

Thompson, J.F., Lira, M.E., Durham, L.K., Clark, R.W., Bamberger, M.J., Milos, P.M., 2003. Polymorphisms in the CETP gene and association with CETP mass and HDL levels. Atherosclerosis 167, 195-204.

Yamada, T., Kawata, M., Arai, H., Fukasawa, M., Inoue, K., Sato, T., 1995. Astroglial localization of cholesteryl ester transfer protein in normal and Alzheimer's disease brain tissues. Acta Neuropathol. 90(6), 633-6.

CHAPTER 3:

SPATIAL AND TEMPORAL PATTERNS OF CHANGE IDENTIFIED IN LONGITUDINAL STUDY OF LEWY BODY DEMENTIA USING VOLUMETRIC AND DIFFUSION TENSOR IMAGING

Abstract

Although neurodegenerative change in Alzheimer's disease has been fairly well characterized by longitudinal neuroimaging, relatively few studies have addressed the Lewy body spectrum disorders. Magnetic resonance (MR) imaging techniques such as volumetry and diffusion tensor imaging (DTI) provide a quantitative means to assess spatial and temporal patterns of neurodegeneration in these disorders. One-hundred and fifty subjects in the following diagnostic groups were prospectively enrolled in a longitudinal MR imaging study: probable Alzheimer's disease (AD, n=28), probable dementia with Lewy bodies (DLB, n=31), probable Parkinson's disease dementia (PDD, n=20), Parkinson's disease with questionable cognitive impairment (PD-other, n=7), Parkinson's disease without cognitive impairment (PD, n=21) and healthy elderly controls (NC, n = 43). Subjects were scanned longitudinally for the acquisition of high-resolution structural images and 51-direction diffusion-weighted data. Baseline volumetrics, volumetric change and DTI data were assessed at both the individual and diagnostic group level. Additionally, post-mortem pathological data was collected and compared to pre-mortem imaging data for eleven subjects who passed away during the study. Volumetric data revealed a pattern of change in the

Lewy body spectrum disorders intermediate between that of AD and healthy controls whereas DTI data revealed relatively equivalent severities between AD and DLB, suggesting that Lewy body dementia may be characterized by microstructural disruption and dysfunction rather than neuronal loss.

Introduction

Among neurodegenerative diseases, Alzheimer's disease (AD) is the most prevalent and best characterized using neuroimaging. There are relatively few neuroimaging studies aimed at the Lewy body (LB) spectrum disorders even though they constitute the second most common form of neurodegenerative dementia after AD and account for over 15 percent of all dementia cases at autopsy (McKeith et al, 2004). There have been especially few studies designed to image subjects longitudinally in order to detect patterns of change in these disorders. A more thorough characterization of LB disease using non-invasive neuroimaging is needed to address clinical need and enable insight into the biologic basis of these disorders.

Specifically, neuroimaging may provide a clinically useful means to enhance early detection and differential diagnosis by revealing a unique spatial and temporal pattern of brain change. Like AD, LB disorders are currently diagnosed and monitored *in vivo* using clinical observation as there is no definitive pre-mortem diagnosis (Lewis et al, 2009). Clinical diagnosis of these disorders tends to have high specificity (90-100%) but notoriously low sensitivity (49-63%) (Luis et al, 1999) due to significant heterogeneity in the clinical presentation and substantial overlap with the

clinical presentations of other neurodegenerative diseases including AD. However, treatment decisions for LB disease do necessitate accurate differential diagnosis from other neurodegenerative diseases. For example, it is best to avoid the use of neuroleptic medications due to the potential of adverse reactions.

Additionally, neuroimaging may allow better assessment of disease progression and treatment effects, which is especially important in guiding therapeutic trials aimed at these diseases. Further, a linked examination between *in vivo* neuroimaging and post-mortem pathology is critical to understand the neuroanatomical substrate for cognitive changes.

The LB spectrum disorders are clinically challenging due to a fundamental lack of understanding as to precisely how the brain changes in these disorders—both at a cellular and gross anatomical level. It is even unclear whether the disorders in this spectrum represent distinct pathological syndromes or temporal variations of a single pathology (Antonelli et al, 2010). The spectrum's two main constituents, dementia with Lewy bodies (DLB) and Parkinson's disease dementia (PDD), are currently distinguished by the clinical "one-year rule" wherein a patient whose cognitive impairment occurs prior to the onset of Parkinsonian motor symptoms or within one year of the onset of motor symptoms is designated as DLB, and a Parkinson's disease (PD) patient with later onset cognitive impairment is designated as PDD (McKeith et al, 2004). Not all subjects with PD do experience cognitive impairment, but prevalence rates for dementia in PD are roughly 30 percent (Aarsland et al, 2008), and the risk of eventual development of dementia in PD is believed to be as high as 80

percent (Hely et al, 2008). Further, a significant portion of PD patients have sub-threshold cognitive deficits, which is sometimes diagnosed as PD-mild cognitive impairment (PD-MCI) (Caviness et al, 2007).

Cognitive impairment in these disorders is typified by fluctuations in attention, frontal executive dysfunction, visuospatial deficits, recurrent visual hallucinations and impairments in language and memory. Dysfunction tends to be more severe in DLB than in PDD, and DLB patients tend to experience a shorter disease course than PDD patients. Clinical presentation is highly variable and often shares considerable overlap with the cognitive profile of AD; however, AD tends to involve greater memory impairment whereas LB dementia is characterized by greater attentional and visuospatial impairment (Calderon et al, 2001).

There is debate in the literature regarding the pathophysiological changes that underlie cognitive impairment in LB dementia. The hallmark pathological feature is abnormal aggregation of the presynaptic protein α-synuclein into Lewy body inclusions in neurons and glial cells, but it is unclear the degree to which Lewy bodies explain the clinical dementia that occurs in these disorders. There is evidence, however, that Lewy body density strongly correlates with cognitive impairment seemingly independent of other brain pathologies (Vernon et al, 2010). Lewy body burden does tend to be higher in DLB brains than in PDD brains, which is consistent with the more severe cognitive impairment found in DLB (Lee et al, 2009).

Location of Lewy bodies in the brain varies and seems to be relevant. Braak et al (2003) proposed a six-stage system suggesting a predictable progression of LB

pathology throughout the brain, starting in the brain stem and olfactory bulb and eventually progressing to the entire cortex. Dementia often occurs in the context of abundant cortical and limbic Lewy bodies (Braak et al, 2005), but the extent to which Lewy bodies exert functional effects on cognition is unclear.

The pathology of LB disorders is further confounded by a high prevalence of concomitant Alzheimer's-related pathology in patients with these disorders, especially in patients with DLB. It has thus been posited that the likelihood a clinical dementia is due to Lewy-related pathology is directly related to the severity of Lewy-related pathology and inversely related to the severity of concomitant Alzheimer's-related pathology (McKeith et al, 2005). In fact, the Third Report of the DLB Consortium criteria requires that the pathologic diagnosis of DLB be made by considering both AD and LB pathologies (McKeith et al, 2005). The strong rate of co-occurrence between Lewy-related and Alzheimer's-related pathology and a number of *in vitro* studies demonstrating protein interactions between α-synuclein, tau and β-amyloid (Deramecourt et al, 2006; Masliah et al, 2001; Jensen et al, 1999; Lashhley et al, 2008; Rowe et al, 2007; Galpern and Lang, 2006; Kazmierczak et al, 2008) suggest the possibility of a linked pathological cascade whereby the presence of one pathology may increase susceptibility to the other and the same brain regions may be affected by both. This pathological link may also explain the strong overlap in clinical presentation between many AD and DLB patients.

A number of additional theories have been proposed for the etiology of cognitive impairment in LB disorders, including striatal dysfunction that impacts the

frontal lobe, primary frontal lobe dysfunction, global neurotransmitter system deficits resulting in widespread cortical dysfunction, and cerebrovascular disease (Silbert and Kaye, 2010).

The neuroimaging profile of these disorders using magnetic resonance imaging (MRI) is likewise poorly understood. In general, LB dementia is believed to have a subcortical rather than cortical pattern of atrophy with relative sparing of medial temporal lobe structures compared to AD (Tam et al, 2005). The most consistent imaging findings seem to be striatal atrophy (Apostolova et al, 2010), scattered cortical loss in frontal and parietal lobes (Whitwell et al, 2007; Junque et al, 2005; Weintraub et al, 2011) and medial temporal lobe atrophy intermediate between healthy aging and AD (Tam et al, 2005) with particular involvement of the amygdala (Marui et al, 2002; Junque et al, 2005). More severe atrophy is typically found in DLB than in PDD (Beyer et al, 2007; Sanchez et al, 2009). Very few diffusion tensor imaging (DTI) studies have been applied to LB dementia, but those that have been done seem to implicate a role for white matter disease, particularly in parieto-occipital fiber tracts (Catani et al, 2003; Matsui et al, 2007; Bozzali et al 2005; Watson et al, 2012; Lee et al, 2010). Even fewer longitudinal studies have been done to track brain changes over time in individual subjects to assess progression of these diseases.

To more thoroughly characterize the neuroimaging profile of LB dementia, we prospectively enrolled 51 subjects with LB dementia (31 DLB and 20 PDD), 28 AD subjects, 21 subjects with PD and no cognitive impairment, 7 subjects with PD and

questionable cognitive impairment, and 43 healthy elderly controls in a longitudinal MRI study involving volumetric and diffusion-weighted imaging.

Methods

Study Population

A total of 150 subjects were recruited and prospectively enrolled in this study between May 2007 and December 2012. Written informed consent was obtained from all subjects or the subjects' legal guardians, and the study was conducted with institutional review board approval and in compliance with Health Insurance Portability and Accountability Act regulations. General inclusion criteria were men and women between the ages of 55 and 100 years old with a clinical diagnosis of Alzheimer's disease (AD, n=28), dementia with Lewy bodies (DLB, n=31), Parkinson's disease dementia (PDD, n=20), Parkinson's disease with questionable cognitive impairment (PD-other, n=7), Parkinson's disease without cognitive impairment (PD, n=21) or cognitively normal (NC, n=43). The PD-other group consisted of 4 subjects referred to us by clinicians as having PD-Mild Cognitive Impairment (PD-MCI) and 3 subjects referred to us by clinicians as having PD with questionable dementia. Subjects with MR imaging contraindications and/or history of symptomatic stroke or other major neurologic or psychiatric disorder were excluded.

Group demographic data are presented in Table 1. The PD group was significantly younger in age than the DLB and PDD groups, reflecting the earlier age at onset of PD versus DLB and PDD. The groups did not significantly differ in

Table 3.1: Subject characteristics

Clinical Diagnosis	**Age (y)**	**Males (n): Fem (n)**	**Education (y)**	**MMSE Score**, Mean (Min, Max)
AD (*n* = 28)	74.45 ± 10.15	12:16	15.37 ± 2.88	21.59 (7, 28)
DLB (*n* = 31)	76.27 ± 7.96	23:8	15.36 ± 3.69	20.74 (4, 30)
PDD (*n* = 20)	76.11 ± 9.11	12:8	15.74 ± 2.35	24.21 (13, 30)
PD-Other (*n* = 7)	71.71 ± 7.11	7:0	16.43 ± 2.15	26.29 (23, 29)
PD (*n* = 21)	67.90 ± 8.03	17:4	16.83 ± 2.77	29.11 (27, 30)
NC (*n* = 43)	73.36 ± 8.42	21:22	17.09 ± 2.27	29.16 (27, 30)
Significant Comparisons ($p < .01$)	PD < DLB, PDD			AD, DLB < PDD, PD-Other < PD, NC

Data are given as mean ± SD unless otherwise specified. MMSE = Mini Mental State Exam. PD subjects were significantly younger than DLB and PDD subjects. AD and DLB subjects were matched on MMSE score at baseline and significantly more impaired than all other subjects. PDD and PD-other subjects were more impaired than PD and NC subjects.

education levels, although there was a trend of lower education among the AD, DLB and PDD groups compared to the PD and NC groups. MMSE scores were significantly lower in the AD and DLB groups, intermediate in the PDD and PD-other groups, and higher in the PD and NC groups. AD and DLB groups were matched on dementia severity level.

Baseline volumetric data was analyzed for 24 AD, 28 DLB, 15 PDD, 5 PD-other, 18 PD and 38 NC subjects. Exclusion of baseline volumetric data was due to excessive motion (2 AD, 3 DLB, 4 PDD, 2 PD-other, 3 PD, 3 NC), subject inability to tolerate duration of complete scan (1 AD, 1 PDD), imaging processing error (1 AD) and incidental mass findings (2 NC). Of subjects with valid baseline volumetric data, longitudinal volumetric data was collected for all subjects willing and able to participate in follow-up visits at 6 months, 12 months, 18 months and 24 months after the initial visit. Longitudinal data with at least one follow-up visit was available for 14 AD, 6 DLB, 9 PDD, 5 PD-other, 12 PD and 30 NC subjects. DTI data was collected on a subset of subjects who could tolerate additional scan time consisting of 18 AD, 17 DLB, 9 PDD, 4 PD-other, 11 PD and 32 NC subjects. During the study period, 21 subjects passed away, and autopsy data was available for 11 of these subjects (Table B) at the time of publication.

MR Imaging Acquisition

MRI was performed at the UCSD Radiology Imaging Laboratory on a General Electric 1.5 T EXCITE HD scanner with an eight-channel phased-array head coil.

Image acquisitions included a conventional three-plane localizer, GE calibration scan, a high-resolution, three-dimensional, T1-weighted volume (TE=3.8ms, TR=8.5 ms, TI=500 ms; flip angle 10º; matrix size = 192 x 192, voxel size = 0.9375 x 0.9375 x 1.2000 mm) and three diffusion-weighted sequences. Diffusion data were acquired using single-shot echo-planar imaging with isotropic 2.5 mm voxels (matrix size = 96 x 96, 47 axial slices, slice thickness = 2.5 mm) covering the entire cerebrum. One volume series was acquired with 51 diffusion gradient directions using a *b*-value of 1000 s/mm² with an additional *b*=0 volume. For use in nonlinear β0 distortion correction, an additional *b*=0 volume was acquired with reverse phase encoding polarity.

Image Processing

Image files in DICOM format were transferred to a Linux-based system for processing via a customized, automated processing stream written in MATLAB and C++. Baseline T1-weighted volumes were reviewed for quality and automatically corrected for spatial distortion due to gradient nonlinearity (Jovicich et al, 2006) and B1 field inhomogeneity (Sled et al, 1998). Volumetric segmentation (Fischl et al, 2002) and cortical surface reconstruction (Dale et al, 1999; Fischl et al 1999; Fischl and Dale, 2000) and parcellation (Fischl et al 2004, Desikan et al 2006) were used to quantify baseline cortical thickness and subcortical volumes within distinct regions of interest (ROIs) using a locally modified version of the FreeSurfer software package (version 3.02) as described in detail elsewhere (Holland et al, 2009). Results from

each of these automated steps were inspected for accuracy and manual corrections were applied as necessary by EAM, who was trained by experts in the field and has three years experience in editing data from more than 100 examinations.

The methods to obtain longitudinal volumetric change were developed at the Multimodal Imaging Laboratory, University of California, San Diego and are described in detail in Holland et al (2009). Briefly, follow-up images were fully affine-registered to the baseline images using 12 parameters and corrected for intensity nonuniformity using an interative process. Nonlinear registration was then used to align voxel centers in the baseline with the appropriate location in the follow-up scans, and a volume-change field was calculated. This field was averaged over each ROI to compute the percentage change from baseline. This longitudinal analysis method has been demonstrated to be free of bias from overestimations of change in serial registration, a bias that is often present in other longitudinal analysis methods (Thompson and Holland, 2011). Additionally, this method has been validated using models where amount of change was known and where noise was added to approximate that seen in human brain imaging of demented patients. In these studies, technical measurement error for the computed change in volume was within 0.2 percent of the structure volume. That is, for a 6000 mm^3 hippocampal volume undergoing a change of 1 percent, the technical measurement error in estimating the 60 mm^3 volumetric change would be ±12 mm^3 in an individual subject if voxels were each 1mm isotropic (Murphy et al., 2010).

T1-weighted volumes underwent a secondary, fully-automated segmentation using the commercially available NeuroQuant software, which has been validated against manual methods and has obtained 501K approval by the Food and Drug Administration as a device for providing quantitative segmental volumes. The procedure produces volumetric data for certain regions of interest in the aged population as well as age-related percentiles for each subject's volumetric data as compared to a normative database (Brewer, 2009).

Processing of diffusion-weighted images is described in full in Hagler et al (2009). Five preprocessing steps were performed: (1) head motion between scans was removed by rigid body registration between the *b*=0 images of each DW scan; (2) within-scan motion was removed by calculating diffusion tensors, synthesis of DW volumes from those tensors, and rigid body registration between each data volume and its corresponding synthesized volume; (3) image distortion in the DW volumes caused by eddy currents was minimized by nonlinear optimization; (4) image distortion caused by magnetic susceptibility artifacts was minimized with a nonlinear β0-unwarping method; and (5) images were resampled using linear interpolation to 1.875 mm^3 isotropic voxels. Fiber tract values for fractional anisotropy (FA), average diffusion coefficient (ADC) and fiber number were obtained using a probabilistic diffusion tensor atlas developed at the Multimodal Imaging Laboratory, University of California, San Diego using software written in Matlab and C++. T1-weighted images were used to nonlinearly register the brain to common space, and diffusion tensor orientation estimates were compared with the atlas to obtain a map of the relative

probability that a voxel belongs to a particular fiber given the location and similarity of diffusion orientations. Average measures were calculated for each fiber ROI, weighted by fiber probability, so that voxels with low probability of belonging to a given fiber contributed minimally to average values. Visual quality control was done for the unwarping, registration and fractional anisotropy mapping.

Statistical Analysis

All statistical analyses were performed using PASW Statistics 18. Analyses of variance followed by two-sample *t*-tests were used to compare continuous demographic and imaging measures between the diagnostic groups. All *t*-test results made no assumption of equal variance between groups. Uncorrected *p*-values < .01 were considered significant before Bonferroni correction for multiple comparisons was applied. Significances from before and after correction for multiple comparisons are given. Prior to the analyses, the effects of sex and age were regressed from all brain measures, and intracranial volume (ICV) was regressed from all subcortical volume measures. The volumetric investigation was restricted to particular regions of interest chosen because either (a) they are regions known to differentiate AD data from healthy control subject data (McEvoy et al, 2009) or (b) they are regions believed to be affected in LB dementia. These regions include bilateral amygdala, hippocampus, pallidum, putamen, caudate, thalamus, lateral ventricle, inferior lateral ventricle, caudal anterior cingulate gyrus, rostral anterior cingulate gyrus, entorhinal cortex, fusiform gyrus, inferior temporal gyrus, middle temporal gyrus, superior

temporal gyrus, lateral orbitofrontal cortex, medial orbitofrontal cortex, parahippocampal gyrus, postcentral gyrus, precuneus, superior parietal gyrus and supramarginal gyrus. Exploration of diffusion-weighted data was likewise restricted to the following fiber tracts and regions of interest: fornix, cingulate cingulum, parahippocampal cingulum, inferior longitudinal fasiculus (ILF), inferior-fronto-occipital fasiculus (IFOF), corpus callosum, superior longitudinal fasiculus (SLF), temporal SLF, parietal SLF, brain stem, amygdala, hippocampus, pallidum, putamen and caudate.

Results

Baseline Volumetrics: Subcortical Volumes

There were no statistically significant differences in subcortical volumes between PD and NC subjects. In general, subjects with DLB and PDD demonstrated volumes intermediate between that of AD subjects and non-demented subjects (PD and NC), with a trend toward greater severity in DLB than PDD (Figure 1). Whole brain volumes exhibited this pattern with statistical significance.

In comparison to non-demented subjects, DLB and PDD subjects had significantly larger lateral ventricles and inferior lateral ventricles bilaterally and smaller left thalami, left hippocampus and left amygdala. Additionally, DLB subjects had smaller right thalami, right pallidum, right hippocampus and right amygdala. After correction for multiple comparisons, differences with PDD only remained significant in the left inferior lateral ventricle and left hippocampus.

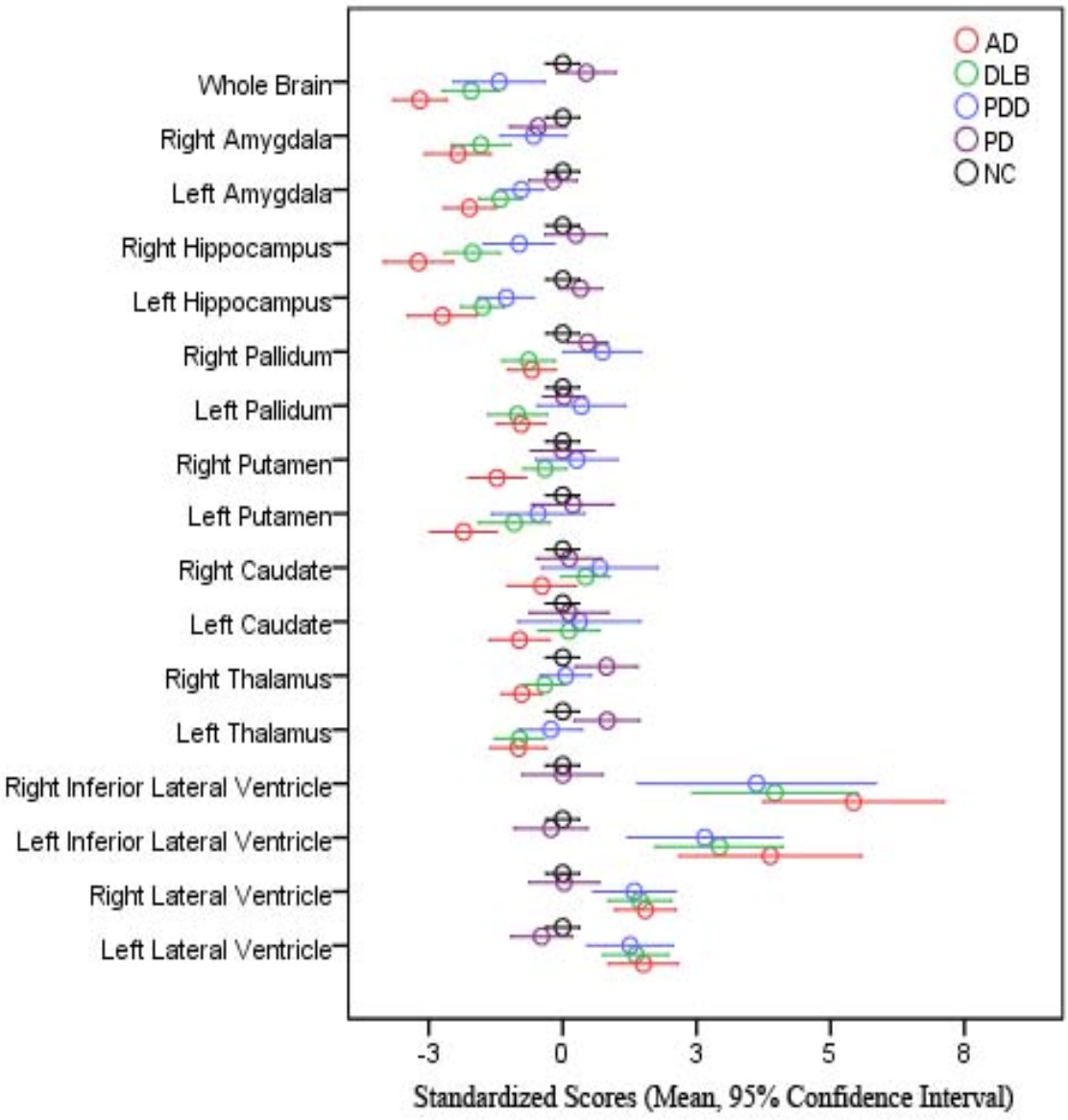

Figure 3.1: Mean of standardized subcortical volumes at baseline by diagnostic group. A value of zero represents what is expected in a normal control of a given age and gender. Error bars represent 95% confidence intervals. Subcortical regions of interest were selected *a priori* as being either regions known to differentiate AD data from healthy control subject data (McEvoy et al, 2009) or regions believed to be affected in the Lewy body spectrum disorders.

In comparison to AD subjects, DLB subjects had significantly larger right putamen volume. PDD subjects had significantly larger volumes than AD subjects in the right thalamus, right putamen, right pallidum, bilateral hippocampus and bilateral amygdala. Of these, the only difference that survived correction for multiple comparisons was that PDD subjects had larger right hippocampal volumes than AD subjects.

PD subjects with questionable cognitive impairment demonstrated volumes intermediate between that of PDD subjects and non-demented subjects.

Baseline Volumetrics: Cortical Thickness

Similar to the pattern seen in subcortical structures, subjects with DLB and PDD demonstrated cortical thickness intermediate between that of AD subjects and non-demented subjects (PD and NC), with a trend toward greater severity in DLB than PDD (Figure 2). The only significant difference in cortical thickness between PD and NC subjects was that PD subjects had greater right inferior temporal thickness, though this did not survive correction for multiple comparisons.

Compared to non-demented subjects, DLB and PDD subjects had decreased thickness in bilateral fusiform, right inferior temporal, right middle temporal, left lateral orbitofrontal, left medial orbitofrontal, right parahippocampal, left postcentral, and bilateral superior temporal. Additionally, DLB subjects had decreased thickness in bilateral entorhinal, left inferior temporal, bilateral isthmus cingulate, left middle temporal, right lateral orbitofrontal, right medial orbitofrontal, left parahippocampus,

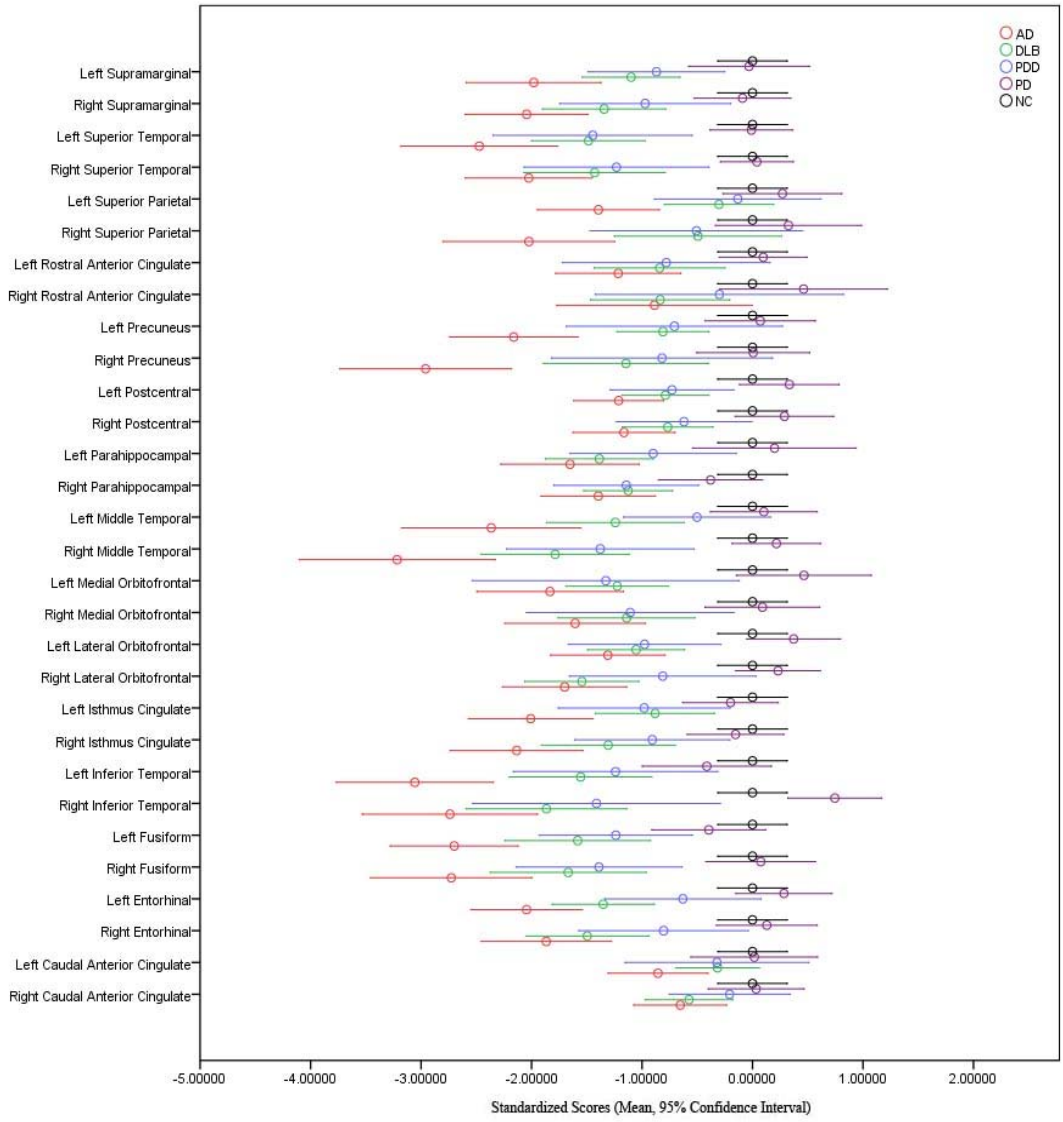

Figure 3.2: Mean of standardized cortical thicknesses at baseline by diagnostic group. A value of zero represents what is expected in a normal control of a given age, gender and intracranial volume. Error bars represent 95% confidence intervals. Cortical regions of interest were selected *a priori* as being either regions known to differentiate AD data from healthy control subject data (McEvoy et al, 2009) or regions believed to be affected in the Lewy body spectrum disorders.

right postcentral, bilateral precuneus and bilateral supramarginal. After correction for multiple comparisons, differences between non-demented and DLB subjects remained significant in all regions except left isthmus cingulate, bilateral precuneus and right medial orbitofrontal. Differences between non-demented and PDD subjects only remained significant in right fusiform, right inferior temporal, left lateral orbitofrontal and left postcentral.

When compared to AD, DLB and PDD showed spared thickness in the left fusiform, left inferior temporal and right precuneus. Additionally, DLB had spared thickness in the left isthmus cingulate, left precuneus and bilateral superior parietal. PDD had spared thickness in left entorhinal and bilateral middle temporal. After correction for multiple comparisons, DLB continued to show spared thickness in bilateral precuneus and DLB showed spared thickness in left middle temporal.

Again, PD subjects with questionable cognitive impairment demonstrated cortical thickness intermediate between that of PDD subjects and non-demented subjects.

Longitudinal Volumetrics

Fewer significant comparisons were found at the diagnostic group level in the longitudinal volumetric data, likely due to the decreased sample size with follow-up data; however examination of longitudinal data at the level of individual subjects allows subjective comparison of spatial and temporal patterns (Figures 3-8). Whole brain atrophy rates were 1.58% in AD, 0.45% in DLB, 0.26% in PDD, 0.60% in PD-

other, 0.28% in PD and 0.66% in NC. Whole brain atrophy was significantly greater in AD than in PDD, PD-other, PD and NC (Figure 9).

In no regions did longitudinal change meet statistical significance for differing between DLB and PDD subjects and non-demented subjects. However, when compared to AD subjects, DLB and PDD subjects were shown to have significantly slower decline in the left fusiform, left middle temporal, left precuneus and left superior parietal. Additionally, PDD subjects were shown to have significantly slower decline in the right isthmus cingulate, right hippocampus and right rostral anterior cingulate. After correction for multiple comparisons, all differences between PDD and AD subjects remained significant except in the left precuneus and right rostral anterior cingulate. The only difference that remained significant between DLB and AD subjects was in the left fusiform.

Diffusion Tensor Imaging: Fiber Number

Fiber number showed a binary separation between demented (AD, DLB, PDD) and non-demented (NC, PD) subjects with a high degree of overlap between AD and DLB subjects and more intermediate values in PDD subjects (Figure 10).

When compared to non-demented subjects, DLB subjects exhibited decreased fiber number in the right fornix, bilateral cingulate cingulum, bilateral inferior longitudinal fasiculus (ILF), bilateral inferior-fronto-occipital fasiculus (IFOF), corpus callosum, bilateral superior longitudinal fasiculus (SLF), bilateral temporal SLF and bilateral parietal SLF. After correction for multiple comparisons, the trend remained

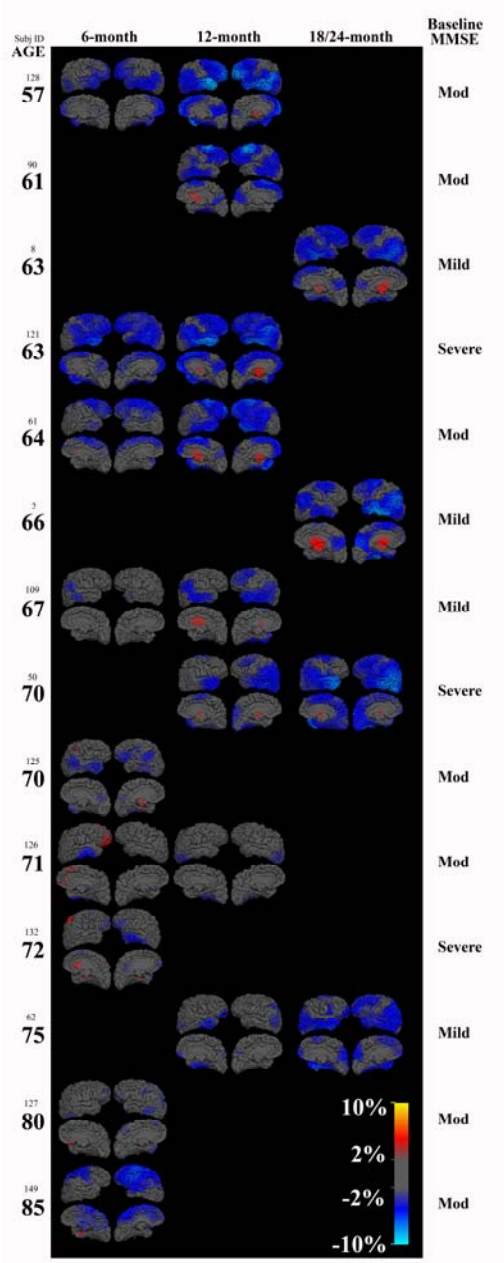

Figure 3.3: Longitudinal data depicted on the cortical surface of 14 individual subjects with a clinical diagnosis of probable Alzheimer's disease. Each individual cortical surface is overlain with a heat-map representation of the estimates of volumetric change at six months, 12 months and 18-24 months. The color scale bar depicts percent volumetric change with blue representing shrinkage and red expansion. Each subject's ID and baseline age are listed to the left, and dementia severity level to the right. Dementia severity level was determined by baseline MMSE score, where Mild = 25-30, Moderate = 18-24 and Severe <18.

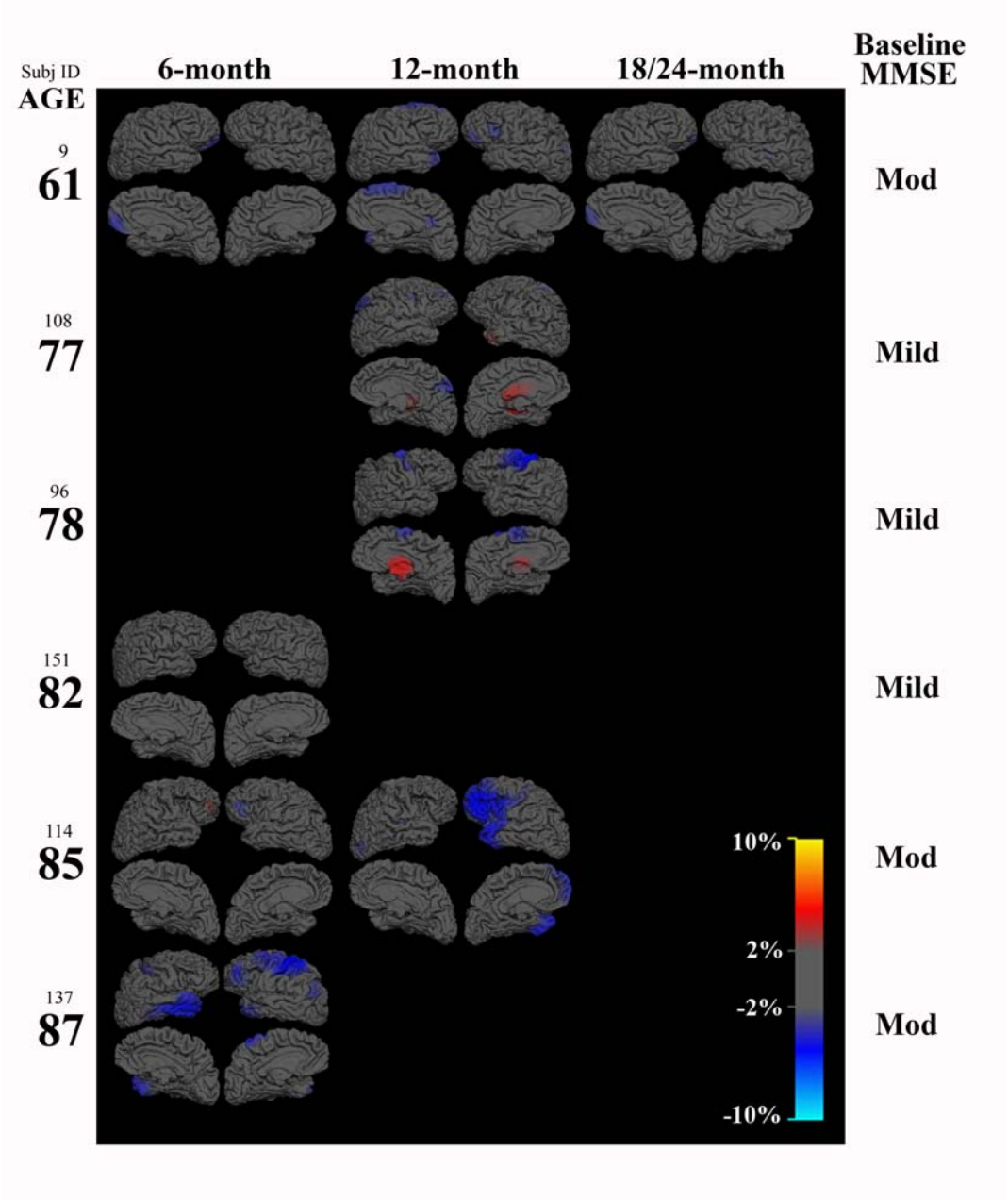

Figure 3.4: Longitudinal data depicted on the cortical surface of six individual subjects with a clinical diagnosis of probable dementia with Lewy bodies (DLB). Each individual cortical surface is overlain with a heat-map representation of the estimates of volumetric change at six months, 12 months and 18-24 months. The color scale bar depicts percent volumetric change with blue representing shrinkage and red expansion. Each subject's ID and baseline age are listed to the left, and dementia severity level to the right. Dementia severity level was determined by baseline MMSE score, where Mild = 25-30, Moderate = 18-24 and Severe <18.

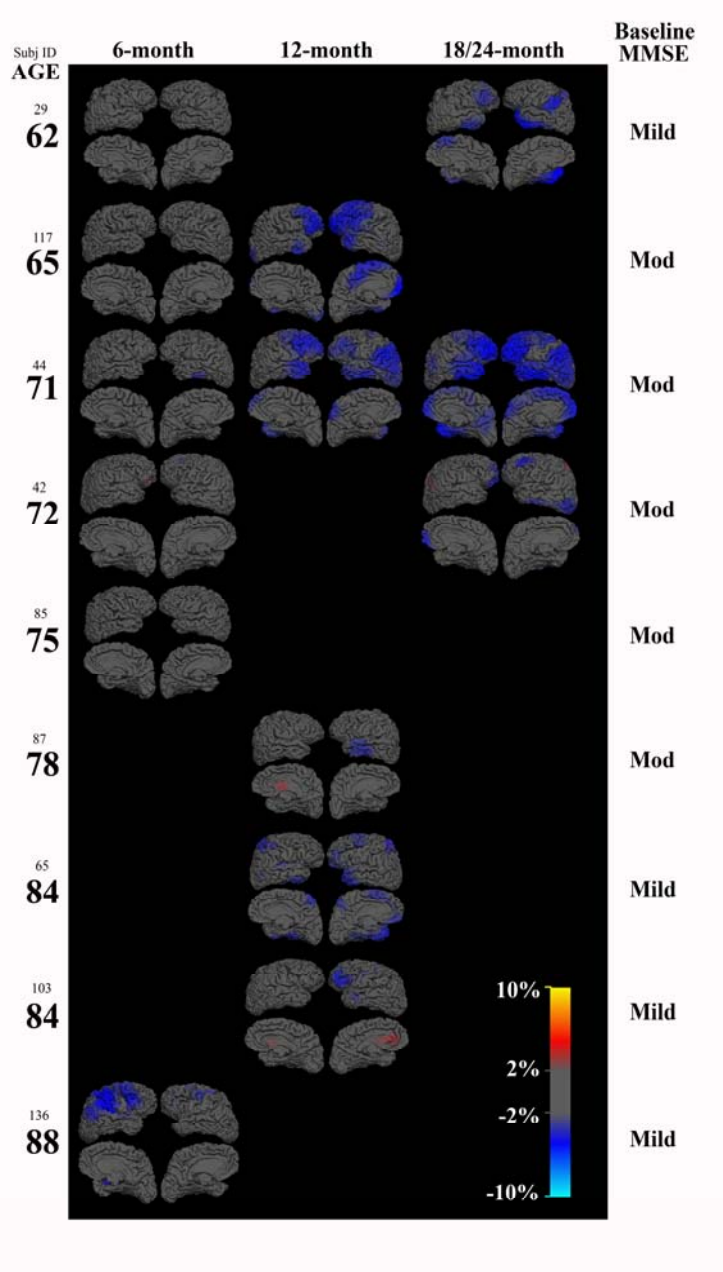

Figure 3.5: Longitudinal data depicted on the cortical surface of nine individual subjects with a clinical diagnosis of probable Parkinson's disease dementia (PDD). Each individual cortical surface is overlain with a heat-map representation of the estimates of volumetric change at six months, 12 months and 18-24 months. The color scale bar depicts percent volumetric change with blue representing shrinkage and red expansion. Each subject's ID and baseline age are listed to the left, and dementia severity level to the right. Dementia severity level was determined by baseline MMSE score, where Mild = 25-30, Moderate = 18-24 and Severe <18.

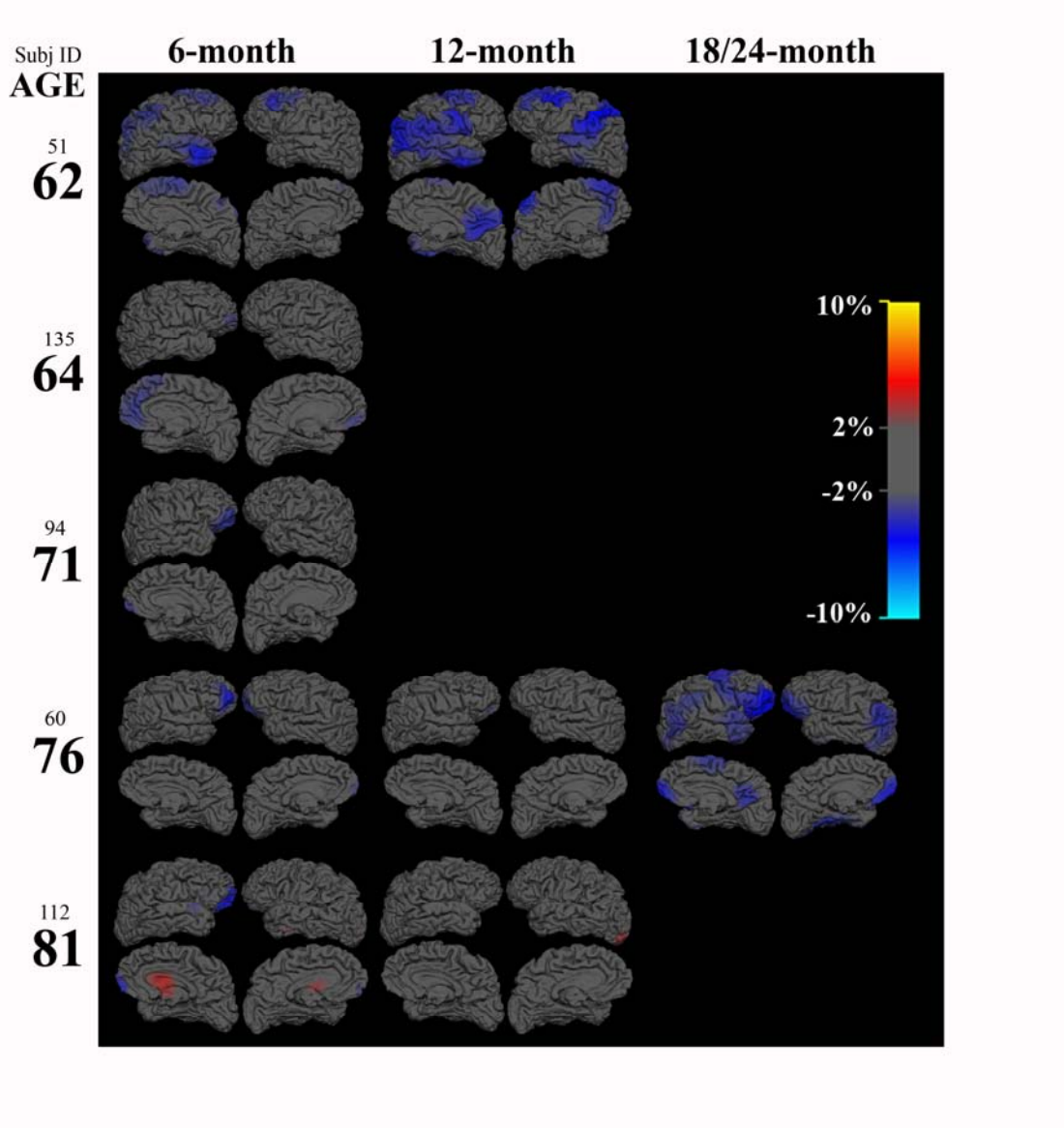

Figure 3.6: Longitudinal data depicted on the cortical surface of five individual subjects with a clinical diagnosis of either Parkinson's disease with mild cognitive impairment (PD-MCI) or Parkinson's disease with questionable dementia. Each individual cortical surface is overlain with a heat-map representation of the estimates of volumetric change at six months, 12 months and 18-24 months. The color scale bar depicts percent volumetric change with blue representing shrinkage and red expansion. Each subject's ID and baseline age are listed to the left.

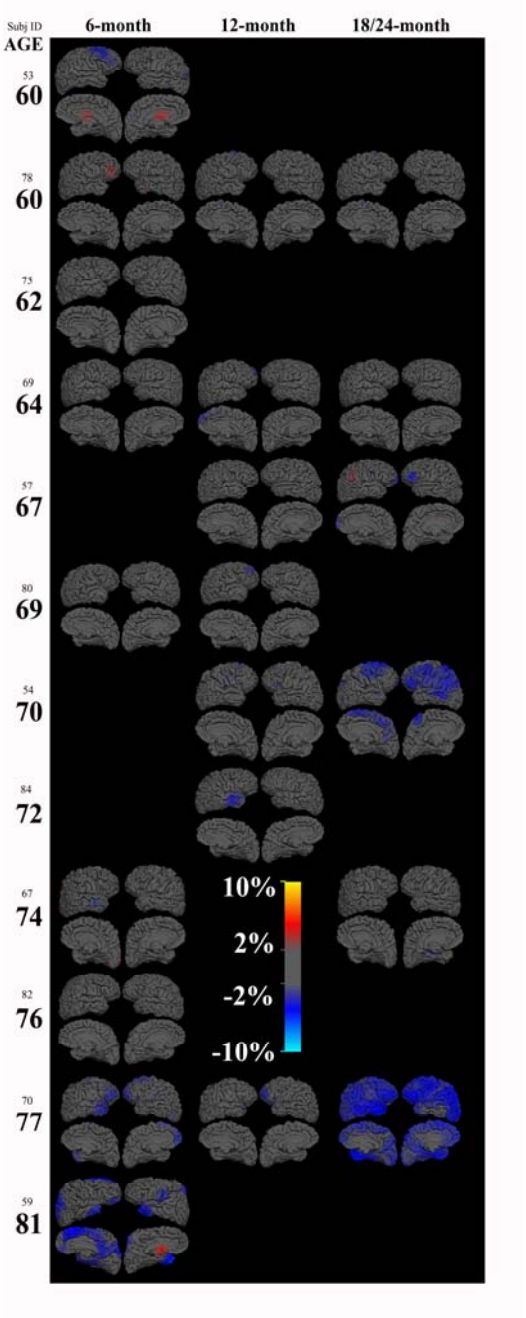

Figure 3.7: Longitudinal data depicted on the cortical surface of 12 individual subjects with a clinical diagnosis of Parkinson's disease without cognitive impairment. Each individual cortical surface is overlain with a heat-map representation of the estimates of volumetric change at six months, 12 months and 18-24 months. The color scale bar depicts percent volumetric change with blue representing shrinkage and red expansion. Each subject's ID and baseline age are listed to the left.

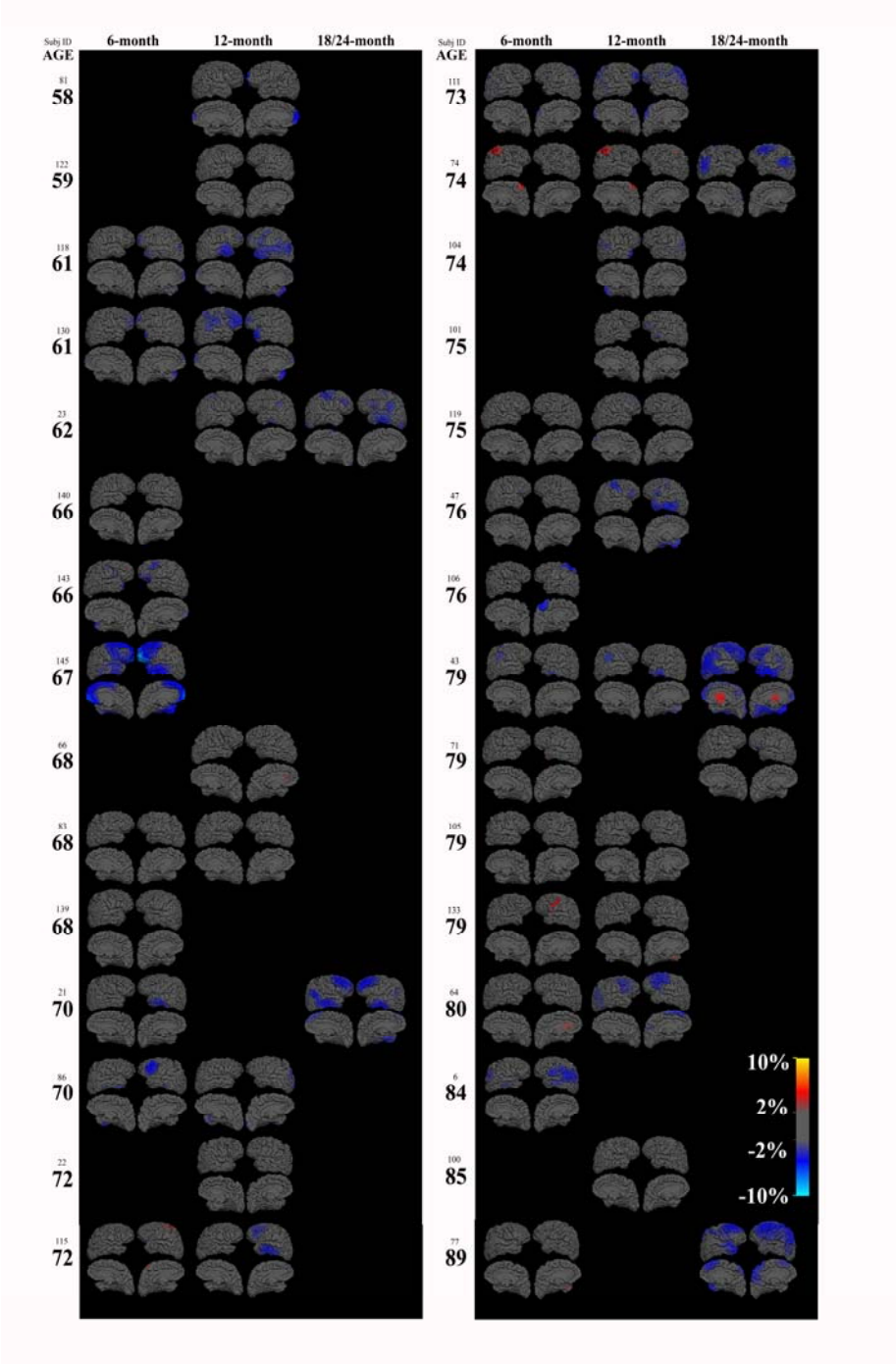

Figure 3.8: Longitudinal data depicted on the cortical surface of 30 individual subjects with normal cognition. Each individual cortical surface is overlain with a heat-map representation of the estimates of volumetric change at six months, 12 months and 18-24 months. The color scale bar depicts percent volumetric change with blue representing shrinkage and red expansion. Each subject's ID and baseline age are listed to the left.

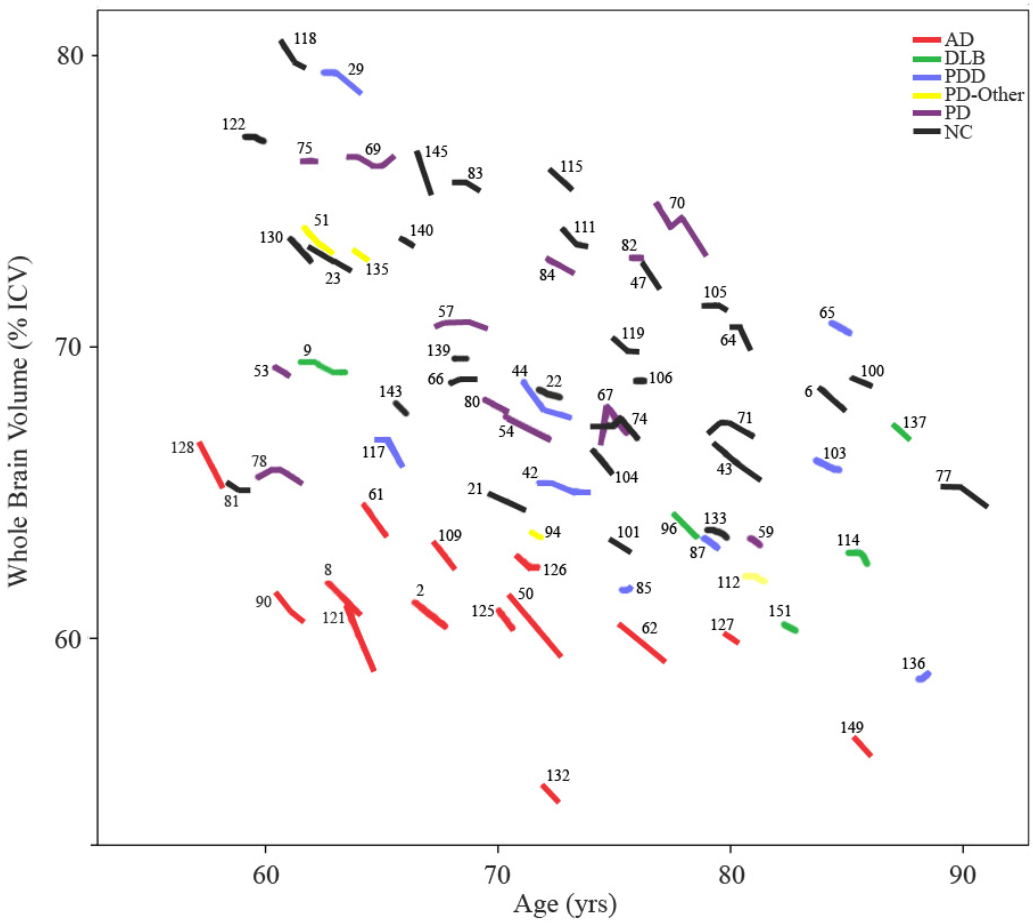

Figure 3.9: Spaghetti plot illustrates whole brain volumes (as percentages of intracranial volume) and volume changes across follow-up visits as a function of age and diagnostic group. Subject ID is listed adjacent to each subject's individual trajectory. Whole brain volume excludes ventricles, CSF and brainstem.

significant in all regions except left ILF, right IFOF, left SLF, left tSLF and left pSLF. There were no significant differences between AD and DLB subjects.

Data from PDD subjects was intermediate between that of AD and DLB subjects and that of non-demented subjects. It was not statistically significant from either group.

Diffusion Tensor Imaging: Average Diffusion Coefficient

Average diffusion coefficient (ADC) tended to be highest and fairly well-matched between AD and DLB groups except in the hippocampus, where AD values were significantly higher than all other groups (Figure 11). PDD values were intermediate, and there were no significant differences among non-demented subjects in the PD and NC groups.

Relative to non-demented subjects, DLB and PDD subjects showed increased ADC in right fornix, right IFOF, corpus callosum and right amygdala. Additionally, DLB subjects had increased ADC in left fornix, bilateral cingulate cingulum, bilateral ILF, left IFOF, right SLF, right pSLF and left amygdala. No comparisons between PDD and non-demented subjects survived correction for multiple comparisons. Results remained significant for DLB subjects in right fornix, right cingulate cingulum, bilateral ILF, bilateral IFOF and corpus callosum.

Compared to AD subjects, both DLB and PDD had lower ADC values in left hippocampus and PDD had lower ADC values in right hippocampus. Relative to PDD,

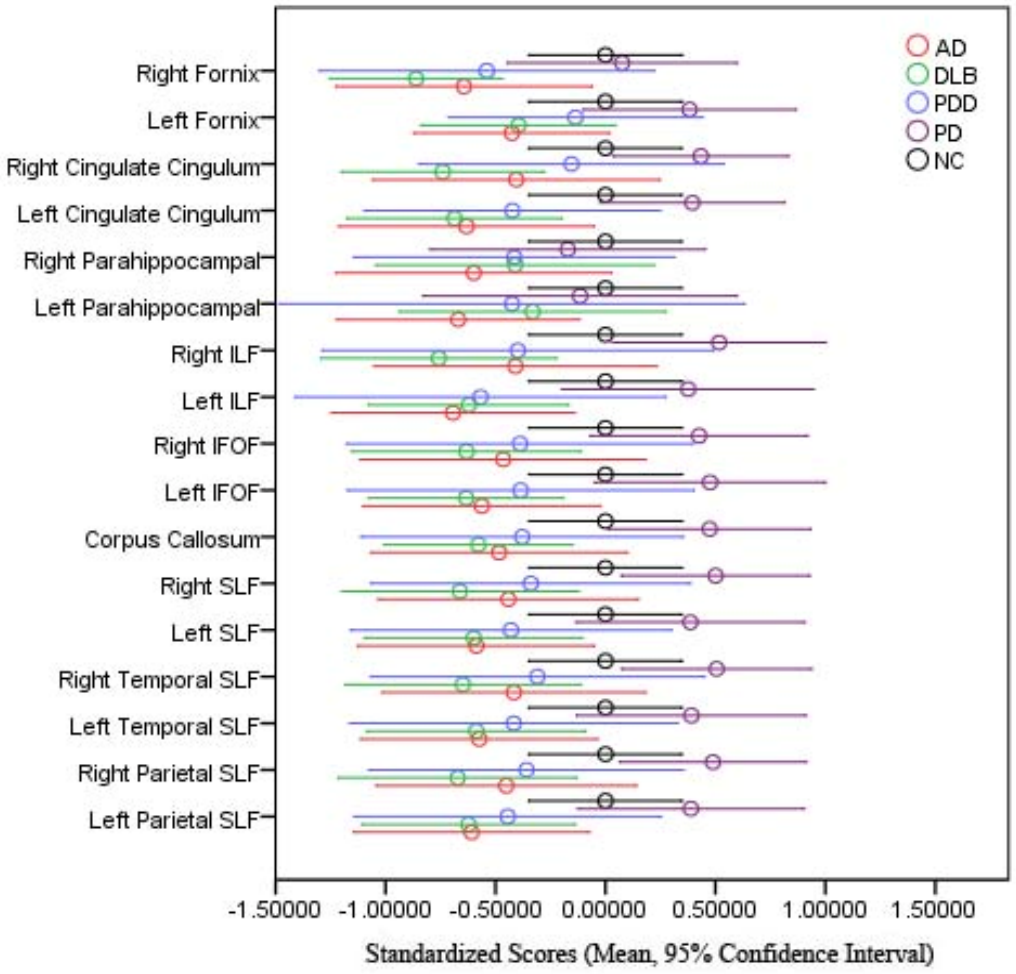

Figure 3.10: Mean of standardized number of fibers within a given tract by diagnostic group. A value of zero represents what is expected in a normal control of a given age, gender and intracranial volume. Error bars represent 95% confidence intervals. Tracts of interest were selected *a priori*.

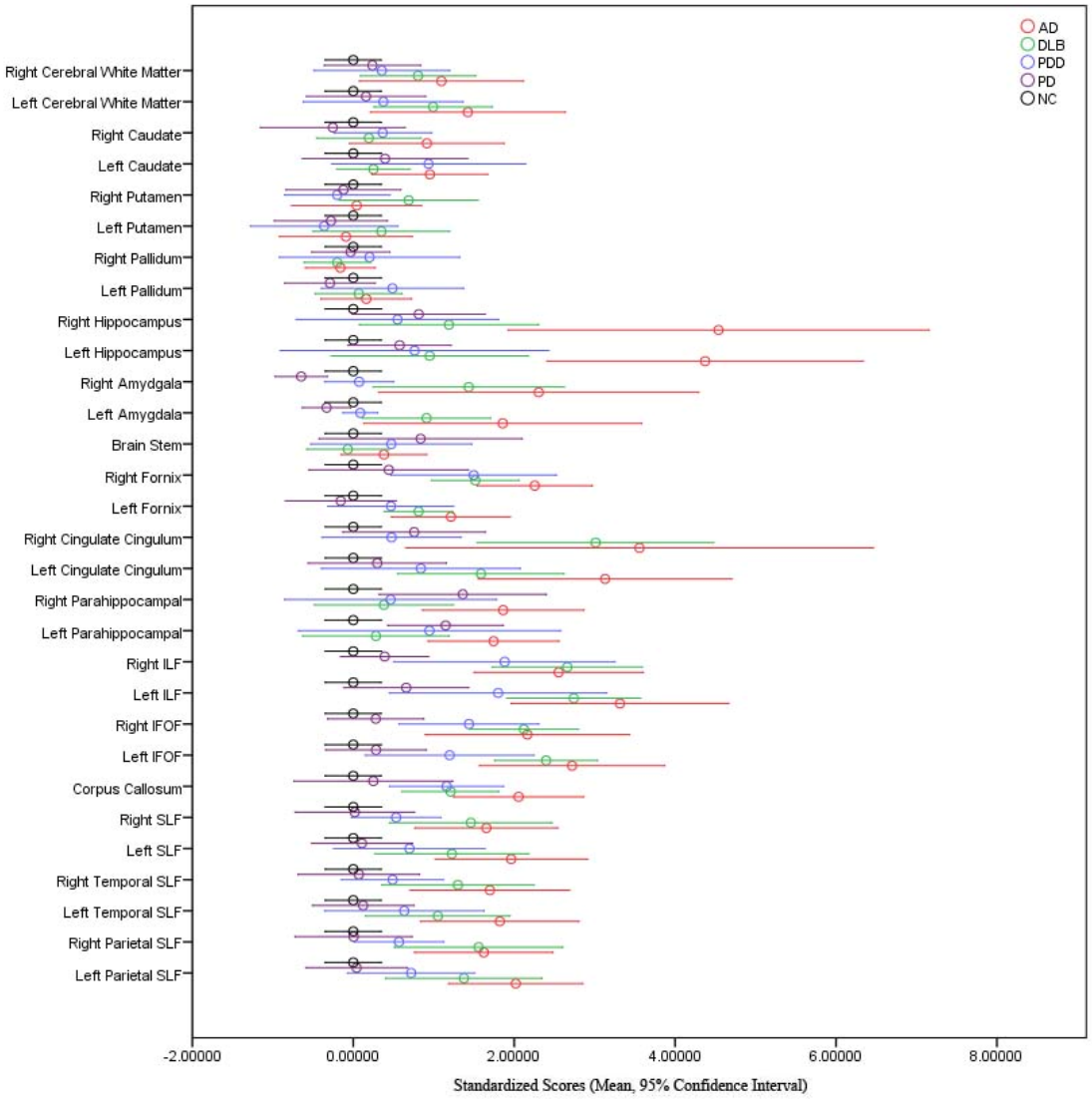

Figure 3.11: Mean of standardized average diffusion coefficient (ADC) by diagnostic group. ADC reflects mean diffusivity of water molecules within a given region and is known to increase with degeneration of structural barriers. A value of zero represents what is expected in a normal control of a given age, gender and intracranial volume. Error bars represent 95% confidence intervals. Regions and tracts of interest were selected *a priori*.

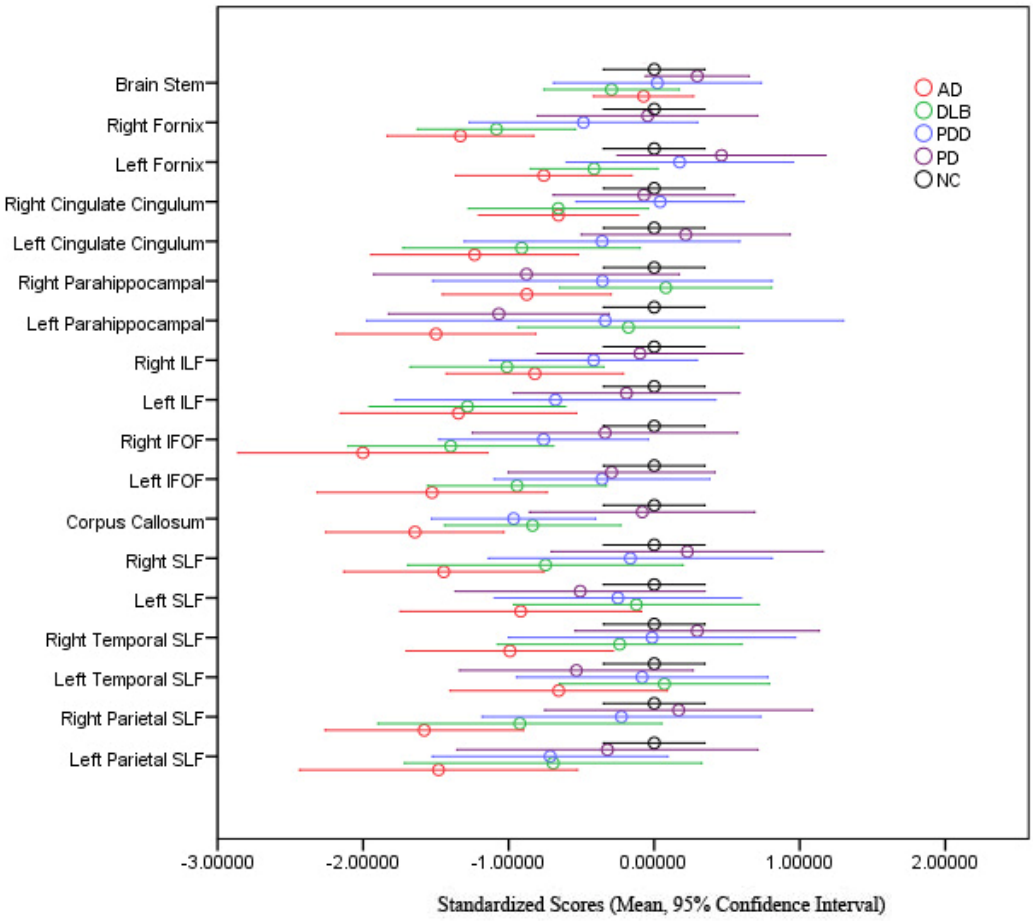

Figure 3.12: Mean of standardized fractional anisotropy (FA) by diagnostic group. FA describes directional preference of water molecules, and values tend to decrease with loss of microstructural integrity. A value of zero represents what is expected in a normal control of a given age, gender and intracranial volume. Error bars represent 95% confidence intervals. Regions and tracts of interest were selected *a priori*.

DLB subjects had significantly increased ADC in the right cingulate cingulum, though none of these survived correction for multiple comparisons.

Diffusion Tensor Imaging: Fractional Anisotropy

The diagnostic group pattern of fractional anisotropy (FA) values is not as distinct as that of ADC values, although the trend is greatest severity (decreased FA) in AD subjects and intermediate severity in DLB and PDD subjects (Figure 12). One region in which this pattern did not hold is the left parahippocampal cingulum, in which AD subjects had significantly reduced FA compared to DLB and NC subjects, but PD subjects also had reduced FA compared to NA subjects.

PDD differed from non-demented subjects in the corpus callosum. DLB differed from non-demented subjects in bilateral fornix, left cingulate cingulum, bilateral ILF, bilateral IFOF and corpus callosum. The only comparison that survived correction for multiple comparisons was that DLB had significantly reduced FA in the right fornix and right IFOF.

Relative to AD, DLB subjects had higher FA values in bilateral parahippocampal; PDD subjects had higher FA values in left fornix, bilateral IFOF, right SLF and right pSLF. None of these differences survived correction for multiple comparisons.

Data from autopsy-confirmed cases

Autopsy reports were obtained for eleven subjects who passed away during the course of the study. A summary of their autopsy reports is presented in Table 2, and their pre-mortem imaging findings with regard to hippocampal and inferior lateral ventricle volume are presented in Figure 13.

Case 5 was a 58 year-old female who had been clinically diagnosed with AD. On pre-mortem imaging, she showed only moderate hippocampal atrophy, although there was significant change between the two imaging time points, which were separated by 42 months. Post-mortem autopsy revealed Braak neurofibrillary stage V/VI with extensive neurofibrillary tau pathology. There was also extensive white matter tau pathology with many "coiled bodies" and extensive amyloid angiopathy. No LB pathology was found.

Case 10 was an 81 year-old male who had been clinically diagnosed with DLB. On pre-mortem imaging, he showed severely reduced hippocampal volume (less than the first percentile for his age) but normal-sized inferior lateral ventricles. His pathology report revealed Braak neurofibrillary stage V with frequent neuritic and diffuse plaques and diffuse neocortical LB pathology. The primary pathologic diagnosis of AD was given with a contributing diagnosis of LB disease.

Case 11 was an 80-year-old male also clinically diagnosed with DLB. He similarly showed reduced hippocampal volume (less than the first percentile) and moderately increased inferior lateral ventricles on pre-mortem imaging. On autopsy, he was found to have Braak neurofibrillary stage IV with moderate neuritic plaques

Table 3.2: Imaging and autopsy findings for 11 subjects

Subj ID	Clinical Dx	Age at Imaging (y)	Imaging to death period (mo)	Age-related HippVol Norm %	Age-related Inf Lat Vent Vol Norm %	Path Dx	LB-related Pathology	Braak NFT Stage	Neuritic Plaques
5	AD	58	5	80 → 39	20 → >99	AD	None	V/VI	Freq
10	DLB	81	7	<1	56	AD with LBD	Diffuse neocortical	V	Freq
11	DLB	80	13	<1	92	LBD with AD	Diffuse neocortical	IV	Mod
12	DLB	74	51	<1	>99	AD, hipp scl, PSP-P	None	VI	Freq
17	DLB	81	17	<1	>99	LBD, hipp scl	Transitional (limbic)	I	None
18	AD	75	11	<1	>99	AD	Unspecified	VI	Freq
20	DLB	84	31	<1	>99	AD with LBD	Diffuse, neocortical	IV	Freq
24	DLB	74	36	<1	>99	AD and LBD	Diffuse, neocortical	V	Freq
31	DLB	70	6	17 → 15 → <1	>99	LBD	Unspecified	I	Unspec
39	DLB	76	3	24	>99	LBD	Diffuse, neocortical	I	Freq
146	PDD	76	3	<1	>99	LBD with AD	Diffuse, neocortical	IV	Mod

DLB = Dementia with Lewy bodies. AD = Alzheimer's Disease. LBD = Lewy body dementia (encompasses both DLB and PDD). Hipp Scl = hippocampal sclerosis. PSP-P = progressive supranuclar palsy-parkinsonism. Imaging and autopsy data are presented for 11 subjects who came to autopsy during the study. Age-related volume normative percentiles were obtained using Cortechs Labs NeuroQuant software.

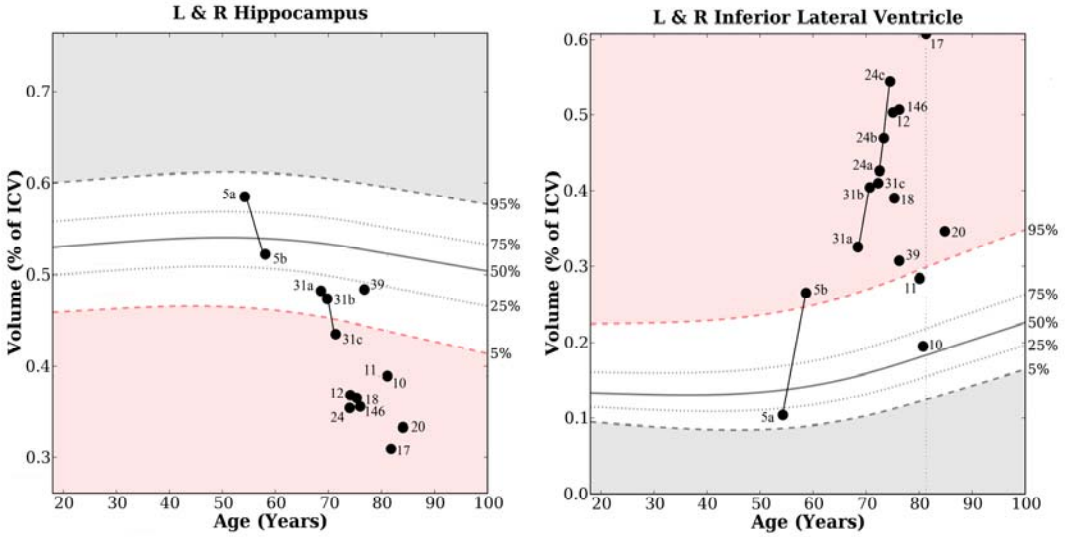

Figure 3.13: Hippocampal and inferior lateral ventricle volumes (as percentages of intracranial volume) plotted as age-related normative percentiles for eleven subjects who came to autopsy. Normative percentiles are generated by Cortechs Labs NeuroQuant software using age-appropriate reference distributions. Subject ID is listed adjacent to each subject's data. Subjects with data from more than one imaging time-point are represented by multiple dots connected by lines.

and frequent diffuse plaques as well as diffuse neocortical LB pathology. He was given a primary pathologic diagnosis of LB disease with a contributing pathologic diagnosis of AD.

Case 12 was a 74-year-old male clinically diagnosed with DLB. On pre-mortem imaging, he had both severely reduced hippocampal volume and elevated inferior lateral ventricles. Upon autopsy, severe AD pathology but no LB pathology was found in his brain. He was given a primary pathologic diagnosis of AD, Braak stage VI with secondary diagnoses of hippocampal sclerosis and progressive supranuclear palsy – Parkinsonism.

Case 17 was an 81-year-old male clinically diagnosed with DLB. He showed severe hippocampal atrophy and inferior lateral ventricle expansion on pre-mortem imaging. Autopsy revealed intermediate or transitional (limbic) type LB pathology and hippocampal sclerosis in the absence of AD pathology (Braak stage I). He was given a primary pathologic diagnosis of LB disease with a contributing pathologic diagnosis of hippocampal sclerosis.

Case 18 was a 75-year-old male clinically diagnosed with AD. He too showed reduced hippocampal volume and increased inferior lateral ventricle volume on pre-mortem imaging. His autopsy confirmed the diagnosis of AD with Braak neurofibrillary stage VI with frequent neuritic and diffuse plaques and severe amyloid angiopathy.

Case 20 was an 84-year-old female clinically diagnosed with DLB. She showed severely reduced hippocampal volume and moderately increased inferior

lateral ventricles on pre-mortem imaging. Both AD pathology (Braak stage IV with frequent neuritic plaques) and LB pathology of diffuse cortical type were found in her brain at autopsy. She was given a primary pathologic diagnosis of AD with contributing LB disease.

Case 24 was a 74-year-old male clinically diagnosed with DLB. He showed decreased but relatively stable hippocampal volumes across three imaging time-points spanning 18 months, but rapid expansion of the inferior lateral ventricles during this time. His autopsy report revealed advanced Braak stage V AD pathology and frequent, diffuse cortical Lewy bodies. The pathologist cited that either AD or LB pathology could have been more important in explaining cognitive symptoms, so both were included in the primary pathologic diagnosis.

Case 31 was a 70-year-old male with a clinical diagnosis of DLB. He was imaged three times over the course of a year. Although his hippocampal volume was relatively normal at the start of this period, it decreased significantly during the last six months of imaging, although not to the level of severity seen in the above cases. His inferior lateral ventricles showed severe expansion during the first six months of imaging. His autopsy report revealed pure LB disease with diffuse cortical Lewy bodies in the absence of AD-related pathology.

Case 39 was a 76-year-old male with a clinical diagnosis of DLB who showed normal hippocampal volume and only slightly increased inferior lateral ventricles. On autopsy, he too was found to have pure LB disease with diffuse cortical Lewy bodies and only age-related AD changes.

Case 146 was a 76-year-old male diagnosed clinically with PDD. He had both severely reduced hippocampal volume and increased inferior lateral ventricles on pre-mortem imaging. On autopsy, his brain showed diffuse cortical LB pathology and moderately severe AD pathology Braak stage IV. His primary pathologic diagnosis was LB disease with a contributing diagnosis of AD.

Discussion

The results of this study demonstrate that gross anatomical change in LB dementia seems to be intermediate between that of AD and healthy aging, even though subjects with DLB and AD were matched on dementia severity level. Significant cortical loss was observed in subjects with LB dementia throughout frontal, temporal and parietal lobe regions, but there were no regions in which cortical loss was significantly greater in the LB dementias than in AD. Similarly, subjects with LB dementia exhibited volume loss in basal ganglia, thalamus and limbic structures but not to the extent of AD subjects. Examination of global change in whole brain volumes (Figure 9) and localized cortical change across individual subjects (Figures 3 -8) revealed that AD subjects were clearly distinguishable from other subjects, both on the basis of cross-sectional measurements and also on their rates and patterns of change. Figure 3 demonstrates a clear Alzheimer's pattern of fronto-temporal cortical loss consistent with the known pathology of AD. Subjects with LB dementias are not as clearly distinguished from non-demented subjects in terms of gross anatomical

change. These findings are supported by previous MRI studies (Duda et al, 2004; O'Brien et al, 2001; Whitwell, 2007).

In contrast, when comparing AD, DLB and PDD subjects using diffusion-weighted data, change in LB dementia seems to be nearly as severe as change in AD, particularly in white matter tracts involving limbic, parietal-ocipital and temporal regions. Previous studies of LB dementia similarly report significant changes in diffusion-weighted measurements in these regions (Matsui et al, 2007; Bozzali et al, 2005; Kantarci et al, 2010; Watson et al, 2012). One tract of particular interest in LB dementia is the inferior longitudinal fasiculus (ILF), which projects from the occipital lobe visual association cortex to the medial and anterior temporal lobe and also carries feedback from the amygdala to the visual cortex (Catani et al, 2003). It is thought that damage to this tract may be responsible for the visuospatial impairments and visual hallucinations common to LB dementia (Yamamoto et al, 2006).

DTI assesses local microstructure of the brain, and is believed to be sensitive to changes in white matter integrity, fiber density, myelination and axonal diameter (Hagler et al, 2009). As degenerative changes occur, diffusivity of water in the brain increases (represented by an increase in ADC) due to the break-down of structural barriers that restrict Brownian motion, and directionality of diffusion becomes more random and less-defined by white matter tracts (represented by a decrease in FA). In this study, FA seemed to be a less powerful measure than ADC in differentiating among diagnostic groups, perhaps reflecting its greater usefulness in identifying tract location rather than tract degeneration.

The increased severity of diffusivity changes relative to structural changes found in this study suggests that—unlike in AD—cognitive impairment in LB dementia may reflect degenerative change in which neuronal loss is not prominent. This hypothesis is supported by pathological studies showing that cortical neuronal loss is not, in fact, a principal feature of LB disease (Higuchi et al, 2000). A recent study by Rodriguez et al (2012) posited that AD pathology may induce greater structural change whereas LB pathology may induce functional effects in disproportion to its structural effects. A number of theories have been proposed regarding the etiology of functional effects in LB dementia. Hattori et al (2011) suggested that a multi-faceted degeneration of white matter may occur in LB disease, including small Lewy pathologies, disruption of axonal transport, alterations in axonal structure, spongiform changes and demyelination. Another study suggested that disruption of diffusivity within white matter may indicate early microvascular ischemic disease and contribute to both the motor and nonmotor symptoms in LB dementia (Silbert and Kaye, 2010).

It is likely that in addition to these proposed etiologies, interplay between LB and AD pathologies significantly influences the clinical dementia of many patients with LB spectrum disorders. The co-occurrence of these pathologies is common, and some brain regions, such as the amygdala, are particularly susceptible to both pathologies (Braak et al, 2004), raising the possibility of a linked pathological cascade. *In vitro* studies have shown evidence for interactions between α-synuclein (the primary component of Lewy bodies), β-amyloid and tau. Specifically, α-synuclein has

been shown to bind to tau and induce its phosphorylation (Jensen et al 1999); extracellular α-synuclein can increase release of β-amyloid peptides and enhance neuronal toxicity (Kazmierczak et al, 2008); and amyloid aggregates enhance aggregation of α-synuclein (Lashley et al, 2008).

Thus, understanding the interplay between AD-related and LB-related pathology seems critical to deciphering the neuroimaging patterns produced by each. It is likely that a considerable portion of structural change observed in subjects in this study can, in fact, be explained by concomitant AD pathology, especially in DLB subjects who are expected to have a high prevalence of Alzheimer's changes. PDD subjects are less likely than DLB subjects to have amyloid pathology (Edison et al, 2008), and this may account for the less severe patterns of structural change seen in them. Ballard et al (2006) proposed that a combination of amyloid and LB pathology may explain cognitive problems in DLB whereas LB pathology alone may explain the slower decline experienced in PDD.

Of the nine subjects clinically diagnosed as DLB or PDD for whom we obtained autopsy reports, only three were found to have pure LB disease (including one subject who additionally had hippocampal sclerosis). Five of these cases showed substantial AD pathology, either as a primary or contributing pathologic diagnosis, and one of these cases did not have any LB pathology. In this latter case, the presence of AD and supranuclear palsy – Parkinsonism, which mimics the motor symptoms of Parkinson's disease but does not involve Lewy bodies, presented a symptomatic profile clinically indistinguishable from LB dementia. It can be assumed that a

significant proportion of subjects clinically diagnosed with DLB or PDD in this sample have concomitant AD pathology, which may be driving the intermediate level of structural change we saw in their brains.

Reliance on clinical diagnosis to determine group-level comparisons is a significant limitation of this study and all *in vivo* imaging studies. The high prevalence of mixed and atypical pathology confounding clinical diagnosis is clearly demonstrated among our eleven autopsy cases. This limitation gives rise to the need for future, larger-scale studies to bridge *in vivo* MRI and post-mortem pathology. Further, the high degree of heterogeneity among these disorders—both at a pathologic and clinical level—suggests it may be useful to invest greater effort in studying individual subjects over time, which is accomplished to a small extent in this study, rather than lumping subjects under umbrella-term diagnoses with little pathological correlation.

Acknowledgments

Chapter 3, in full, is currently being prepared for submission for publication of the material. Murphy EA; Seibert TM; Holland D; Hagler Jr. DJ; Dale AM; Brewer JB. The dissertation author was the primary investigator and author of this paper.

The authors thank collaborators at the UCSD Parkinson's Disease Research Consortium, Shiley-Marcos Alzheimer's Disease Research Center, Multi-modal Imaging Laboratory, Radiology Imaging Laboratories and clinicians at the UCSD medical center. We also express our appreciation to Kelly Landy for help with subject

recruitment and to Jerlyn Tolentino, Erik Kaestner and Nichol Ferng for help with recruitment and data acquisition.

J.B.B. is supported by NINDS K02 NS067427, NIA U01 AG10483, NIA P50 AG005131, NIA RC2AG036535 and General Electric Medical Foundation and is an investigator for, and receives research funds from Janssen Alzheimer Immunotherapy. He has served on advisory boards for Elan and Avanir Pharmaceuticals, holds stock options in CorTechs Labs, Inc., and serves as an editor for the International Journal of Alzheimer's Disease; E.A.M. is supported in part by NIGMS Training Grant GM007198.

References

Aarsland D, Beyer MK, Kurz MW. Dementia in Parkinson's disease. Curr Opin Neurl 2008;21**:** 676-682.

Antonelli F, Ray Nicola and Strafella AP. Imaging Cognitive and Behavioral Symptoms in Parkinson's Disease. Expert Rev. Neurother 2010;10(12):1827-1838.

Apostolova LG, Beyer M, Green AE, Hwang KS, Morra JH, Chou Y, Avedissian C, Aarsland D, Janvin CC, Larsen JP, Cummings J, Thompson PM. Hippocampal, Caudate and Ventricular changes in Parkinson's disease with and without dementia. Movement Disorders 2010; 25(6):687-695.

Ballard C, Ziabreva I, Perry R, Larsen JP, O'Brien J, McKeith I, Perry E, Aarsland D. Differences in neuropathologic characteristics across the Lewy body dementia spectrum. Neurology 2006; 67(11):1931-34.

Beyer MK, Larsen JP, Aarsland D. Gray matter atrophy in Parkinson disease with dementia and dementia with Lewy bodies. Neurology 2007;69;747-754.

Bozzali M, Falini A, Cercignani M, Baglio F, Farina E, Alberoni M, Vezzulli P, Olivotto F, Mantovani F, Shallice T, Scotti G, Canal N, Nemni R. Brain tissue

damage in dementia with Lewy bodies: an in vivo diffusion tensor MRI study. Brain 2005;128(7):1595-1604.

Braak H, Del Tredici K, Rub U, de Vos RA, Jansen Steur EN, Braak E. Staging of brain pathology related to sporadic Parkinson's disease. Neurobiol Aging 2003;24(2):197-211.

Braak H, Ghebremedhin E, Rub U, Bratzke H, Del Tredici K. Stages in the development of Parkinson's disease-related pathology. Cell Tissue Res 2004;318:121-134.

Braak H, Rub U, Jansen Steur EN, Del Tredici K, de Vos RA. Cognitive status correlates with neuropathologic stage in Parkinson disease. Neurology 2005; 64:1404-10.

Brewer JB. Fully-automated volumetric MRI with normative ranges: Translation to clinical practice. Behavioural Neurology 2009;21:1-8.

Calderon J, Perry RJ, Erzinclioglu SW, Berrios GE, Dening TR, Hodges JR. Perception, attention, and working memory are disproportionately impaired in dementia with Lewy bodies compared with Alzheimer's disease. J Neurol Neurosurg Psychiatry 2001;70:157-164.

Catani M, Jones DK, Donato R, Ffytche DH. Occipito-temporal connections in the human brain. Brain 2003;126:2093-2107.

Caviness JN, Driver-Dunckley E, Connor DJ, Sabbagh MN, Hentz JG, Noble B, Evidente VG, Shill HA, Adler CH. Defining mild cognitive impairment in Parkinson's disease. Mov Disord 2007;22:1272-1277.

Dale AM, Fischl B, Sereno MI. Cortical surface-based analysis. I. Segmentation and surface reconstruction. Neuroimage 1999;9(2):179-194.

Deramecourt V, Bombois S, Maurage CA, Ghestern A, Drobecq H, Vanmechelen E, Levert F, Pasquier F, Delacourte A. Biochemical staging of synucleinopathy and amyloid deposition in dementia with Lewy bodies. J Neuropathol Exp Neurol 2006;65:278-288.

Desikan RS, Ségonne F, Fischl B, Quinn BT, Dickerson BC, Blacker D, Buckner RL, Dale AM, Maquire RP, Hyman BT, Albert MS, Killiany RJ. An automated labeling system for subdividing the human cerebral cortex on MRI scans into gyral based regions of interest. Neuroimage 2006;31(3):968-980.

Duda JE. Pathology and neurotransmitter abnormalities of dementia with Lewy bodies. Dement Geriatr Cogn Disord 2004; 17:3-14.

Edison P, Rowe CC, Rinne JO, Ng S, Ahmed I, Kemppainen N, Villemagne VL, O'Keefe G, Nagren K, Chaudhury KR, Masters CL, Brooks DJ. Amyloid load in Parkinson's disease dementia and Lewy body dementia measured with [11C]PIB positron emission tomography. J Neurol Neurosurg Psych 2008;79:1331-1338.

Fischl B, Sereno MI, Dale AM. Cortical surface-based analysis. II. Inflation, flattening, and a surface-based coordinate system. Neuroimage 1999;9(2):195-207.

Fischl B, Dale AM. Measuring the thickness of the human cerebral cortex from magnetic resonance images. Proc Natl Acad Sci USA 2000;97(20):11050-11055.

Fischl B, Salat DH, Busa E, Albert M, Dieterich M, Haselgrove C, van der Kouwe A, Killiany R, Kennedy D, Klaveness S, Montillo A, Makris N, Rosen B, Dale AM. Whole brain segmentation: automated labeling of neuroanatomical structures in the human brain. Neuron 2002;33(3):341-355.

Fischl B, van der Kouwe A, Destrieux C, Halgren E, Segonne F, Salat DH, Busa E, Seidman LJ, Goldstein J, Kennedy D, Caviness V, Makris N, Rosen B, Dale AM. Automatically parcellating the human cerebral cortex. Cereb Cortex 2004;14(1):11-22.

Galpern WR, Lang AE. Interface between tauopathies and synucleinopathies: a tale of two proteins. Ann Neurol. 2006;59(3);449-458.

Hagler DJ Jr, Ahmadi ME, Kuperman J, Holland D, McDonald CR, Halgren E, Dale AM. Automated white-matter tractography using a probabilistic diffusion tensor atlas: Application to temporal lobe epilepsy. Hum Brain Mapp 2009;30(5):1535-1547.

Hattori T, Orimo S, Aoki S, Ito K, Abe O, Amano A, Sato R, Sakai K, Mizusawa H. Cognitive status correlates with white matter alteration in Parkinson's disease. Human Brain Mapping 2011.

Hely MA, Reid WG, Adena MA, Halliday GM, Morris JG. The Sydney multicenter study of Parkinson's disease: the inevitability of dementia at 20 years. Mov Disord 2008;23:837-844.

Higuchi M, Tashiro M, Arai H, Okamura N, Hara S, Higuchi S, Itoh M, Shin RW, Trojanowski JQ, Sasaki H. Glucose hypometabolism and neuropathological correlates in brains of dementia with Lewy bodies. Exp Neurol 2000;162:247-256.

Holland D, Brewer JB, Hagler DJ, Fennema-Notestine C, Dale AM; Alzheimer's Disease Neuroimaging Initiative. Subretional neuroanatomical change as a biomarker for Alzheimer's disease. Proc Natl Acad Sci USA 2009;106(49):20954-20959.

Jensen PH, hager H, Nielsen MS, Hojrup P, Gliemann J, Jakes R. alpha-synuclein binds to Tau and stimulates the protein kinase A-catalyzed tau-phosphorylation of serine residues 262 and 356. J Biol Chem 1999;274:25481-25489.

Jovicich J, Czanner S, Greve D, Haley E, van der Kouwe A, Gollub R, Kennedy D, Schmitt F, Brown G, Macfall J, Fischl B, Dale A. Reliability in multi-site structural MRI studies: effects of gradient non-linearity correction on phantom and human data. Neuroimage 2006;30(2):436-43.

Junque C, Ramirez-Ruiz B, Tolosa E, Summerfield C, Marti MJ, Pastor P, Gomez-Anson B, Mercader JM. Amygdalar and hippocampal MRI volumetric reductions in Parkinson's disease with dementia. Mov Disord 2005;20:540-544.

Kantarci K, Avula R, Senjem ML, Samikoglu AR, Zhang B, Weigand SD, Przybelski SA, Edmonson HA, Vemuri P, Knopman DS, Ferman TJ, Boeve BF, Petersen RC, Jack CR Jr. Dementia with Lewy bodies and Alzheimer disease: neurodegenerative patterns characterized by DTI. Neurology 2010;74:1814-1821.

Kazmierczak A, Strosznajder JB, Adamczyk A. alpha-synuclein enhances secretion and toxicity of amyloid beta peptides in PC12 cells. Neurochem Int 2008;53(6-8):263-9.

Lashhley T, Holton JL, Gray E, Kirkham K, O'Sullivan SS, Hilbig A, Wood NW, Lees AJ, Revesz T. Cortical alpha-synuclein load is associated with amyloid-Beta plaque burden in a subset of Parkinson's disease patients. Acta Neuropathol 2008;115:417-425.

Lee JE, Park Bosuk, Song SK, Sohn YH, Park H-J, Lee PH. A Comparison of gray and white matter density in patients with Parkinson's disease dementia and dementia with Lewy bodies using voxel-based morphometry. Movement Disorders 2009;25(1):28-34.

Lee J E, Park H-J, Park B, Song S K, Sohn Y H, Lee JD, Lee PH. A comparative analysis of cognitive profiles and white matter alterations using voxel-based diffusion tensor imaging between patients with Parkinson's disease dementia and dementia with Lewy bodies. J Neurol Psychiatry. 2010;81(3):320-326.

Lewis SJ, Barker RA.Understanding the dopaminergic deficits in Parkinson's disease: insights into disease heterogeneity. J Clin. Neurosci 2009;16:620-625.

Luis CA, Barker WW, Gajaraj K, Harwood D, Petersen R, Kashuba A, Waters C, Jimison P, Pearl G, Petito C, Dickson D, Duara R. Sensitivity and specificity of three clinical criteria for dementia with Lewy bodies in an autopsy-verified sample. Int J Geriatr Psychiatry 1999;14:526-533.

Marui W, Iseki E, Nakai T, Mirura S, Kato M, Ueda K, Kosaka K. Progression and staging of Lewy pathology in brains from patients with dementia with Lewy bodies. J Neurol Sci 2002;195:153-59.

Masliah E, Rockenstein E, Veinbers I, Sagara Y, Mallory M, Hashimoto M, Mucke L. β-amyloid peptides enhance alpha-synuclein accumulation and neuronal deficits in a transgenic mouse model linking Alzheimer's disease and Parkinson's disease. Proc Natl Acad Sci USA 2001;98:12245-12250.

Matsui H, Nishinaka K, Oda M, Niikawa H, Kubori T, Udaka F. Dementia in Parkinson's disease: diffusion tensor imaging. Acta Neurol Scand 2007;116:177-181.

McEvoy LK, Fennema-Notestine C, Roddey JC, Hagler DJ Jr, Holland D, Karow DS, Pung CJ, Brewer JB, Dale AM; Alzheimer's Disease Neuroimaging Initiative. Alzheimer disease: quantitative structural neuroimaging for detection and prediction of clinical and structural changes in mild cognitive impairment. Radiology 2009;251(1):195-205.

McKeith J, Mintzer J, Aarsland D, Burn D, Chiu H, Cohen-Mansfield J, Dickson D, Dubois B, Duda J, Feldman H, Gauthier S, Halliday G, Lawlor B, Lippa C, Lopez OL, Manchado JC, O'Brien J, Playfer J, Reid W. DLB on behalf of the International Psychogeriatric Association Expert Meeting on DLB: Dementia with Lewy bodies. Lancet Neurol 2004;3:19-28.

McKeith IG, Dickson DW, Lowe J, Emre M, O'Brien JT, Feldman H, Cummings J, Duda JE, Lippa C, Perry EK, Aarsland D, Arai H, Ballard CG, Boeve B, Burn DJ, Costa D, Del Ser T, Dubois B, Galasko D, Gauthier S, Goetz CG, Gomez-Tortosa E, Halliday G, Hansen LA, Hardy J, Iwatsubo T, Kalaria RN, Kaufer D, Kenny RA, Korczyn A, Kosaka K, Lee VM, Lees A, Litvan I, Londos E, Lopez OL, Minoshima S, Mizuno Y, Molina JA, Mukaetova-Ladinska EB, Pasquier F, Perry RH, Schulz JB, Trojanowski JQ, Yamada M; Consortium on DLB. Diagnosis and management of dementia with Lewy bodies: third report of the DLB consortium. Neurology 2005;65:1863-72.

Murphy, E.A., Holland, D., Donohue, M., McEvoy, L.K., Hagler, D.J., Jr., Dale, A.M., Brewer, J.B., Alzheimer's Disease Neuroimaging Initiative. Six-month

atrophy in MTL structures is associated with subsequent memory decline in elderly controls. Neuroimage 2010;53(4):1310-1317.

O'Brien JT, Paling S, Barber R, Williams ED, Ballard C, McKeith IG, Gholkar A, Crum WR, Rossor MN, Fox NC. Progressive brain atrophy on serial MRI in dementia with Lewy bodies, AD, and vascular dementia. Neurology 2001;56:1386-1388.

Rodriguez MJ, Potter E, Shen Q, Barker W, Greig-Custo M, Agron J, Loewenstein D, Duara R. Cognitive and structural magnetic resonance imaging features of Lewy body dementia and Alzheimer's disease. Alzheimer's & Dementia 2012;8:211-218.

Rowe CC, Ng S, Ackermann U, Gong SJ, Pike K, Savage G, Cowie TF, Dickinson KL, Maruff P, Darby D, Smith C, Woodward M, Merory J, Tochon-Danguy H, O'Keefe G, Klunk WE, Mathis CA, Price JC, Masters CL, Villemagne VL. Imaging beta-amyloid burden in aging and dementia. Neurology 2007;68:1718-1725.

Sanchez-Castaneda C, Rene R, Ramirez-Ruiz B, Campdelacreu J, Gascon J, Falcon C, Calopa M, Jauma S, Juncadella M, Junque C. Correlations between gray matter reductions and cognitive deficits in dementia with Lewy bodies and Parkinson's disease with dementia. Mov Disord 2009;24:1740-1746.

Silbert LC and Kaye J. Neuroimaging and cognition in Parkinson's disease dementia. Brain Pathology 2010;20:646-653.

Sled JG, Zijdenbos AP, Evans AC. A non-parametric method for automatic correction of intensity nonuniformity in MRI data. IEEE Trans Med Imaging 1998;17(1):87-97.

Tam CW, Burton EJ, McKeith IG, Burn DJ, O'Brien JT. Temporal lobe atrophy on MRI in Parkinson's disease with dementia: a comparison with Alzheimer's disease and dementia with Lewy bodies. Neurology 2005;65:1863-1872.

Thompson WK, Holland D; Alzheimer's Disease Neuroimaging Initiative. Bias in tensor based morphometry Stat-ROI measures may result in unrealistic power estimates. Neuroimage 2011;57(1):1-4.

Vernon AC, Ballard C, Modo Michel. Neuroimaging for Lewy body disease: Is the in vivo molecular imaging of alpha-synuclein neuropathology required and feasible? Brain Res. Rev. 2010;65(1):28-55.

Watson R, Blamire AM, colloby SJ, Wood JS, Barber R, He J, O'Brien JT. Characterizing dementia with Lewy bodies by means of diffusion tensor imaging. Neurology 2012;79:906-914.

Weintraub D, Doshi J, Koka D, Davatzikos C, Siderowf AD, Duda JE, Wolk DA, Moberg PJ, Xie SX, Clark CM. Neurodegeneration across stages of cognitive decline in Parkinson Disease. Arch Neurol. 2011;68(12):1562-1568.

Whitwell JL, Weigand SD, shiung MM, Boeve BF, Ferman TJ, Smith GE, Knopman DS, Petersen RC, Benarroch EE, Josephs KA, Jack CR Jr: Focal atrophy in dementia with Lewy bodies on MRI: a distinct pattern from Alzheimer's disease. Brain 2007;130:708-719.

Yamamoto R, Iseki E, Murayama N, Minegishi M, Marui W, Togo T, Katsuse O, Kato M, Iwatsubo T, Kosaka K, Arai H. Investigation of Lewy pathology in the visual pathway of brains of dementia with Lewy bodies. J Neurol Sci 2006;246:95-101.

CONCLUSION

The studies described in this dissertation demonstrate three applications of quantitative neuroimaging to the study of aging and neurodegenerative disease. The findings suggest that MRI has considerable potential to enhance understanding of these processes at a biologic level and to influence clinical practice.

Chapter One presents a study in which six-month neurodegeneration was quantified in 142 healthy elderly subjects using longitudinal structural analysis. Even in healthy elderly subjects, loss of cortical thickness and subcortical volume could be quantified in a time period as short as six months and was shown to associate with subsequent performance on neuropsychological measures. Specifically, neurodegeneration in certain medial temporal lobe structures correlated with two-year decline in memory performance. Of the 142 subjects examined, seven subjects converted to a diagnosis of mild cognitive impairment (MCI) during the follow-up period. A qualitative analysis of their imaging data revealed accelerated change in a pattern consistent with what is expected in the early forms of Alzheimer's disease (AD). These findings suggest that longitudinal MRI might be useful in identifying rapid atrophy in otherwise healthy subjects and therefore enhance early detection of neurodegenerative disease.

Chapter Two applies these same neuroimaging techniques to an analysis of two polymorphisms in the cholesteryl ester transfer protein (CETP) gene, which had been

previously implicated in risk of Alzheimer's disease. This study investigates the effect of these polymorphisms on brain structure, atrophy rate and risk of AD in 188 elderly controls and 318 subjects with AD or MCI. Associations were shown to be dependent on APOE ε4 carrier status, suggesting that CETP may contribute to the genetic variability of brain structure and dementia susceptibility in an APOE-dependent manner. The use of imaging measures in studies such as this one demonstrate the advantage of neuroimaging genetics, in which phenotypes are defined by quantitative measures of brain structure or function rather than clinical characteristics such as disease, symptoms or behaviors. This enables a closer description of the biologic impact of genes in the brain.

Lastly, Chapter Three illustrates how these imaging techniques may be used to enhance understanding of the neurodegenerative process and to thus aid in the detection and differential diagnosis of these disorders. By following 150 subjects who were either healthy elderly controls or had been clinically diagnosed with AD, dementia with Lewy bodies (DLB), Parkinson's disease dementia (PDD) or Parkinson's disease (PD), this study provided a longitudinal description of the changes that occur in these disorders. Findings show that gross structural change in Lewy body dementias is intermediate between that of AD and healthy controls, whereas microstructural change detected by diffusion tensor imaging is of relatively equal severity between Lewy body dementias and AD. This suggests that Lewy body dementia may be unique from AD in that it is characterized by microstructural disruption and dysfunction but not neuronal loss. Further, the collection of both *in vivo*

imaging data and post-mortem pathological data in eleven individual subjects enables direct comparison between changes detected by MRI *in vivo* and pathological changes demonstrated post-mortem. This analysis revealed a high level of concomitance between Lewy body and Alzheimer's-related pathology, perhaps explaining the overlap in imaging patterns and clinical presentations of these disorders.

Together, these three studies demonstrate considerable potential for MRI data to be translated beyond the academic setting to clinical practice. In the near future, it is likely that MRI will not only be used in neurology clinics to identify gross pathology such as a tumor or a bleed but to also identify individuals at risk for dementia and track neurodegenerative disease progression.